

# Generation of functional striatal neurons from human pluripotent stem cells

Thesis submitted for the degree of Doctor of Philosophy

School of Biosciences, Cardiff University

2016

Zoe Noakes



**DECLARATION**

This work has not been submitted in substance for any other degree or award at this or any other university or place of learning, nor is being submitted concurrently in candidature for any degree or other award.

Signed .....(candidate)      Date .....

**STATEMENT 1**

This thesis is being submitted in partial fulfilment of the requirements for the degree of PhD.

Signed .....(candidate)      Date .....

**STATEMENT 2**

This thesis is the result of my own independent work/investigation, except where otherwise stated, and the thesis has not been edited by a third party beyond what is permitted by Cardiff University's Policy on the Use of Third Party Editors by Research Degree Students. Other sources are acknowledged by explicit references. The views expressed are my own.

Signed .....(candidate)      Date .....

**STATEMENT 3**

I hereby give consent for my thesis, if accepted, to be available online in the University's Open Access repository and for inter-library loan, and for the title and summary to be made available to outside organisations.

Signed .....(candidate)      Date .....

**STATEMENT 4: PREVIOUSLY APPROVED BAR ON ACCESS**

I hereby give consent for my thesis, if accepted, to be available online in the University's Open Access repository and for inter-library loans after expiry of a bar on access previously approved by the Academic Standards & Quality Committee.

Signed .....(candidate)      Date .....

## Acknowledgements

First and foremost, I would like to thank my primary supervisor, Prof Meng Li, for giving me this opportunity and providing her continuous guidance and support. I have really appreciated her open door policy and readiness to listen. I also wish to thank the whole Li lab, but specific thanks go to Claudia, who taught me so much about stem cell culture when I knew so little; Marija, who always gave help when I needed it and for giving me valuable feedback on this thesis; Shanthi, for being the backbone of the lab and keeping us in line; and of course Ines, for being there at the start and getting me through my first departmental talk. I would also like to thank my second supervisor, Prof Steve Dunnett, and the whole Brain Repair Group, especially Mariah and Claire for their help and supervision with the transplantation experiments. Thanks also go to Mic and Adam for their help with the electrophysiology studies.

Finally, I would like to thank my friends and family for their continuous support, reassurance and inspiration – particularly my parents and brother for the stimulating debates and pragmatic solutions, and Charlotte for reading a thesis she didn't understand. Most of all, I want to thank my partner Philip, for providing me with endless support and encouragement to follow my chosen career path when I doubted myself most, getting me to where I am now.

## Abstract

The striatal neuronal populations comprise medium spiny projection neurons (MSNs) and GABAergic and cholinergic interneurons. Huntington's disease (HD) involves massive degeneration of striatal neurons. The derivation of MSNs and interneurons from human pluripotent stem cells (hPSCs) would allow modelling of striatal function and HD *in vitro*, as well as provide a viable source of tissue for cell replacement therapy.

Our lab has previously demonstrated that Activin A can induce MSN fate in hPSCs, and that these cells can survive and differentiate *in vitro* and *in vivo*. In this study, it was found that this effect occurs via the Activin receptor, independently of SHH signalling. Furthermore, blockade of BMP signalling accelerated MSN differentiation. Electrophysiological analysis demonstrated their potential to acquire functional membrane properties and synaptic activity *in vitro*.

Wnt inhibition and SHH activation have been shown to pattern hPSCs into medial ganglionic eminence (MGE) progenitors and cortical interneurons. Both cortical and striatal interneurons are born in the MGE. This thesis presents the first account of generating MGE progenitors for the purpose of producing striatal interneurons *in vitro*. They expressed subtype markers such as parvalbumin, somatostatin, calretinin and choline acetyltransferase. When transplanted into neonatal rat striatum, hPSC-derived MGE progenitors migrated to the septum and hippocampus within 6 weeks. The majority of differentiated neurons became calretinin GABAergic interneurons, and a few in the striatum acquired cholinergic interneuron fate. Patch clamp analysis both *in vitro* and *in vivo* revealed functional neuronal characteristics and synaptic connectivity, although a more mature neuronal phenotype was achieved *in vivo*.

In conclusion, functional striatal MSNs and interneurons can be generated using hPSCs, which will be invaluable for research into striatal function and dysfunction in HD and other striatum relevant disorders. They may also serve as a desperately needed therapy for HD, pending further preclinical studies in HD animal models.

# Contents

List of figures.....	vii
List of tables.....	vii
List of abbreviations.....	viii
1 Introduction .....	1
1.1 The striatum and Huntington’s disease.....	1
1.1.1 Striatal anatomy and function .....	1
1.1.2 Huntington’s disease.....	4
1.1.2.1 Disease mechanisms .....	5
1.1.2.2 Animal models .....	7
1.1.2.3 Cell replacement therapy.....	8
1.1.2.4 Novel therapeutic strategies.....	9
1.2 Striatal development .....	11
1.2.1 Neural induction .....	11
1.2.2 Key morphogens and signalling pathways in forebrain development.....	12
1.2.2.1 Sonic hedgehog (SHH) signalling.....	12
1.2.2.2 Wnt signalling.....	13
1.2.2.3 Transforming growth factor (TGF)- $\beta$ family signalling .....	13
1.2.3 Forebrain development .....	15
1.2.4 Development of the striatum .....	16
1.3 Human pluripotent stem cells.....	19
1.3.1 hPSCs as a model of embryonic development.....	19
1.3.2 hPSCs for disease modelling and drug screening.....	20
1.3.3 hPSCs for regenerative medicine .....	20
1.3.4 Neural differentiation of hPSCs .....	21
1.3.5 Directed differentiation of hPSCs towards striatal neurons.....	23
1.3.5.1 Generation of MSNs from hPSCs .....	23
1.3.5.2 Generation of striatal interneurons from hPSCs.....	25

1.3.6	Direct reprogramming of somatic cells into striatal neurons .....	27
1.4	Aims.....	29
2	Methods and materials .....	30
2.1	Cell culture .....	30
2.1.1	hPSC culture .....	30
2.1.2	hPSC freezing and thawing.....	30
2.1.3	hESC transfection (with Claudia Tamburini) .....	30
2.1.4	hPSC neural differentiation.....	31
2.2	Cell analysis.....	32
2.2.1	Immunocytochemical staining .....	32
2.2.2	Quantitative real-time PCR .....	33
2.2.2.1	RNA extraction .....	33
2.2.2.2	DNase treatment.....	33
2.2.2.3	Reverse transcription PCR.....	33
2.2.2.4	Quantitative real-time PCR (qPCR) .....	33
2.2.3	Electrophysiological analysis.....	34
2.3	Transplantation of hESC-derived neural progenitors .....	35
2.3.1	Transplantation of hPSC-derived MGE progenitors into neonatal rats (with Claire Kelly)	35
2.3.1.1	Cell suspension preparation.....	35
2.3.1.2	Postnatal care of mother and pups.....	35
2.3.1.3	Transplantation procedure .....	35
2.3.1.4	Experimental groups and time points.....	35
2.3.2	Tissue preparation .....	36
2.3.3	Immunohistochemistry .....	36
2.3.4	Section imaging and analysis .....	36
2.3.5	<i>Ex vivo</i> brain slice recording (Michael Laing) .....	36
2.4	Statistical analysis .....	37

3	The role of TGF $\beta$ signalling in hPSC differentiation towards functional MSN fate .....	40
3.1	Introduction .....	40
3.2	Results.....	42
3.2.1	Activin acts independently of SHH signalling.....	42
3.2.2	Activin acts selectively via ALK5 receptor .....	44
3.2.3	Inhibition of BMP signalling accelerates Activin effects .....	46
3.2.4	Electrophysiological characterisation of hESC-derived MSNs <i>in vitro</i> .....	48
3.3	Discussion.....	51
4	Characterisation of hPSC-derived MGE-like interneurons.....	56
4.1	Introduction .....	56
4.2	Results.....	58
4.2.1	Activation of SHH signalling induces MGE fate in hPSCs .....	58
4.2.2	MGE progenitors mature into cortical and striatal interneurons.....	59
4.2.3	hESC-derived MGE progenitors can become functional GABAergic neurons .....	60
4.3	Discussion.....	62
5	Transplantation of hPSC-derived MGE progenitors into neonatal rat striatum.....	66
5.1	Introduction .....	66
5.2	Results.....	68
5.2.1	Generation of a tau-GFP-expressing hESC line .....	68
5.2.2	Neonatal transplantation does not avoid immune response to xenograft .....	68
5.2.3	Transplanted hESC-derived MGE progenitors migrate within the first 6 weeks of transplantation .....	70
5.2.4	Transplanted hESC-derived MGE progenitors become striatal interneurons .....	73
5.2.5	Transplanted cells adopt region-specific morphologies .....	75
5.2.6	Patch clamping of transplanted hESC-derived neurons .....	75
5.3	Discussion.....	77
6	General discussion .....	83
6.1	Summary .....	83



6.2	Implications for the study of human development .....	83
6.3	Implications for disease modelling .....	85
6.4	Implications for regenerative medicine.....	86
6.5	Conclusions .....	87
7	References .....	88

## List of figures

Figure 1.1:	Schematic diagram of classical direct/indirect pathway model of basal ganglia organisation and function.....	3
Figure 1.2:	Potential intracellular mechanisms of HTT-induced pathology in HD.....	6
Figure 1.3:	Schematic diagram of a coronal section through the developing telencephalon.....	16
Figure 3.1:	Activin exerts LGE-inducing effects independently of SHH .....	43
Figure 3.2:	Activin exerts its effects selectively via the ALK5 receptor.....	45
Figure 3.3:	LDN accelerates the effects of Activin.....	47
Figure 3.4:	hESC-derived MSNs display neuronal membrane properties and synaptic activity <i>in vitro</i> . .....	49
Figure 4.1:	SHH activation induces MGE fate in hESCs.....	59
Figure 4.2:	MGE progenitors mature into cortical and striatal interneurons.....	61
Figure 4.3:	hESC-derived MGE progenitors become functional GABAergic neurons.....	63
Figure 5.1:	Generation of tau-GFP hESC line TG4.....	69
Figure 5.2:	Neonatal transplantation does not avoid host immune response and graft rejection .....	71
Figure 5.3:	Transplanted cells migrate within the first 6 weeks of transplantation.....	72
Figure 5.4:	Transplanted MGE progenitors differentiate into striatal interneurons.....	74
Figure 5.5:	Transplanted MGE progenitors adopt region-specific morphologies.....	76
Figure 5.6:	Transplanted hESC-derived MGE progenitors can mature into functional neurons.....	78

## List of tables

Table 1.1:	Summary of TGFB superfamily of ligands, their Type I and II receptors (Rs) and associated Smads.....	15
Table 2.1:	List of primary antibodies used for immunostaining.....	38
Table 2.2:	List of primers used for qPCR.....	39

## List of abbreviations

AP	action potential
CGE	caudal ganglionic eminence
aCSF	artificial cerebrospinal fluid
AMD	age-related macular degeneration
ASD	autism spectrum disorder
BDNF	brain derived neurotrophic factor
BMP	bone morphogenetic protein
CAG	cytosine-adenine-guanine
ChAT	choline acetyltransferase
ChIP	Chromatin immunoprecipitation
CR	calretinin
CsA	cyclosporine A
DARPP32	dopamine and cAMP-regulated neuronal phosphoprotein 32kDa
DBS	deep brain stimulation
DKK1	dickkopf1
Dsh	Dishevelled
EB	embryoid body
FGF8	fibroblast growth factor 8
Frz	Frizzled
GFP	green fluorescent protein
GPCR	G protein coupled receptor
GPe	globus pallidus externa
GPi	globus pallidus interna
GSK3 $\beta$	glycogen synthase kinase 3 $\beta$
HD	Huntington's disease
hESCs	human embryonic stem cells
hPSCs	human pluripotent stem cells
HTT	Huntingtin
iN	induced neurons
iPSCs	induced pluripotent stem cells
LGE	lateral ganglionic eminence

MGE	medial ganglionic eminence
MSN	medium spiny neuron
NPY	neuropeptide Y
PD	Parkinson's disease
PSP	post-synaptic potential
Ptc	Patched
PV	parvalbumin
QA	quinolinic acid
RA	retinoic acid
RMP	resting membrane potential
ROCK	Rho associated kinase
SCID	severe combined immunodeficiency
SHH	Sonic hedgehog
Smo	Smoothed
SNc	substantia nigra pars compacta
SNr	substantia nigra pars reticulata
SST	somatostatin
STN	subthalamic nucleus
SVZ	subventricular zone
TG4	tau-GFP cell line 4
TGF $\beta$	transforming growth factor $\beta$
TH	tyrosine hydroxylase
VZ	ventricular zone
WGE	whole ganglionic eminence

# 1 Introduction

## 1.1 The striatum and Huntington's disease

### 1.1.1 Striatal anatomy and function

The striatum is the main input nucleus of the basal ganglia, an assembly of subcortical nuclei involved in the control of voluntary actions, reward and habit formation. The dorsal striatum is the largest part and comprises the caudate and putamen, which regulate the motor and associative roles of the striatum. The ventral striatum includes the nucleus accumbens and olfactory tubercle, which also form part of the limbic system and reward pathways. The basal ganglia circuit is a complex feedback loop with the cortex and thalamus that processes motivation and reward levels to filter out unnecessary actions and allow purposeful actions. The model by which this is widely agreed to occur is based around the two distinct populations of striatal projection neurons, or medium spiny neurons (MSNs), which form the direct and indirect pathways through the basal ganglia (Bolam *et al.*, 2000).

MSNs are GABAergic projection neurons making up 75% and 95% of striatal neurons in primates and rodents respectively. The remainder of striatal neurons are GABAergic and cholinergic interneurons (Wu and Parent, 2000). MSNs are identified by their expression of the dopamine- and cAMP-regulated phosphoprotein (DARPP32), which is involved in integrating dopamine and NMDA receptor signalling. This is a crucial function in MSNs, as they receive strong glutamatergic innervation from the cortex and thalamus, and dopaminergic input from the substantia nigra pars compacta (SNc). MSNs can belong to either the direct or indirect pathway, and can be distinguished by their connectivity, dopamine receptor expression and anatomical location. Direct pathway MSNs express D1 dopamine receptors and substance P, and innervate the substantia nigra pars reticulata (SNr) and the internal segment of the globus pallidus (GPi; or entopeduncular nucleus in rodents). MSNs of the indirect pathway express D2 dopamine receptors and enkephalin, and project to the external segment of the globus pallidus (GPe). These two populations are also largely anatomically segregated, with direct pathway MSNs concentrating in the striosomal (patch) compartments and indirect pathway MSNs assembling in the matrix (Davis and Puhl, 2011). The SNr and GPi are the basal ganglia output nuclei, populated with GABAergic projection neurons that innervate the thalamus. The GPe is an intermediate nucleus that sends inhibitory projections to the SNr and GPi, as well as the subthalamic nucleus (STN) (Bolam *et al.*, 2000). Another pathway was proposed by Nambu *et al.* to send even faster excitation from the cortex to the GPi and SNr via the STN, which they termed the hyperdirect pathway (Nambu, Tokuno and Takada, 2002).

Using movement as an example of the behavioural output controlled by the basal ganglia, at rest the GPi and SNr are tonically active while MSNs are quiescent. Upon excitatory input from the motor cortex, direct pathway activation causes inhibition of the GPi and SNr, and disinhibition of the thalamus, promoting movement. Activation of the indirect pathway however, inhibits the GPe, disinhibiting the GPi and SNr, allowing inhibition of the thalamus and suppressing motor output. The excitability of the two opposing MSN groups is constantly modulated by dopaminergic input from the SNc, which increases excitability of D1-expressing MSNs and decreases excitability of D2-expressing MSNs (Beaulieu and Gainetdinov, 2011) (**Figure 1.1**). Meanwhile, the hyperdirect pathway activates GPi and SNr neurons to inhibit the thalamus and suppress movement. It is thought that together, these pathways work in a specific spatiotemporal manner to disinhibit a specific population of output neurons while inhibiting the surrounding cells, such that a specific action is permitted (Nambu, Tokuno and Takada, 2002). This classical model of basal ganglia function has come under recent scrutiny based around the antagonistic and parallel nature of the two striatal pathways (Calabresi *et al.*, 2014). Rather, in light of recent evidence showing the expression of heteromeric complexes of D1 and D2 dopamine receptors in MSNs of both pathways, Calabresi *et al.* have proposed a revised model in which the pathways work together in constant communication to initiate and stop movement (Calabresi *et al.*, 2014). Cholinergic and GABAergic interneurons synapse onto MSNs of both pathways as well as dopaminergic axons, facilitating synaptic plasticity.

This revised model provides well-deserved acknowledgement of the role of striatal interneurons in striatal function. Striatal interneurons fall into several categories based on neurotransmitters, molecular markers and firing properties. Cholinergic interneurons are identified chemically by their expression of choline acetyltransferase (ChAT) and are tonically active. They were known to play a role in reward and associative learning, and their activation was shown to cause inhibitory currents in MSNs. The mechanism behind this was recently found to be that they synapse directly onto dopaminergic axons, stimulating action potential-independent release of dopamine and GABA onto MSNs (Threlfell *et al.*, 2012; Nelson *et al.*, 2014). GABAergic interneurons can be further subdivided into those that express parvalbumin (PV), somatostatin (SST) and calretinin (CR). PV interneurons receive direct glutamatergic input from cortical neurons and synapse onto MSNs, providing feed forward inhibition. Their electrophysiology is characterised by extremely fast spiking and narrow action potentials (Plotkin *et al.*, 2005). SST-expressing interneurons are also often referred to by other markers that are co-expressed in the majority of this subtype: neuropeptide Y (NPY), nitric oxide synthase (NOS) or NADPH-diaphorase (Figueredo-Cardenas *et al.*, 1996). In addition to GABA release near MSN dendritic spines, these cells have been shown to release nitric oxide (NO) following simultaneous glutamate and dopamine receptor activation, which diffuses into MSN dendrites and

reduces their excitability (Fino and Venance, 2011). Strangely, there have been no studies that have matched electrophysiological analysis with post-hoc identification of calretinin-expressing striatal interneurons, leaving their role in striatal function somewhat elusive.

Notably, most research on striatal interneurons has been done in rodents, and from numbers alone it is clear that they have substantial differences to primate striatal interneurons. In particular, interneurons make up 23% of primate striatal neurons, and only 5% in rodents. Furthermore, in the rat striatum, PV interneurons are the most abundant, with about the same numbers of CR and SST-expressing cells (PV:CR:SST, 4:3:3), while in primates there are more than double the proportion of CR interneurons over PV or SST (Wu and Parent, 2000). This shows how more research into human and primate striatal interneurons is necessary to better understand their physiological function.

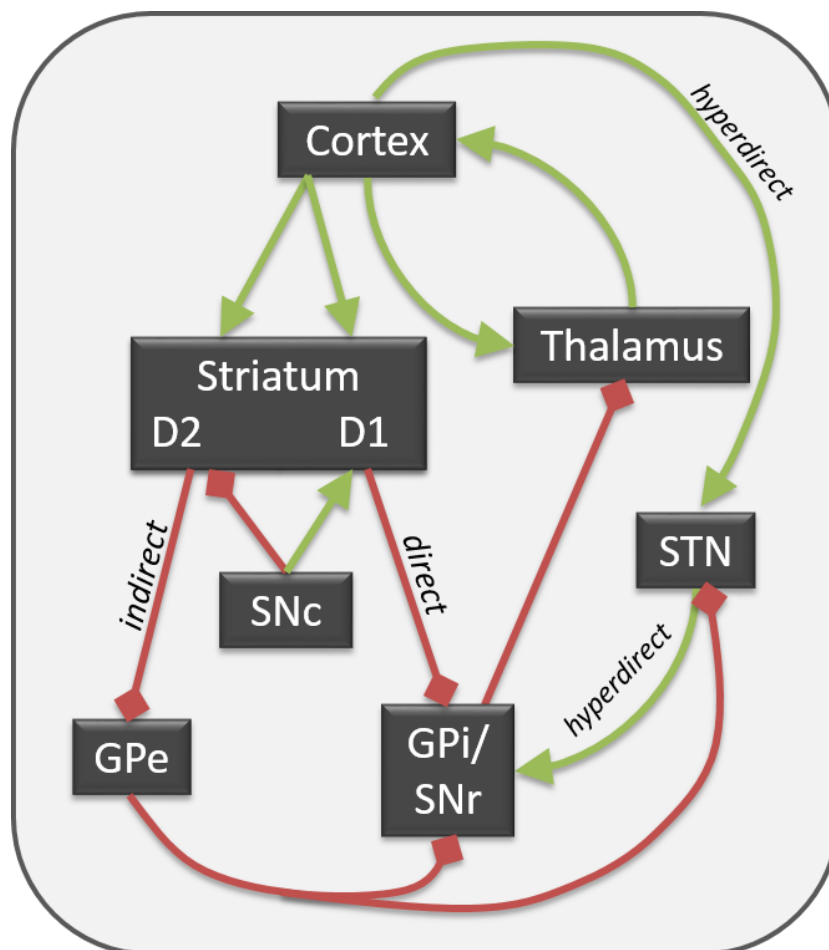


**Figure 1.1: Schematic diagram of classical direct/indirect pathway model of basal ganglia organisation and function.**

Cortical input to the striatum activates the GABAergic direct and indirect pathways, which are modulated by dopaminergic innervation from the SNc. At rest, the GPi and SNr tonically inhibit the thalamus. Upon cortical and SNc activation, the direct pathway inhibits the GPi causing disinhibition of the thalamus. Meanwhile the indirect pathway is inhibited by SNc input to cause further inhibition of the GPi. The hyperdirect pathway proposed by Nambu et al. (2002) is an excitatory projection from the cortex via the STN that stimulates the output nuclei to exert inhibition on the thalamus. D1/D2 = dopamine receptors; SNc/r = substantia nigra pars compacta/reticulata; GPe/i = globus pallidus externa/interna; STN = subthalamic nucleus.

### 1.1.2 Huntington's disease

Huntington's disease (HD) is a progressive neurodegenerative disorder caused by an inherited cytosine-adenine-guanine (CAG) repeat in the *Huntingtin (HTT)* gene. This autosomal dominant mutation produces a poly-glutamine stretch in the HTT protein giving it gain-of-function that is particularly toxic to neurons (MacDonald *et al.*, 1993). Despite its ubiquitous expression, striatal MSNs are by far the most susceptible to the excitotoxicity caused by HTT, but the mechanism behind this is unclear. Although cortical grey matter volume is reduced by around 23%, the caudate and putamen show the largest reduction in volume, between 46 and 62% (Monte, Vonsattel and Richardson, 1988; Halliday *et al.*, 1998). This was found to be relatively specific to MSNs, while striatal interneurons were thought to be largely spared. Indeed, MSNs in the rat striatum were found to express endogenous Htt at much higher levels than any of the interneuron subtypes (Kosinski *et al.*, 1997). The different MSN populations were found to be differentially affected in human patients, particularly in the early stages of HD, in which the abundance of indirect pathway enkephalin-positive fibres was reduced to 34% of those in control brains, while substance P-positive fibres of the direct pathway were only reduced to 71% (Deng *et al.*, 2004). At the latest stage of HD however, both populations were reduced to less than 10% of controls. The early loss of indirect pathway MSNs is believed to cause the involuntary movements associated with chorea, one of the most prominent motor symptoms of HD (Starr *et al.*, 2008). Later loss of the direct pathway MSNs results in bradykinesia and rigidity. Before onset of motor symptoms, psychiatric and cognitive deficits can go unnoticed for years before diagnosis, and manifest as increased irritability and impaired executive functions such as planning and organisation (Ross and Tabrizi, 2011). These impairments are also caused by striatal degeneration and its usual rich innervation of the prefrontal cortex and limbic system.

Due to the established vulnerability of MSNs, striatal interneurons are often dismissed when discussing HD pathogenesis as "selectively spared" (Ross and Tabrizi, 2011). However, in rodent models, PV interneurons were shown to contain Htt-positive intranuclear inclusions in the R6/2 HD transgenic mouse model and a reduction in phosphorylated CREB in quinolinic acid-lesioned rats (Kosinski *et al.*, 1999; Giampà *et al.*, 2006). Reiner *et al.* compared healthy brains with the brains of HD patients spanning all 4 symptomatic grades as defined by Vonsattel *et al.* (Vonsattel *et al.*, 1985; Reiner *et al.*, 2013). At grade 1 there is little atrophy but moderate astrocytosis and loss of 50% of striatal neurons; by grade 4, more than 95% of neurons are lost causing massive striatal atrophy and enlargement of the lateral ventricles, as well as marked atrophy of the globus pallidus (Vonsattel *et al.*, 1985). Reiner *et al.* showed that PV interneurons are significantly reduced in the rostral caudate at grade 1, and all over the striatum by more than 80% at the latest stages of the disease, which is unsurprising considering the 95% neuronal loss characterised at grade 4 (Reiner *et al.*, 2013). The PV

interneuron loss is thought to have a profound impact on the types of motor symptoms experienced around grade 3, which typically sees a transition from chorea to dystonia. Other striatal interneurons have been confirmed several times to resist degeneration in HD, although the large cholinergic calretinin-expressing interneurons have been shown to downregulate ChAT and calretinin expression rather than degenerate, which is still likely to impact their function (Massouh *et al.*, 2008). Going forward, it will be important to consider all striatal cell types when conducting research into HD pathophysiology.

There are currently no disease modifying drugs available for HD, and all treatment is aimed at relieving the myriad of symptoms. Motor symptoms such as chorea, myoclonus, dystonia and rigidity can be treated with anticonvulsants, levodopa, benzodiazepines and muscle relaxants, but these drugs have their own debilitating side effects such as depression, sedation or causing an opposite motor symptom. Neuroleptics and anti-depressants are often used to treat the psychosis, depression and anxiety, causing a whole host of sympathetic nervous system-related side effects (Ross and Tabrizi, 2011). However, symptomatic treatment of HD does not provide any increase to lifespan compared to patients in parts of the world where medical treatment is unavailable (Walker, 2007). The full penetrance and hereditary nature of the disease means that preventative measures would be relatively easy to administer in future generations, but more needs to be known about the mechanisms by which mutant HTT causes HD for this to become a reality. Because currently diagnosis usually occurs once striatal degeneration is already well under way, novel therapies must also aim to repair the lost striatal circuitry, or at least cease any further damage.

#### 1.1.2.1 Disease mechanisms

The Huntingtin protein is expressed in all mammalian cells, but despite the discovery of the *HTT* gene more than 20 years ago, its physiological function remains relatively unknown (MacDonald *et al.*, 1993). It is a largely cytoplasmic protein that occasionally translocates to the nucleus, it has a role in vesicular transport and gene transcription, and may also regulate trafficking of RNA (Ross and Tabrizi, 2011). Homozygous *Htt* deletion is embryonically lethal in animals, whereas heterozygous knockouts develop normally (Nasir, Floresco and O'Kusky, 1995). This opposes the view that HD could be caused by *HTT* loss-of-function in one allele, and supports the growing consensus that HTT gain-of-function is toxic to cells. Furthermore, it has been shown that the number of CAG repeats, and therefore the polyglutamine length, is inversely associated with the age of HD onset (Andrew *et al.*, 1993). Polyglutamine aggregates are formed *in vitro* when there are more than 36 consecutive glutamine residues on a protein, which lines up with the finding that HD only manifests itself in people with 36 or more CAG repeats (Walker, 2007). The mechanisms by which mutant HTT causes HD are many and diverse, from truncated toxic N-terminal fragments and abnormal aggregate formation, to changes in



gene transcription and impaired cell metabolism (see Ross and Tabrizi (2011) for review of mechanisms).

These varied pathways result in selective early degeneration of striatal MSNs, thought to be mediated by their susceptibility to excitotoxicity from cortical and thalamic innervation and their rich expression of glutamate receptors. Specifically, one proposed mechanism of HD is that reduced glutamate uptake by astrocytes leads to increased glutamate at corticostriatal synapses, causing overstimulation of NMDA receptors and excessive calcium ion influx (**Figure 1.2**) (Ross and Tabrizi, 2011; Schwarcz *et al.*, 2011). *Brain-derived neurotrophic factor (BDNF)* is one gene of interest whose expression is reduced in HD patients. MSNs and PV interneurons are particularly dependent on BDNF, released from corticostriatal neurons, for neurotrophic support and maintenance of GABAergic synapses (Ghiglieri *et al.*, 2012). Another gene whose transcription is altered in HD is *NF- $\kappa$ B*, which regulates the expression of many pro-inflammatory cytokines, causing microglia to become activated and the presence of more reactive oxygen species, increasing levels of oxidative stress and perpetuating the excitotoxicity in MSNs (Ross and Tabrizi, 2011). Inflammation is likely to have a far more important role in striatal degeneration than previously thought. The striatum is the only region in HD that undergoes reactive astrocytosis, giving an indication as to why the striatum might be the most affected (Vonsattel and DiFiglia, 1998). Furthermore, innate immune activation was detected in subjects carrying the HD mutation 16 years prior to predicted onset of clinical symptoms, heavily implicating cell-autonomous immune activation as a mechanism for causing striatal degeneration (Björkqvist *et al.*, 2008).

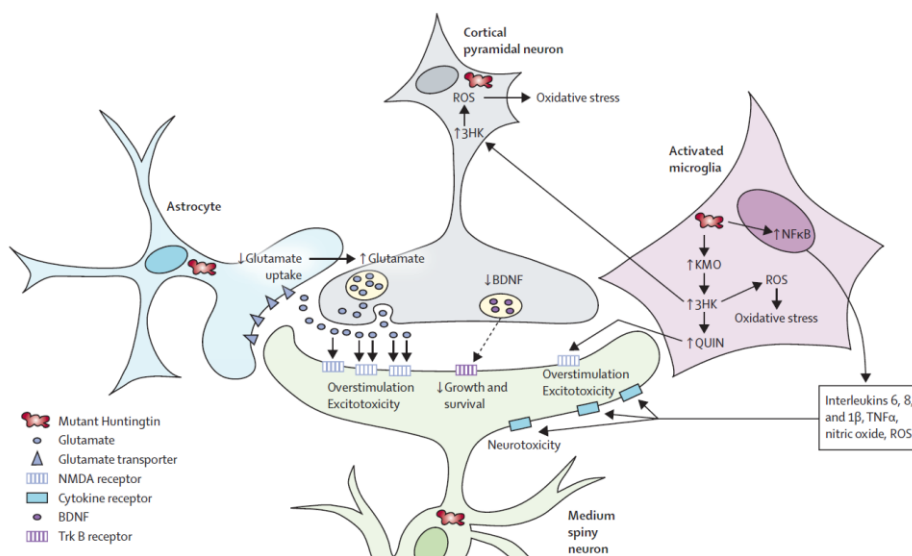


**Figure 1.2: Potential intracellular mechanisms of HTT-induced pathology in HD.**

Mutant HTT causes reduced BDNF release from cortical projection neurons. Glutamate uptake by astrocytes is impaired and activated microglia release quinolinic acid, causing increased NMDA receptor activation on MSNs and excitotoxicity. 3HK=3-hydroxykynurenine. QUIN=quinolinic acid. KMO=kynurenine 3-monoxygenase. ROS=reactive oxygen species. Trk B=tyrosine kinase B receptor. NMDA=N-methyl-D-aspartic acid. From Ross and Tabrizi (2011).

### 1.1.2.2 Animal models

HD is a strictly human disease, so any attempts to model the disorder *in vivo* must be induced in the animals, mostly rodents, and this has been done either genetically or by lesioning the striatum with an excitotoxin. There are many different transgenic mouse models with broadly three types of mutation (Ferrante, 2009). First, those that express the N-terminus of the human *HTT* gene containing the CAG repeats, for example the R6/2 mouse, which is one of the most widely used and displays progressive neurodegeneration and behavioural impairment that resembles HD, with a shortened lifespan of 14 to 21 weeks. Second, mice that have extra CAG repeats inserted into their own *Htt* gene, which may in theory be more genetically accurate but in reality produces a much subtler phenotype. The *HdhQ111* mouse has a normal lifespan, but does encounter MSN-specific neuropathology and late-onset motor deficits. Thirdly, yeast or bacterial artificial chromosomes (YAC/BAC) have been employed to express the full-length human mutant *HTT* in mice, and show behavioural and cognitive deficits similar to HD patients, as well as striatal degeneration. Transgenic mouse models have been invaluable in researching the cellular mechanisms of HD and investigating potential therapeutic mechanisms.

Excitotoxic lesion models aim to recreate MSN-specific degeneration by injecting an excitotoxin directly into the striatum, to which MSNs are more vulnerable than other neurons or glial cells. By far the most commonly used excitotoxin for this approach is quinolinic acid (QA), a NMDA receptor agonist. QA is an endogenous metabolite in the kynurene pathway, which has been shown to be over-activated in the microglia of 3 different transgenic mouse models and early grade (0/1) HD patients, when there is marked neuronal loss but little macroscopic change to the striatum (**Figure 1.2**) (Guidetti *et al.*, 2004, 2006). QA injected intrastrially had previously been shown to specifically target MSNs, sparing large cholinergic interneurons, glia and afferent axons from the cortex and thalamus (Roberts *et al.*, 1993). However, there has been much conflicting evidence on whether the GABAergic interneurons are spared or also killed by QA. SST interneurons were severely depleted in many studies, but this effect differed greatly depending on the type of analysis conducted and the age of the rats receiving the injection (Roberts *et al.*, 1993; Figueredo-Cardenas, Chen and Reiner, 1997). PV interneurons have been less widely analysed, but were reduced comparatively to MSNs in one study and selectively spared with cholinergic interneurons in another (Figueredo-Cardenas *et al.*, 1998; Liang *et al.*, 2005). The massive neuronal loss caused by QA in rodents provides a robust model of the later stages of HD, displaying severe motor and cognitive impairments, allowing the testing of reparative therapeutic strategies to replace lost striatal neurons or to protect those that do survive the insult. Furthermore, excitotoxin-induced lesions delivered the only non-human primate HD models until

recent advances in genetic primate models, providing a more human-related model on which to test new therapies before going into clinical trials (Ghiglieri *et al.*, 2012).

#### 1.1.2.3 Cell replacement therapy

Brain repair by cell replacement therapy has long been a suggested therapeutic strategy, stemming from the use of foetal ventral midbrain tissue to replace lost nigral dopaminergic cells in Parkinson's disease (PD) (Björklund and Stenevi, 1979; Björklund *et al.*, 2003). The success of *in vivo* studies in this area prompted the suggestion that the same could be applied to HD by isolating whole ganglionic eminence (WGE), the developmental birthplace of striatal neurons, from fetuses and transplanting it into the striatum of lesioned animal models or human patients. This was understood to be a bigger challenge than PD due to the complex circuitry to which the striatal MSNs belong as well as the comparatively long distances travelled by MSN axons (Peschanski, Cesaro and Hantraye, 1995). Initial studies grafting rat foetal WGE into excitotoxin-lesioned rat striatum gave promising histological results, showing formation of MSN-rich P-zones that expressed typical mature striatal molecular markers (Graybiel, Liu and Dunnett, 1989). There was also good evidence showing formation of afferent connections from the relevant host cortical and subcortical regions, as well as efferent connections from the graft to the globus pallidus (Wictorin *et al.*, 1988, 1989; Wictorin and Björklund, 1989). Behavioural studies using sensitive motor testing have shown that allografts can restore motor impairment in the lesioned rats (Döbrössy and Dunnett, 2005; Klein, Lane and Dunnett, 2012). Importantly, *ex vivo* brain slice recordings from grafted cells have demonstrated functional integration of the cells through long term potentiation and depression from corpus callosum stimulation (Mazzocchi-Jones, Döbrössy and Dunnett, 2009, 2011). This supports the idea that grafts are not just producing neurotrophic factors aiding the remaining host neurons, but are in fact restoring striatal circuitry. Xenografting of human foetal tissue into rodent HD models has been vital for the progression of the technique towards clinical trials. However, human tissue grafts appear to take as long to mature as in normal development, perhaps explaining the reduced P zone formation and limited behavioural recovery when compared with rat WGE grafts (Grasbon-Frodl *et al.*, 1996; Pundt *et al.*, 1996; Sanberg *et al.*, 1997; Lelos *et al.*, 2015). The most promising results have come from allografting studies of non-human primate WGE into excitotoxin-lesioned monkeys, causing recovery of skilled motor function up to 7 months post-transplantation (Kendall, Rayment and Torres, 1998; Palfi *et al.*, 1998).

On the basis of the successful allografting studies in rodents and non-human primates, clinical trials transplanting human WGE into HD patients was approved in several centres around the world (Kopyov *et al.*, 1998; Bachoud-Lévi *et al.*, 2000; Rosser *et al.*, 2002). The principal aim of these trials was the safety and tolerability of intrastriatal transplantation with foetal WGE tissue. While there were small improvements in motor and cognitive symptoms in 3 of 5 patients until 2 years post-transplantation

in the French trial, this effect had disappeared by 4-6 years (Bachoud-Lévi *et al.*, 2006). The NEST-UK trial followed up 3-10 years post-transplantation and similarly showed no significant differences on any measure between patient groups (Barker *et al.*, 2013). However, there were no foetal tissue graft-related adverse events in these studies, and the number of cells transplanted was considered quite small for any functional improvement to occur. Post-mortem analyses of 6 and 18 month old grafts has confirmed the presence of DARPP32-positive neurons as well as SST and CR interneurons, TH fibre innervation and lack of mutant HTT in grafted cells (Freeman *et al.*, 2000; Capetian *et al.*, 2009). Around 10 years after transplantation, post mortem grafts still showed the presence of P-zones with MSNs and interneurons, but there was also evidence of MSN-specific degeneration and fewer blood vessels throughout the graft area than the surrounding host tissue (Cicchetti *et al.*, 2009; Cisbani *et al.*, 2013). Overall, the clinical trials have demonstrated the safety of the procedure, and opened up the possibility to transplant more tissue in following trials, possibly subject to further optimisation of the graft composition (Barker *et al.*, 2013). On the point of graft composition, the vast majority of preclinical studies have been done using WGE tissue. A handful of studies have either used only lateral GE (LGE) or compared it with medial GE grafts (MGE; striatal MSN or interneuron birthplaces respectively). While one study suggested that the greater the number of DARPP32-positive cells the better the functional recovery, others found that the presence of MGE tissue in the WGE grafts gave better overall survival as well as added functional benefits (Nakao *et al.*, 1996; Grasbon-Frodl *et al.*, 1997; Watts, Brasted and Dunnett, 2000).

The high quantity of tissue needed per graft in HD patients (5 WGEs per transplanted hemisphere), the very limited supply of viable foetal tissue from abortions and the lack of quality control possible on the tissue, all mean that it is not a feasible source of tissue for widespread treatment of HD. Therefore, clinical trials and *in vivo* studies using foetal tissue must act as a proof-of-principle, while another source of tissue is found. Recent advances in human pluripotent stem cell (hPSC) differentiation have made them a strong contender to replace foetal tissue. It is now possible to direct their differentiation towards a MSN fate, both *in vitro* and after transplantation into HD models (Aubry *et al.*, 2008; Ma *et al.*, 2012; Carri *et al.*, 2013; Nicoleau *et al.*, 2013; Arber *et al.*, 2015). However, if WGE is the gold standard against which to compare, hPSC-derived grafts will likely require interneurons and perhaps glial cells in addition to MSNs to produce a functional graft.

#### 1.1.2.4 Novel therapeutic strategies

It has been 23 years since the mutant *HTT* gene was discovered to cause HD, but despite this, disease-modifying drug targets have been slow to emerge. Novel drug targets include lowering HTT levels in cells by RNA interference, antisense oligonucleotides or zinc finger proteins to lower mutant *HTT* transcript levels (Harper *et al.*, 2005; Garriga-Canut *et al.*, 2012; Kordasiewicz *et al.*, 2012). Reduction

in mutant HTT has led to improvements in behavioural impairments but mostly when given early in the modelled disease. However, delivery of these potential therapies would need to be frequent and direct into the brain as they are unable to cross the blood brain barrier, creating a technical challenge that requires novel delivery methods. A pharmacological approach to this idea is inhibition of sirT1, a sirtuin deacetylase whose inhibition has been demonstrated to cause a selective decrease in mutant HTT. A clinical trial testing the effects of Selisistat, a SirT1 inhibitor, in HD patients has confirmed that it is safe and well tolerated (Süssmuth *et al.*, 2015). Despite showing no signs of clinical benefit or effects on mutant HTT blood levels, biological samples were collected with the aim of developing SirT1-specific assays that will aid future trials.

BDNF or other neurotrophic factor administration targeting the brain is an avenue that has shown promise *in vivo*. These are administered by gene therapy or synthetic polymer implants into the striatum, promoting survival of the remaining striatal neurons (Géral, Angelova and Lesieur, 2013). Of relevance to **Chapter 3** is that administration of intrastriatal Activin A significantly reduced neuronal loss following QA lesion in rats, demonstrating neurotrophic effects on striatal neurons (Hughes *et al.*, 1999). A phase I clinical trial tested implantation of a device containing BHK cells (baby hamster kidney) programmed to release ciliary neurotrophic factor (CNTF) in the striatum of HD patients (Bloch *et al.*, 2004). Although no clinical benefit was seen over the 2 years, the technique was deemed safe and feasible, and did show improved electrophysiological measurements in half the patients. Another delivery method is transplantation of genetically engineered mesenchymal stem cells to secrete BDNF that is being proposed for a Phase I clinical trial following their demonstration of safety and tolerability in trials for other diseases (Deng *et al.*, 2016). Pharmacological increase in BDNF levels may be achieved using fingolimod, an approved therapy for multiple sclerosis that has a number of effects including immune modulation, MAP kinase activation, increased BDNF production and reduced NMDA-mediated excitotoxicity. Fingolimod has been shown to improve motor function and reduce brain atrophy in the R6/2 mouse model, promising findings suggesting it could be clinically beneficial in HD patients (Di Pardo *et al.*, 2014).

Deep brain stimulation (DBS) is a surgical approach based on the findings that pallidotomy could be beneficial for dystonia and chorea in HD. Long term follow up of patients with GPi DBS showed significant improvement of chorea in all patients but had no effect on bradykinesia or dystonia (Gonzalez *et al.*, 2014). It will be important to measure quality of life outcomes in these studies in order to evaluate the long term benefits of such therapies.

Overall, cell replacement therapy is by far the most thoroughly researched potential therapy for HD and does hold promise for reversing the impact of striatal degeneration. However, more easily

administered pharmacological approaches that can inhibit the toxic actions of mutant HTT earlier in the disease would be the ideal early intervention.

## 1.2 Striatal development

### 1.2.1 Neural induction

Gastrulation of the embryo leads to the formation of the three germ layers – ectoderm, mesoderm and endoderm. The innermost layer, the endoderm, forms the respiratory and gastrointestinal tracts. The mesoderm is the middle layer and becomes tissues such as muscle and cartilage. Finally, the outer layer, the ectoderm, gives rise to the hair, skin, sweat glands and nervous system. A dorsal part of the mesoderm forms Spemann's Organiser region, first discovered in 1924 by Spemann and Mangold. They transplanted what is now known as the Organiser region from a *Xenopus* embryo onto the ventral side of another embryo, causing the formation of 2 separate neural axes, demonstrating that this region alone is enough to trigger neural induction (Spemann and Mangold, 1924). Later, the key morphogens that were discovered to be released from the Organiser were identified as noggin, chordin and follistatin, which act by inhibiting BMP and TGF $\beta$  signalling that induce endoderm and mesoderm in the adjacent tissues (Smith and Harland, 1992; Hemmati-Brivanlou, Kelly and Melton, 1994; Sasai *et al.*, 1994; Zimmerman, De Jesús-Escobar and Harland, 1996; Bachiller *et al.*, 2000). The equivalent structure in mouse was termed the "node", but was found to only induce posterior structures and lacked the anterior forebrain. In mammals, the anterior visceral endoderm (AVE) is also required for telencephalon formation (Tam and Steiner, 1999; Andoniadou and Martinez-Barbera, 2013). Over time, the central notochord arises from the cells of the Organiser as the embryo elongates along the rostro-caudal axis, and the neural plate overlying the notochord folds inwards to create the neural tube in a process called neurulation. Depending on the dorso-ventral and rostro-caudal location along the neural tube, cells release and are exposed to different levels and types of morphogens, which play a key role in instructing cell fate (Bronner-Fraser and Fraser, 1997).

The notochord releases a morphogen called Sonic hedgehog (SHH), exposing cells all along the ventral neural tube to high concentrations of this protein (Rubenstein *et al.*, 1998). The caudal part of the neural tube forms the spinal cord, while more rostrally the hindbrain, midbrain and forebrain form distinct swellings in the neural tube. The forebrain is largely patterned by the anterior neural ridge (ANR), a patterning centre at the most rostral end of the neural plate that releases fibroblast growth factor 8 (FGF8) and Wnt inhibitor Dickkopf1 (DKK1) (Backman *et al.*, 2005). Some of the relevant signalling pathways and morphogens involved specifically in forebrain development are described in the following sections.

## 1.2.2 Key morphogens and signalling pathways in forebrain development

### 1.2.2.1 *Sonic hedgehog (SHH) signalling*

*Shh* was discovered in mouse as one of three genes related to the *Drosophila* hedgehog gene, an important patterning factor in its development. *Shh* was found to be expressed in late stages of gastrulation, strictly in the midline, then extends along the entire notochord and head process. Its expression is then induced in the developing CNS, further than the rostral limit of the head process, where it spreads into the ventral forebrain and ventrolaterally in the midbrain. Expression is maintained in both the notochord and the floorplate midline along the hindbrain and spinal cord (Echelard *et al.*, 1993). As indicated by its strict spatial expression profile, SHH signalling is heavily involved in dorso-ventral patterning of the neural tube, creating a morphogen gradient that patterns cells by concentration.

Following release from ventral midline cells along the neural tube, SHH binds to the membrane receptor Patched (Ptc). In the absence of SHH, Ptc represses the G-protein coupled receptor (GPCR) Smoothed (Smo) while Gli(1-3) transcription factors are retained in a cytoplasmic pool. When SHH binds Ptc, the receptor is internalised and Smo is able to initiate an intracellular signalling cascade involving Gli proteins, which target Ptc and Gli genes in a feedback loop (Hooper and Scott, 2005; Traiffort, Angot and Ruat, 2010). Gli1 expression is consistently associated with SHH pathway activation and acts only as a transcriptional activator, therefore its ectopic expression mimics SHH expression (Hynes *et al.*, 1997; Lee *et al.*, 1997). Gli2 has a similar activating role to Gli1 but to a lesser extent (Ruiz I Altaba, 1998). In contrast, Gli3 appears to be downregulated by SHH signalling, and has a high propensity to form a protein kinase A (PKA)-dependent cleaved repressor version of itself (Gli3R) that forms an inverse gradient with SHH and represses its target genes (**Figure 1.3**) (Wang, Fallon and Beachy, 2000; Rallu *et al.*, 2002). Indeed, in *Shh* knockout mouse embryonic telencephalon, dorsal markers spread to much of the ventral region, which loses its usual structure. In Gli3 knockouts the opposite is true – ventral markers are expressed in the dorsal regions, although some dorsal markers are still expressed. In mice lacking both *Shh* and one copy of Gli3, the dorso-ventral molecular profile is largely restored, with clear dorsal and ventral regions demarcated by their usual transcription factor expression profiles (Rallu *et al.*, 2002).

In this thesis, alongside recombinant SHH itself, Purmorphamine, a small molecule SHH agonist, is used that has been shown to activate SHH signalling by direct Smo activation (Sinha and Chen, 2006). The chemical inhibitor of SHH signalling used here, Cyclopamine, also binds Smo directly but suppresses its activity (Chen *et al.*, 2002).

### 1.2.2.2 *Wnt signalling*

Wnt signalling is crucial for telencephalic patterning. Initial antagonism of Wnt by DKK1 is key for inhibiting posterior patterning and establishing the telencephalon (Yamaguchi, 2001). Several Wnt genes are then expressed in the dorsal midline of the telencephalon where they regulate proliferation and specification of the developing cortex (Lee *et al.*, 2000). Specifically, Wnt3a has been shown to induce dorsal markers such as Pax6, Ngn2 and Emx1 while suppressing the ventral marker NKX2.1 (Gunhaga *et al.*, 2003).

Wnts are secreted glycoproteins and their signalling involves three main intracellular pathways: the canonical Wnt pathway, the Wnt/calcium ion pathway and the planar cell polarity pathway (Huelsken and Behrens, 2002). The canonical Wnt pathway has been shown to be active in the dorsal pallium and not at all in the subpallium, and indeed is required to suppress ventral cell fates in telencephalic development (Backman *et al.*, 2005). Wnts bind to Frizzled (Frz) transmembrane putative GPCRs along with LRP co-receptors that are crucial for canonical signalling. In the absence of Wnt,  $\beta$ -catenin is phosphorylated and bound to a destruction complex including glycogen synthase kinase 3  $\beta$  (GSK3 $\beta$ ), axin and adenomatous polyposis coli (APC). This causes its ubiquitylation and degradation by the proteasome. When Wnts bind Frz, dishevelled (Dsh) prevents  $\beta$ -catenin degradation by removing GSK3 $\beta$  from the destruction complex. This allows  $\beta$ -catenin to enter the nucleus and interact with various transcription factors that upregulate Wnt target genes. The Wnt/Ca<sup>2+</sup> pathway involves G-protein activation of phospholipase C and protein kinase C (PKC), which leads to increased intracellular Ca<sup>2+</sup> and calcineurin activation. Calcineurin dephosphorylates NF-AT, which suppresses canonical Wnt signalling in the nucleus. Finally, the planar cell polarity pathway recruits JNK and Rho-associated kinase (ROCK) for regulation of cytoskeletal organisation and polarity of cells (Huelsken and Behrens, 2002).

DKK1 blocks Wnt activity by inhibiting its binding to co-receptor LRP6 (Semenov *et al.*, 2001). In this thesis, selective inhibition of canonical Wnt signalling is achieved using the small molecule XAV939, which is a tankyrase inhibitor, preventing the degradation of axin, thereby promoting persistence of the destruction complex and degradation of  $\beta$ -catenin (Huang *et al.*, 2009).

### 1.2.2.3 *Transforming growth factor (TGF)- $\beta$ family signalling*

The TGF $\beta$  superfamily of ligands is large and diverse, including two broad subfamilies according to their sequence similarity and binding receptors. The first subfamily includes TGF $\beta$ s, Activins, and Nodal, and the second subfamily comprises bone morphogenetic proteins (BMPs), growth and differentiation factors (GDFs) and Mullerian inhibiting substance (MIS) (Shi and Massagué, 2003).



Between them, the superfamily of ligands have roles in regulation of cell proliferation, identification, differentiation and death, throughout embryogenesis as well as adulthood.

The TGF $\beta$  ligands signal by binding to type I and II transmembrane receptor serine/threonine kinases, which phosphorylate intracellular receptor-regulated Smad proteins (R-Smad: 1/2/3/5/8). The R-Smad then forms a heteromeric complex with the Co-Smad, Smad4, and translocates to the nucleus where the complex interacts with other factors to alter gene transcription. Inhibitory Smads (I-Smad: 6/7) block TGF $\beta$  signalling by competing with R-Smads for receptor or Co-Smad binding (Massagué, 1998). TGF $\beta$  family ligands and receptors are summarised in **Table 1.1**. The TGF $\beta$ /Activin/Nodal subfamily ligands bind first to the type II receptor followed by recruitment of the type I receptor, typically ALK4/5/7, which phosphorylate Smad2/3 (Massague 1998 or Hart 2002). The BMP subfamily have higher affinity for the type I receptors (ALK2/3/6) so form first a complex with type I then type II receptors, leading to Smad1/5/8 phosphorylation (Kirsch 2000).

There are many endogenous inhibitors of TGF $\beta$  family signalling, including noggin, chordin and cerberus, which inhibit BMPs by binding to its receptor binding sites, and follistatin, which does the same to Activins and BMPs (Shi and Massagué, 2003). The neural induction role of noggin, chordin and follistatin can be mimicked *in vitro* using small molecules LDN193189, dorsomorphin and SB431542, which are used throughout this thesis (Chambers *et al.*, 2009; Boergermann *et al.*, 2010).

BMPs are the largest subfamily of TGF $\beta$  ligands and play an important role in dorso-ventral patterning of the telencephalon. They are expressed and secreted at the dorsal midline of the telencephalon, in regions corresponding to the future hippocampus and choroid plexus (Furuta, Piston and Hogan, 1997). BMP-soaked beads reduced *Shh* expression by up to 96% in telencephalic explants, demonstrating that dorsalisation of chordin and noggin double mutants is due to an increase in BMP signalling (Anderson *et al.*, 2002). This study also highlighted a role for noggin and chordin lasting beyond initial neural induction (Bachiller *et al.*, 2000; Anderson *et al.*, 2002).

Activins (A/B/AB) have a less obvious role in forebrain development that requires some further research. Activin subunits and ActR-IIB were found to be expressed in the telencephalon of E12.5 mouse embryos (Feijen, Goumans and van den Eijnden-van Raaij, 1994). Phosphorylated Smad2 was also found to co-localise with subpallial marker DLX2, and a direct upregulatory interaction was demonstrated using chromatin immunoprecipitation (ChIP) (Maira *et al.*, 2010). These findings laid the foundation for the discovery in our lab that Activin A induces subpallial progenitor identity in hPSC-derived forebrain progenitors, which will be described further in later sections (Cambray *et al.*, 2012; Arber *et al.*, 2015).

Ligands	Type I Rs	Type II Rs	Smads
<b>TGFβ</b>	ALK5 (TβR-I)	TβR-II	Smad2/3
<b>Activin</b>	ALK4	ActR-IIB	Smad2/3
<b>Nodal</b>	ALK4/7	ActR-IIB	Smad2/3
<b>BMPs</b>	ALK2/3/6	BMPR-II/B	Smad1/5/8

**Table 1.1: Summary of TGFβ superfamily of ligands, their Type I and II receptors (Rs) and associated Smads.**

### 1.2.3 Forebrain development

After neurulation, morphogen gradients act antagonistically to pattern the forebrain into distinct regions of the dorsal pallium and the ventral subpallium, which form the cortex and ganglionic eminences respectively. The LGE gives rise primarily to striatal MSNs and olfactory bulb interneurons. Cortical and striatal interneurons, as well as globus pallidus projection neurons and basal forebrain cholinergic neurons, are born in the MGE (**Figure 1.3**). The caudal ganglionic eminence (CGE) is thought to produce most calretinin interneurons of the striatum and cortex (Pauly *et al.*, 2013; Pilz *et al.*, 2013).

Division of the forebrain is coincident with the induction of specific transcription factors (**Figure 1.3**). Pallial expression of PAX6 and subpallial expression of GSX2 and DLX1/2 define the pallial-subpallial boundary between the dorsal LGE and developing cortex. Although PAX6 expression is much higher in the pallium, it is still present in the human LGE. Other transcription factors such as GSX2, DLX1/2, ASCL1 (aka MASH1) and OLIG2 are expressed across the whole GE ventricular and subventricular zones (VZ/SVZ) (Hansen *et al.*, 2013; Pauly *et al.*, 2013; Onorati *et al.*, 2014). Shh initiates and maintains ventral expression of Nkx2.1 in the MGE, which gives rise to cortical and striatal interneurons (Gulacsi and Anderson, 2006). In the mouse striatum, Nkx2.1 is restricted to MGE-derived interneurons, and the same has been widely assumed and demonstrated in human foetal brain sections (Marin, Anderson and Rubenstein, 2000; Nóbrega-Pereira *et al.*, 2008; Hansen *et al.*, 2013; Pauly *et al.*, 2013; Wang *et al.*, 2014). Nonetheless, Onorati *et al.* recently showed that NKX2.1 mRNA and protein is present in the 10-11 weeks-post-fertilisation human LGE, albeit at far lower levels than in the MGE. They reported that 74% of striatal cells at this stage were NKX2.1-positive with 96% co-expressing CTIP2 (aka BCL11B), a MSN marker. By 20 weeks, only 6% of cells in the human foetal striatum expressed NKX2.1 (Onorati *et al.*, 2014). It is possible that the low level of NKX2.1 coupled with the short time window of expression in the developing striatum have led to the assertion that it is never expressed in developing human MSNs.

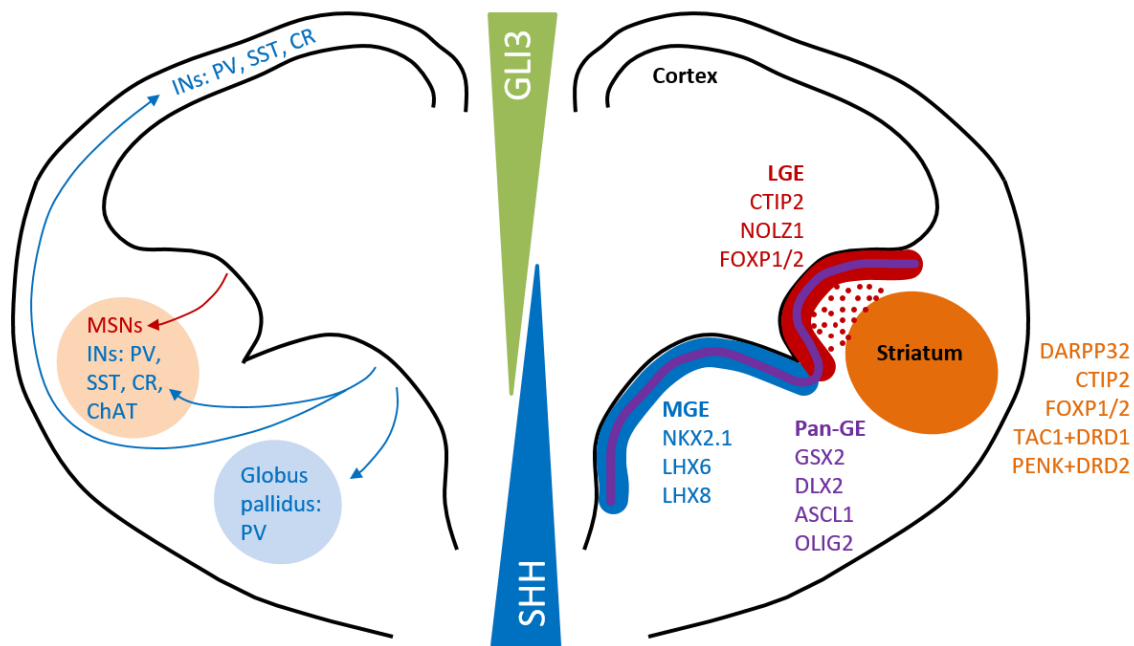


**Figure 1.3: Schematic diagram of a coronal section through the developing telencephalon.**

Cells are patterned by ventral SHH and dorsal Gli3R, which antagonise one another. Cells born in the MGE migrate to the globus pallidus, striatum and cortex, and express different subtype markers, while LGE-born MSNs populate the adjacent striatum (left). The LGE (red) and MGE (blue) have distinct expression patterns of molecular markers, but also share expression of pan-GE transcription factors (purple). LGE progenitors mature into striatal MSNs with their own combination of markers (orange; right). INs = interneurons.

#### 1.2.4 Development of the striatum

GSX2 is heavily involved in the maintenance of LGE progenitor fate specification by repressing PAX6 expression, allowing the expression of key ventral transcription factors. In *Gsx2* knockout mice, there is a delay and reduction in the level of *Dlx2* and *Ascl1* expression in the LGE, leading to a significant reduction in striatal volume, but not a complete abolishment (Szucsik *et al.*, 1997; Toresson, Potter and Campbell, 2000). *Dlx1* and *Dlx2* expression patterns are indistinguishable in the subpallium, and they are vital for the differentiation of the later-born matrix MSNs, which develop abnormally in double homozygous mutants (Anderson *et al.*, 1997). Indeed, *Gsx2* and *Dlx1/2* function upstream of other key transcription factors such as *Helios* and *Nolz1*. *Helios* is expressed at low levels first in mouse LGE progenitors in the SVZ, and then in the developing striatum by new matrix neurons until adolescence, when it co-localises with other MSN markers such as *Ctip2* and *Foxp1*. *Helios* expression was completely abolished in both *Gsx2* and *Dlx1/2* knockout mice, whereas it was unchanged by *Ascl1* mutation (Martín-Ibáñez *et al.*, 2012). *Nolz1* is expressed mostly in SVZ LGE progenitors and appears to have a role in promoting cell cycle exit and neuronal differentiation via *Gsx2*-dependent upregulation of retinoic acid (RA) signalling (Jensen, Björklund and Parmar, 2004; Urbán *et al.*, 2010). RA is released by local glia in the LGE and plays an important role in promoting the GABAergic

phenotype of both striatal MSNs and interneurons (Toresson *et al.*, 1999; Chatzi, Brade and Duester, 2011).

By E14 in the rat and 50 days post fertilisation in the human foetus, juvenile post-mitotic neurons in the mantle zone of the LGE and striatal anlage cease to express GSX2 and DLX2 and are identified instead by the presence of CTIP2, FOXP1 and FOXP2 (Martín-Ibáñez *et al.*, 2012; Pauly *et al.*, 2013). Mature MSNs can be identified by their expression of DARPP32 in combination with the aforementioned transcription factors. Co-expression of these proteins is necessary to reliably identify cells as MSNs, as each of them is individually expressed in cortical cells (Onorati *et al.*, 2014). CTIP2 is a transcription factor that is crucial in the development of the neocortex, hippocampus and olfactory bulb; but within the striatum it is exclusively expressed in MSNs, showing complete co-expression with DARPP32 and FOXP1 (Arlotta *et al.*, 2008; Onorati *et al.*, 2014). *Ctip2* knockout mice appear to have normal birth of MSNs in the LGE followed by migration to the striatum, however at E15.5 they begin to show reduced striatal *Foxp1* expression and disorganised striatal compartments. Specifically, MSNs fail to arrange themselves into striosomes and many MSN markers, particularly those of the direct pathway MSNs found in striosomes, show dramatically reduced expression, including DARPP32. Furthermore, aberrant striosome formation appears to be responsible for abnormal dopaminergic innervation that is usually richest on striosome MSNs (Arlotta *et al.*, 2008). The lack of changes in the LGE progenitor population in *Ctip2* knockout mice shows that it is more likely to play a role in post-mitotic maturation and connectivity of MSNs, as it does in corticospinal motor neurons (Arlotta *et al.*, 2005). Genome-wide ChIP-sequencing of an immortalised mouse striatal cell line over-expressing *Ctip2* further showed a role in BDNF signalling, which is also vital for DARPP32 expression in mouse MSNs (Ivkovic and Ehrlich, 1999; Tang *et al.*, 2011). Most notably, CTIP2 mRNA and protein was found to be significantly decreased in both the R6/1 HD mouse model and human HD patient brains (Desplats, Lambert and Thomas, 2008). Overexpression of *Ctip2* also diminished the toxic effects of mutant HTT on cultured neurons, supporting an important role for CTIP2 in the specific vulnerability of MSNs in HD.

Striatal interneurons born in the MGE and CGE must migrate to the striatum, which happens around E15 in mouse. High *Nkx2.1* expression is the main distinguishing feature of the MGE, and mice lacking *Nkx2.1* develop MGEs that resemble LGE and fail to produce almost any striatal interneurons (Marin, Anderson and Rubenstein, 2000). *Nkx2.1* expression is driven and maintained by *Shh* signalling, which not only arises from the ventro-dorsal *Shh* gradient across the telencephalon, but is also determined by an internal gradient of *Shh* signalling that is higher in the dorsal MGE than in the ventral region (Xu *et al.*, 2010). In this study, mosaic loss of *Shh* signalling by *Smo* knockdown led to *Nkx2.1* downregulation and *Gsx2* upregulation in the cells lacking *Smo*, producing bipolar CR interneurons

reminiscent of those born in the CGE, where *Gsx2* expression is also high. Interestingly, this also caused neighbouring cells expressing *Smo* to upregulate *Shh* pathway genes resulting in a higher number of SST than PV interneurons. This was in agreement with a previous study showing that SST interneurons arise from the dorsal MGE while PV interneurons develop from more ventral progenitor pools (Flames *et al.*, 2007). In addition, the ventral-most region of the MGE appears not to produce any GABAergic interneurons, but instead gives rise to globus pallidus projection neurons and cholinergic neurons of the basal forebrain and striatum (Flandin, Kimura and Rubenstein, 2010).

The mechanism that defines whether MGE-derived interneurons migrate to the striatum or the cortex remains unclear, but the result is that the two populations have distinct responses to migratory cues by expression of specific membrane receptors. Marin *et al.* first demonstrated that expression of semaphorins in the striatum repelled migrating cortical interneurons that expressed neuropilins 1 and 2, and that loss of neuropilin expression led to increased striatal interneurons (Marin *et al.*, 2001). The same group later showed that *Nkx2.1* downregulation in cortical interneurons was the key step in allowing neuropilin expression and repulsion from the striatum (Nóbrega-Pereira *et al.*, 2008). By forcing expression of *Nkx2.1* they were able to increase the number of interneurons in the striatum, while preventing post-mitotic *Nkx2.1* expression led to a reduction in striatal interneurons. This mechanism was further elucidated to show that *Zfhx1b* expression is required downstream of *Dlx1/2* to repress *Nkx2.1* and allow interneuron migration to the cortex (McKinsey *et al.*, 2013). The majority of past research on this subject has been aimed at finding the mechanisms behind interneuron migration to the cortex. A recent study by the Marin group focussed on what causes interneurons to settle in the striatum (Villar-Cerviño *et al.*, 2015). They found that, in a similar way to cortical interneurons, striatal interneurons are both attracted to the striatum through ErbB4/Nrg-1 interactions and simultaneously repelled by the cortex via Eph/ephrin signalling. The EphB expression is therefore likely to be downstream of maintained *Nkx2.1* expression. Also downstream of *Nkx2.1* are *Lhx6* and *Lhx8*, expressed by post-mitotic GABAergic and cholinergic interneurons respectively, in both the cortex and striatum (Marin, Anderson and Rubenstein, 2000; Hansen *et al.*, 2013). These studies highlight the limited knowledge we still have of the processes behind striatal development, and considering the differences between rodent and human striatal cell composition, more studies must be done in human tissue in order to confirm the relevance of these findings.

### 1.3 Human pluripotent stem cells

Human embryonic stem cells (hESCs) are derived from the inner cell mass of a human embryo and have the unique ability to self-renew and maintain their pluripotency in culture, given the correct extrinsic signals (Thomson *et al.*, 1998). A similar type of pluripotent stem cell was discovered by Takahashi *et al.*, whereby they induced pluripotency (iPSCs) in adult human fibroblasts by viral transduction of four key transcription factors: OCT3/4, SOX2, KLF4 and c-Myc (Takahashi *et al.*, 2007). Together, hESCs and iPSCs can be termed human pluripotent stem cells (hPSCs), where pluripotency is defined as both the ability to self-renew and have the potential to differentiate into any cell type in the body. Maintaining cells in the pluripotent state has evolved from requiring feeder layers of mouse embryonic fibroblasts secreting unknown factors, to now widely used fully defined media and matrices on which to grow hPSCs (Ludwig *et al.*, 2006).

Known developmental principles can be applied to hPSCs to pattern them towards a particular cell fate, making them an excellent tool to study unknown developmental pathways as well as to obtain limitless supplies of specific cell types of interest. Human PSC-derived neurons allow access to live human neurons that could only previously be achieved through obtaining human foetal tissue, which cannot be quality-controlled or standardised. The motivation for generating particular cell types comes, inevitably, largely from those affected in disease. For example, there is a strong interest in generating midbrain dopaminergic neurons for cell replacement therapy for PD, and GABAergic interneurons for epilepsy (Kriks *et al.*, 2011; Kirkeby *et al.*, 2012; Maroof *et al.*, 2013; Cunningham *et al.*, 2014). This thesis is focused on producing striatal MSNs and interneurons for cell therapy in Huntington's disease. Nonetheless, the value of hPSCs extends far beyond regenerative medicine to the potential to study the development of live human neurons *in vitro*, as well as compare healthy development and neuronal function with neurons derived from patient iPSCs or hESC lines with targeted gene mutations. This will provide a useful platform for high throughput screening of potential therapies before taking them into animal models.

#### 1.3.1 hPSCs as a model of embryonic development

Pluripotent stem cells are an ideal tool for modelling development and defining the mechanisms of pluripotency and differentiation. A pioneering study demonstrated that inhibition of TGF $\beta$  and BMP signalling lead to neural induction of hESCs in fully defined monolayer conditions, by inhibiting induction of mesoderm or endoderm (Chambers *et al.*, 2009). They provided an easily manipulable tool on which to test different conditions for promoting differentiation of human cells. Over time, it has been confirmed that many of the known signalling events in the developing nervous system can be applied to hESCs to achieve expected gene expression profiles. However, this is generally limited

to broad morphogen gradients across the developing brain. The flexibility of hESCs allows the researcher to make fine adjustments in factor concentration and treatment time windows to optimise the induction of one particular developmental region. For example, varying the concentration of SHH to mimic different dorso-ventral positions and obtain more LGE or MGE-like cells (Li *et al.*, 2009). Similarly, altering SHH application time windows changes their rostro-caudal position to produce more MGE or hypothalamic cells (Maroof *et al.*, 2013). Conversely, novel putative developmental pathways can be discovered that were not previously known, such as the ability of Activin to induce LGE or CGE fate (Cambray *et al.*, 2012; Arber *et al.*, 2015). Finally, once differentiation protocols are reliably established, the role of specific proteins can be probed by targeted genetic mutations. The relatively novel CRISPR-Cas9 technology allows high efficiency and precise gene editing, including insertion or deletion of specific gene sequences (Kearns *et al.*, 2014). This can be applied in a similar way to mouse genetic manipulation studies, to look at the effects of knocking out or over-expressing specific genes on the differentiation of specific cell types.

### 1.3.2 hPSCs for disease modelling and drug screening

The discovery of human iPSCs has opened up a whole new opportunity of *in vitro* disease modelling that allows the production of neurons from patient-derived cells, whose disease symptoms can be profiled and matched to any *in vitro* phenotypes observed (Takahashi *et al.*, 2007). While this is useful for monogenic diseases such as HD, as it avoids the need for editing a hESC line, it is particularly valuable to the study of polygenic diseases with multiple risk factors, such as schizophrenia and autism spectrum disorder (ASD) (Brennand *et al.*, 2011). Further to their applications in developmental biology, patient iPSCs can be compared to healthy PSCs to observe differences in the way the cells differentiate and mature into neurons. The generation of iPSCs from patient fibroblasts enables the expansion of a limited number of cells into an unlimited cell line that can be used for large scale studies and high throughput screening of potential therapies. One limitation to these studies currently is choosing the phenotypes to study, especially in psychiatric disorders where knowledge of disease mechanisms at the cellular level are extremely limited. Because HD is a monogenic disease, decades of *in vivo* and *in vitro* model research have highlighted the key pathways involved in the disease. On this basis, studies have already managed to show some impairments in cell metabolism, adhesion and death using HD iPSC-derived neurons (Zhang *et al.*, 2010; The HD iPSC Consortium, 2012). Enrichment of striatal cell types in these studies would greatly improve their relevance to the disease.

### 1.3.3 hPSCs for regenerative medicine

Cell replacement therapy relies on the possibility that cells can be implanted into a specific part of the body and adopt the identity and function of the damaged cell population such that they can partly or fully restore the tissue. Clinical trials using human foetal tissue to replace lost neurons in PD and HD

have shown that the procedure can be safe and produce positive functional benefits to patients (Wenning *et al.*, 1997; Hagell *et al.*, 1999; Bachoud-Lévi *et al.*, 2006). Difficulties with reproducing consistently successful outcomes in these trials has brought into question whether clinical trials should be open-label or double-blind placebo controlled, however it is also likely that the variation between foetal grafts also plays a large role (Evans, Mason and Barker, 2012). Another huge obstacle in the routine clinical use of foetal tissue is that it is in very limited and declining supply. Human iPSCs represent the most suitable source of cells for progression in this field, as they can be thoroughly quality controlled and produce an unlimited supply of tissue for transplantation.

Preclinical studies in PD models have provided very promising results both of histological and functional integration of the iPSC-derived grafts in rodent and non-human primate models (Kriks *et al.*, 2011; Grealish *et al.*, 2014; Hallett *et al.*, 2015). These cells are likely to enter into clinical trials in the near future.

Researchers at the Jules Stein Eye Institute recently published their findings from a Phase I clinical trial using iPSC-derived retinal pigmented epithelial cells (Schwartz *et al.*, 2012). The treatment caused no adverse effects and appeared safe 4 months post-transplantation, and there were even some improvements in vision measured in both patients. This is the first clinical trial using either iPSCs or iPSCs as the source of cells for transplantation, but other trials are in the pipeline (Carr *et al.*, 2013).

Much research is now focused on devising protocols for robust generation of specific cell types from iPSCs for this purpose.

#### 1.3.4 Neural differentiation of iPSCs

There are several methods by which an enriched population of neurons can be derived from iPSCs. Embryoid bodies (EBs) are formed when iPSCs are grown in suspension in the absence of feeder cells or pluripotency-inducing growth factors. These EBs go through the normal steps of embryonic development, and therefore form the three germ layers – endoderm, mesoderm and ectoderm. Zhang *et al.* demonstrated that exposure of plated EBs to FGF2 was sufficient to promote self-organisation into neural rosettes and neural precursor proliferation (Zhang *et al.*, 2001). Enzymatic isolation of the neural rosettes yielded 96% neural cells, which were subsequently expanded in suspension and then plated in the absence of FGF2 to initiate terminal differentiation. This is a method that is still widely used, and indeed has been applied to the production of ventral telencephalic neurons by adding recombinant SHH and Wnt inhibiting molecules (Li *et al.*, 2009; Danjo *et al.*, 2011). The EB method produces a high yield of neurons and large scale bioreactor culture systems make it easily applied to high throughput screening studies. However, cells within the EB are exposed to different levels of



patterning factors and inevitably produce their own unknown signalling molecules making it difficult to achieve defined and homogeneous cultures enriched for a single neuronal subtype.

Organoids are *in vitro*-derived tissues that exploit the huge capacity of either tissue stem cells or PSCs to self-organise by embedding EBs into a matrix to support their growth into much larger structures. This was first shown using intestinal stem cells to produce tissues containing crypts and villi, including all the relevant cell types (Sato *et al.*, 2009). More recently, this was applied to developing cortex-like tissues, complete with ventricular zone and layer-specific marker expression (Lancaster *et al.*, 2013). This type of research compromises on homogeneity for system complexity, and models well the early developmental processes in the human cortex, but will not be applicable for generating specific neuronal cell types.

Several mouse stromal cell lines are able to induce neural differentiation when co-cultured with hPSCs, however the mechanism by which this occurs remains unknown (Perrier *et al.*, 2004). Stromal co-cultures can induce 30-50% neurons from hPSCs, and was the method behind the first MSN differentiation protocol (Aubry *et al.*, 2008). Nonetheless, its use of animal feeder cells prevents any clinical applications and makes more defined methods more attractive for research purposes.

A defined monolayer differentiation method for neural induction of hPSCs was first described by Chambers *et al.*, in which the organising effects of the TGF $\beta$ -family inhibitors chordin, follistatin and noggin were reproduced *in vitro* (Chambers *et al.*, 2009). "Dual-Smad inhibition" of hPSCs first used recombinant noggin with the small molecule SB431542 (ALK4/5 inhibitor) to efficiently generate a population of forebrain progenitors responsive to additional patterning cues. A later study found that LDN193189 effectively mimics the BMP inhibition induced by noggin (Boergermann *et al.*, 2010). The default fate for hPSCs is of dorsal forebrain identity, but many differentiation protocols have already been devised to generate various other neuronal subtypes including midbrain dopaminergic neurons (Jaeger *et al.*, 2011; Kriks *et al.*, 2011; Kirkeby *et al.*, 2012), cortical interneurons (Cambray *et al.*, 2012; Maroof *et al.*, 2013) and striatal MSNs (Carri *et al.*, 2013; Nicoleau *et al.*, 2013; Arber *et al.*, 2015). The monolayer differentiation method exposes cells uniformly to fully defined culture medium containing specific patterning factors. Cells therefore differentiate in a much more synchronous and homogeneous manner to other methods making it the ideal choice for producing specific neuronal cell types for *in vitro* modelling or for cell therapy.

### 1.3.5 Directed differentiation of hPSCs towards striatal neurons

#### 1.3.5.1 Generation of MSNs from hPSCs

Research that laid the foundation for MSN-specific differentiation protocols found that precise concentrations and timing of SHH with or without Wnt inhibition were able to pattern hESC-derived telencephalic progenitors towards LGE or MGE lineage (Aubry *et al.*, 2008; Li *et al.*, 2009). The first group to publish a method specifically for MSN differentiation used mouse stromal cell co-culture for neural induction of hESCs (Aubry *et al.*, 2008). Isolated neural rosettes were treated with BDNF to anteriorise, and SHH (200 ng/ml) and DKK1 (100 ng/ml) to ventralise the cells. Neural induction with this method was fairly inefficient, with only 22% of cells expressing the neuronal marker MAP2. However, more than half of the neurons were DARPP32-positive, suggesting that SHH and DKK1 are at least somewhat effective in patterning hESCs towards MSN fate. They tested the *in vivo* potential of the cells at different stages of *in vitro* differentiation. Early stage cells produced teratoma-like regions of non-neuroectodermal identity, or neural rosette structures at best, while transplantation of mature neurons caused very poor graft survival. The stage at which cells could be characterised as LGE progenitors, expressing nestin, GSX2 and DLX2, was the best stage for graft survival, DARPP32 expression and lack of teratoma formation. When grafted into QA-lesioned nude rats and left for up to 21 weeks, all animals developed overgrown grafts that compressed the host brain considerably. DARPP32-positive regions were seen throughout the grafts, but the vast majority of cells were still dividing despite neural lineage commitment.

The ventralising effect of SHH was further explored by Ma *et al.*, who used the embryoid body method to generate neuroepithelial cells that were then manually isolated and re-plated (Ma *et al.*, 2012). Cells were treated with SHH (200 ng/ml) at a dose they found to be most effective at down-regulating PAX6 and up-regulating ASCL1, MEIS2 and GSX2, while keeping NKX2.1 expression to a minimum of 30%. Neural induction was far more efficient than in the study by Aubry *et al.*, with 93% of cells expressing  $\beta$ III-tubulin. Of the neurons, 80% were double-positive for DARPP32 and GABA. Whole cell patch clamping demonstrated the cells' ability to generate action potentials during current steps, and blockade of spontaneous synaptic activity using bicuculline, a GABA receptor inhibitor. Transplanted LGE-like progenitors in the QA-lesioned striatum of SCID mice, reportedly produced around 60% GABAergic neurons, the majority of which were DARPP32-positive. There was host innervation of the graft by TH and VGLUT expressing fibres, suggesting integration into the host brain. Animals showed significant functional recovery in rotarod, open field and treadscan testing compared to lesion only animals. While this study demonstrated high efficiency in generating functional DARPP32-positive MSNs, the manual isolation of neural colonies step is crucial for getting rid of unwanted cell types, making this protocol unsuitable for large scale systematic use.

Both Carri *et al.* and Nicoleau *et al.* demonstrated the efficacy of monolayer neural induction (51 and 58% MAP2-expressing cells respectively), and built upon the previous findings of the latter group (Aubry *et al.*, 2008; Carri *et al.*, 2013; Nicoleau *et al.*, 2013). Carri *et al.* added SHH (200 ng/ml) and DKK1 (100 ng/ml) from day 5 for 3 weeks to ventralise the cells, resulting in 52% CTIP2/GABA-positive neurons and 20% DARPP32-positive neurons (Carri *et al.*, 2013). These neurons exhibited MSN-like electrophysiological characteristics of an onset delay in firing the first action potential as well as inhibitory post-synaptic currents indicative of GABAergic signalling. Upon transplantation into QA-lesioned rat striatum, DARPP32-expression was observed at 9 weeks, but massive graft overgrowth meant this was a very small number of cells. There was a significant reduction in apomorphine-induced rotations in the grafted group at 3 and 6 weeks in the absence of mature MSNs, but not at 9 weeks, suggesting this may have been a transient neurotrophic effect of the immature graft rather than due to functional integration. Nicoleau *et al.* optimised their previous factor concentrations, demonstrating that inhibition of Wnt signalling by DKK1 or the small molecule inhibitor, XAV-939, enhanced forebrain patterning of the cells in a dose-dependent manner (Nicoleau *et al.*, 2013). In addition, they showed that a lower concentration of SHH (50 ng/ml) was more effective in generating LGE progenitors, while the higher concentration they used previously resulted in 80% of cells expressing NKX2.1, a MGE marker. Together, SHH (50 ng/ml) and XAV-939 (1  $\mu$ M) generated 28% DARPP32-positive neurons, producing both a higher proportion of neurons and MSNs than Carri *et al.*. They also presented evidence of the two MSN subpopulations expressing DRD1 or DRD2 that form the direct and indirect basal ganglia pathways respectively. Transplantation of the LGE progenitors produced large grafts that contained extensive FOXP1, CTIP2, FOXP1, and DARPP32 expression throughout and innervation by host TH fibres. These protocols demonstrate the ability to produce relatively high proportions of MSNs from hESCs using monolayer differentiation, but also emphasise the need for protocols that produce transplantable cells that will not overgrow *in vivo*.

Our lab has taken a completely novel approach to generating MSNs from hPSCs, by exploiting Activin A (hereafter named Activin) signalling to induce LGE and MSN fate (Arber *et al.*, 2015). Prior to discovering its effects on MSN differentiation, former lab members had found that Activin could induce a CGE-derived calretinin interneuron fate (Cambray *et al.*, 2012). The CGE is often described as a caudal extension of the LGE, and has a highly overlapping transcription factor expression profile including GSX2 and DLX2. Evidence for TGF $\beta$  family signalling in the developing subpallium, specifically the presence of Activin subunits, receptors and phosphorylated Smad2, support the concept of a patterning role for Activin in the ventral forebrain (Feijen, Goumans and van den Eijnden-van Raaij, 1994; Maira *et al.*, 2010). By testing different timing and concentrations of Activin, it was found that an earlier and higher dose of Activin increased pan-GE markers GSX2 and DLX2, but had no effect on

the MGE markers NKX2.1 and LHX8 (Arber *et al.*, 2015). Furthermore, Activin stimulated a large increase in CTIP2 expression after just 12 hours, hinting that it may have a direct regulatory effect on its expression. LGE progenitors at around day 20 of differentiation expressed GSX2, DLX2, CTIP2, FOXP2 and NOLZ1. This protocol has now been applied to multiple hESC and hiPSC lines by several researchers, consistently generating 20-40% DARPP32-positive neurons, with around 80% of cells NeuN-positive. At day 20, LGE progenitors were transplanted into QA-lesioned rat striatum (given immunosuppressant) and analysed 4, 8 and 16 weeks after. DARPP32 staining was visible by 8 weeks, and at 16 weeks 50% of graft cells were DARPP32-positive. FOXP2, calbindin, GABA, substance P and enkephalin were also expressed throughout the grafts at 16 weeks. Host TH fibres appeared to innervate the grafts, and human NCAM-positive fibres were observed extending out of the graft core towards the globus pallidus and midbrain. There was no Ki67 staining at 16 weeks, and no indication of graft overgrowth, however the grafts were actually very small and no improvement was seen in apomorphine-induced rotations. Activin induction of MSN fate in hPSCs is arguably the most efficient monolayer differentiation method for producing MSNs, and appears to have an advantage in not promoting overgrowth *in vivo*. However, because very little is known about Activin signalling in striatal development, more research must be done to decipher the mechanism by which Activin exerts its patterning effects *in vitro*.

#### 1.3.5.2 Generation of striatal interneurons from hPSCs

Striatal interneurons originate from the MGE and CGE and fall into several subtypes defined by their expression of distinct markers (**Figure 1.3**). GABAergic CR interneurons that derive from the CGE can be generated by treating late born hPSC-derived forebrain progenitors with Activin (Cambray *et al.*, 2012). All other interneuron subtypes are born in the MGE, a single developmental structure that gives rise to many cell types, making enrichment of one cell type over another more challenging. Cortical GABAergic interneurons expressing PV or SST are of most interest in current research, due to their emerging role in autism, schizophrenia and epilepsy (Liu *et al.*, 2013; Maroof *et al.*, 2013; Cunningham *et al.*, 2014). However, striatal cholinergic interneurons and basal forebrain cholinergic neurons have also been highlighted as cell types of interest for modelling dystonia and Alzheimer's disease respectively *in vitro* (Crompton *et al.*, 2013; Capetian *et al.*, 2014). Striatal GABAergic interneurons are becoming increasingly implicated in HD and their potential importance in a functioning striatal graft for HD cell therapy has also been recently emphasised (Reiner *et al.*, 2013; Reddington, Rosser and Dunnett, 2014). Fortunately, efforts to generate cortical interneurons from hPSCs have resulted in the production of all the above cell types. In theory, distinguishing between cortical and striatal interneurons is possible by looking at co-expression of NKX2.1 and LHX6 in striatal interneurons, however this involves some practical challenges, not least finding reliable antibodies that can be used

in combination (Nóbrega-Pereira *et al.*, 2008). All protocols for generating cortical interneurons have used a combination of Wnt inhibition followed by SHH activation, due to the strong NKX2.1-inducing effect of high SHH concentrations that pattern the MGE *in vivo*.

The embryoid body neural induction method was used by Li *et al.*, who applied different concentrations of SHH with or without DKK1 to hESC-derived neuroepithelial cells (Li *et al.*, 2009). They found that the higher dose of SHH (500 ng/ml) induced NKX2.1 expression in 84% of cells, 94% of which were FOXG1-positive indicating their ventral forebrain identity. Addition of DKK1 reduced the proportion of PAX6-positive cells and increased NKX2.1 mRNA levels. After further maturation of the cells, many stained positive for GAD67, and a few cells were also CTIP2/DARPP32-positive, showing some LGE induction as well as MGE. However, in this study they did not look at whether there was expression of any interneuron subtype markers.

Following this study, there was a relatively long period of silence in the field of hPSC-derived interneurons, which came to an end in May 2013 with the publication of three new papers in one month, plus another two soon after (Germain *et al.*, 2013; Liu *et al.*, 2013; Maroof *et al.*, 2013; Nicholas *et al.*, 2013; Kim *et al.*, 2014). Liu *et al.* used only a high dose of SHH (1000 ng/ml) to pattern hESCs towards MGE progenitors, and no Wnt inhibition. They obtained 38% and 45% of cholinergic and GABAergic neurons respectively. When transplanted into the hippocampus of a lesioned mouse model of learning and memory impairment they generated 8% and 45% ChAT and GABA-positive cells respectively and caused improvement in the learning and memory deficits (Liu *et al.*, 2013). In contrast, Kim *et al.* used a small molecule-based approach with IWP-2, a Wnt inhibitor, and SAG, a SHH activator (Smo agonist), from day 0. They are also the only group that applied FGF8 to the ventral forebrain progenitors in order to eliminate COUP-TFII expression, a CGE marker, and increase NKX2.1 expression to 80%. They also observed around 1% of cells expressing PV or SST, and in another publication showed that the cells could suppress seizures and improve behavioural impairments in epileptic mice (Cunningham *et al.*, 2014; Kim *et al.*, 2014).

Nicholas *et al.* used a NKX2.1/GFP reporter hESC line to facilitate their study. They applied DKK1 and another SHH activator, Purmorphamine, to EBs from day 9, producing 75% NKX2.1-positive cells, 81% of which co-expressed FOXG1. They followed the maturation of the cells *in vitro* for 30 weeks, and showed that hPSC-derived neurons develop along a similar timeline to human development, dramatically improving in functional maturation by the last time point. Despite the identification of 10% PV-positive cells at 15 weeks, this had reduced to just 1.5% by 30 weeks, with 40% SST and 77% calretinin. A population of NKX2.1/LHX6 double-positive cells indicated the presence of both striatal and cortical interneurons in their cultures (Nicholas *et al.*, 2013).

Finally, Maroof *et al.* used a monolayer differentiation to test different time windows of SHH treatment to optimise NKX2.1-positive cells that were MGE-like rather than the more caudal pre-optic area or hypothalamus, which also express NKX2.1. Also using a NKX2.1/GFP reporter hESC line, they looked at co-expression with OLIG2 and FOXG1 to determine the condition that produced the most MGE-like progenitors. Unlike many of the other groups, they demonstrated that beginning SHH treatment early (day 2-18) lead to the generation of hypothalamic-like progenitors. Intermediate SHH treatment (day 6-18) favoured the generation of cholinergic (50%) over GABAergic (15%) interneurons, while later addition of SHH produced 70% GABAergic and just 5% cholinergic interneurons. Other optimisation experiments found that supplementation of 5nM SHH treatment with 1  $\mu$ M Purmorphamine was able to optimally induce NKX2.1 and reduce the use of expensive recombinant SHH. PV and SST were each expressed by 40% of NKX2.1-positive cells, and no calretinin-expressing cells were detected. NKX2.1-positive progenitors were transplanted into mouse cortex, but after 2 months cells remained immature and had not differentiated into neuronal subtypes (Maroof *et al.*, 2013). This last protocol appears to be the most effective at generating MGE-like GABAergic interneurons, but their *in vivo* potential requires further assessment to see if they can mature over a longer time scale.

These studies have demonstrated that it is relatively easy to generate a high proportion of NKX2.1-positive MGE-like progenitors, but that their maturation into specific subtypes is very slow and requires more research. It appears that both cortical and striatal interneurons can form from these hPSC-derived MGE progenitors, but this remains to be confirmed with *in vivo* experiments.

#### 1.3.6 Direct reprogramming of somatic cells into striatal neurons

Induced neuron (iN) technology involves direct reprogramming of post-mitotic somatic cells into mature neurons by forcing expression of lineage-specific transcription factors (Vierbuchen *et al.*, 2010). Direct conversion of human adult fibroblasts to MSNs was performed by viral transduction of brain-enriched micro-RNAs, miR-9/9\* and miR-124, together with a combination of MSN-specific transcription factors (Victor *et al.*, 2014). While the micro-RNAs efficiently induced neuronal markers, CTIP2 was the only transcription factor tested (of 16) that was able to induce DARPP32 expression. DLX1 and DLX2 were found to increase the proportion of GABAergic neurons, and MYT1L improved the yield of MAP2-positive cells. With immunostaining on cells 5 weeks post-transduction they found that 82% were neurons, and 77% of neurons were DARPP32-positive MSNs. When cells were transplanted into mouse striatum after reprogramming, 91% of cells became DARPP32-positive, and their functional properties very closely resembled those of the native mouse MSNs.

GABAergic interneurons have also been generated using iN technology, this time without the use of micro-RNAs for efficient neuronal conversion (Colasante *et al.*, 2015). ASCL1 has also been shown to induce a high proportion of neurons with this method, so they tested other MGE-specific transcription factors in combination with ASCL1, using a GAD67-GFP mouse embryonic fibroblast line (Vierbuchen *et al.*, 2010). Colasante *et al.* found that FOXG1, SOX2, LHX6 and DLX5 increased the GABAergic population of neurons in an additive way, achieving GFP/GAD67 expression in 15% of plated fibroblasts. More than 90% of the GABAergic neurons were PV-positive, while a very low proportion expressed SST. Repeating this experiment using human iPSCs, more than half of neurons were GABAergic while 90% of neurons were PV-positive, raising the question as to why the other 40% of PV-positive neurons were not GABAergic. They assessed the efficiency of the conversion and estimated it at more than 30%, better than with the mouse cells. A third of cells displayed repetitive action potential firing upon current injection, but this was at a much lower frequency than observed in real PV interneurons.

These two studies demonstrate a novel way of studying the genes involved in fate commitment of specific cell types. For example, the iN-MSN study further confirmed the importance of CTIP2 in MSN development, which had already been suggested in knockout studies and our own research into MSN differentiation from hPSCs (Arlotta *et al.*, 2008; Victor *et al.*, 2014; Arber *et al.*, 2015). It is also a fast and relatively efficient way of generating a small number of mature human neurons from somatic cells, which may be useful for specific tests on skin biopsies. However, such tissue samples are limited in scale and there is no opportunity of expansion of these post-mitotic cells, making them unsuitable for standardised drug screening or regenerative medicine.

## 1.4 Aims

Efficient *in vitro* generation of functional striatal neurons is crucial for the progress of regenerative medicine as well as modelling healthy and diseased striatal development *in vitro*.

The aims of this project are to investigate the mechanisms by which Activin induces an MSN fate in hPSC-derived forebrain progenitors by manipulating the exogenous factors to which they are exposed and measuring intracellular changes, such as protein or gene expression. This will both provide new information on the processes involved in human MSN differentiation and could lead to the discovery of other pathways that further enrich MSN generation.

The second aim is to assess whether current cortical interneuron differentiation protocols can be applied for the generation of striatal interneurons, both *in vitro* and *in vivo*. This involves characterising how these interneurons survive, migrate and differentiate following transplantation into neonatal rat brain.

Together, hPSC-derived striatal MSNs and interneurons will provide a valuable tool for the aforementioned applications.



## 2 Methods and materials

### 2.1 Cell culture

All cell cultures were maintained at 37°C and 5% CO<sub>2</sub> (Galaxy 170 R, New Brunswick). Cell work was carried out under a laminar flow hood (Maxisafe 2020, Thermo Scientific) under sterile conditions. Cells were grown on cell culture-treated plastic multi-well plates (Thermo Scientific) or glass coverslips (VWR).

#### 2.1.1 hPSC culture

All experiments were carried out using H7 hESC line or their tau-GFP-transfected counterparts (TG-H7) unless otherwise stated (2.1.2). Multi-well plates were coated with hESC-qualified Matrigel (Corning) diluted in DMEM/F-12 (Gibco) for at least 1 hour at 37°C. H7 were maintained in mTeSR1 or TeSR-E8 medium and TG-H7 cell lines were maintained in TeSR-E8 medium (Stem Cell Technologies). All media were changed at least every other day and cells were passaged when they reached 80% confluency as follows. All media was aspirated and cells were washed with D-PBS (Gibco) once, then EDTA 0.02% (Sigma) was added and the cells incubated at 37°C for 1-2 mins. EDTA was aspirated and medium added. A serological pipette was used to scratch and manually dissociate the cells by titrating into small clusters. Cell suspension was centrifuged at 1150 rpm for 3 minutes (5810 R, Eppendorf) to create a cell pellet that was resuspended in fresh medium and seeded at a 1:1, 1:2, and 1:5 ratios.

#### 2.1.2 hPSC freezing and thawing

Cells were stored in liquid nitrogen tanks at low passage numbers for future use. Cells were passaged as described above (2.1.1) but kept in large clusters and resuspended in medium containing 10% DMSO. Cell suspension from one well of 80% confluency was transferred into a cryogenic vial and placed inside a cell freezing container to slow the rate of freezing once placed at -80°C. Cells were kept at -80°C for up to 1 week before being placed in liquid nitrogen storage tanks. Cell thawing was carried out as quickly as possible by placing cryogenic vials straight from liquid nitrogen at 37°C. Thawed cell suspension was transferred to pre-warmed medium and centrifuged at 1150 rpm for 3 minutes. The cell pellet was resuspended in fresh medium and plated into a single well.

#### 2.1.3 hESC transfection (with Claudia Tamburini)

H7 hESCs were transfected with a plasmid containing a CAG-tau-GFP construct to drive constitutive expression of a tau-GFP fusion protein, and a puromycin resistance cassette (puromycin acetyltransferase) for selection of cells expressing the transgene. Plasmid DNA was prepared for transfection by ethanol precipitation as follows. 5 µg DNA was made up to 100 µl with TE buffer, sodium acetate (1/10<sup>th</sup> volume, 3M) was added, the tube was filled with 100% ethanol and placed at

-20°C overnight. DNA was centrifuged at 15,000 x g for 15 minutes at 4°C, the pellet was washed with 70% ethanol and the centrifuge step repeated. The pellet was air-dried under a laminar flow hood and resuspended in TE buffer. Two 80% confluent wells of H7 hESCs were pre-treated with ROCK inhibitor (10 µM, Y-27632), dissociated with dispase (7 minutes at 37°C) and medium was added to stop the reaction. Cells were resuspended in P3 buffer (Lonza) with 2 or 4 µg of plasmid DNA and transferred to a cuvette for electroporation with the Lonza 4D-Nucleofector using the CB-150 program. Cells were re-plated in medium with ROCK inhibitor.

Medium was changed 48 hours later with mTeSr1 plus puromycin (1 µg/ml) for selection of cells containing the transgene. Following selection, 5 colonies grew large enough for picking, expanding and freezing. Of those, 4 clones (TG2, 3, 4 and 5) were stable enough for continuous culture and differentiation, but TG2, 3 and 5 switched off the transgene during neural differentiation. TG4 was used for all experiments requiring GFP expression.

#### 2.1.4 hPSC neural differentiation

Cells were passaged as above (**2.1.1**) but plated on Growth Factor Reduced Matrigel (diluted 1/15 in DMEM-F12 and coated for 1 hour at 37°C; Corning) in mTeSR1 or E8. When cells were >90% confluent, medium was changed to N2B27-defined medium: 100 ml DMEM-F12, 50 ml Neurobasal, 1 ml N2 supplement, 1 ml B27 without retinoic acid, 2 mM L-glutamine, penicillin-streptomycin, 0.1 mM β-mercaptoethanol (all from Gibco). This was designated as day 0 of differentiation. For MSN differentiation, the ALK4/5/7 inhibitor SB431542 (SB; 10 µM; Tocris) was added to medium from day 0-5. The ALK2/3/6 inhibitors dorsomorphin (200 nM; Tocris) and LDN193189 (LDN; 100 nM; Tocris) were added to medium from day 0-9. For MGE differentiation, SB431542 and LDN193189 were given from day 0-9, as well as XAV939 (2 µM; Tocris), a Wnt inhibitor.

Cells were passaged at day 9-12 as follows. Manual dissociation was carried out with 0.02% EDTA as above (**2.1.1**) but cells were kept in large clusters and titrated very gently without the centrifugation step. Cells were split at a 2:3 ratio onto fibronectin-coated plates (15 µg/ml, 1 hour at 37°C; Millipore). The 2<sup>nd</sup> passage was carried out between days 19 and 22 using EDTA as above but with more vigorous titration to make very small clusters of cells, which were plated onto poly-D-lysine and laminin-coated plates. Poly-D-lysine (10 µg/ml in ddH<sub>2</sub>O) was added for 30 minutes at room temperature, washed and dried under UV. Laminin (10 µg/ml; Sigma) was then added and incubated overnight at 37°C. When cells started to look neuronal, at around day 25, B27 with retinol (Gibco) replaced the B27 without retinol and growth factors BDNF and GDNF (10 ng/ml; Peprotech) were added to promote neuron survival.

For MSN differentiation, Activin A (25 ng/ml; R&D) was added from day 10 onwards and cells were split 1:1 at passage 2. For MGE differentiation, SHH (200 ng/ml; R&D) and purmorphamine (1  $\mu$ M; Millipore) were added from day 10 to 18 and cells were split 1:3 or 1:4 at passage 2, depending on density. Other molecules were given as stated in the relevant chapter: cyclopamine (1  $\mu$ M), SB525334 (1  $\mu$ M), LY2109761 (5  $\mu$ M).

For electrophysiology experiments, cells were dissociated with Accutase (Gibco) and seeded at a density of 100,000 cells per 13 mm coverslip. SCM1 medium was given for 8 days following the second or third passage and was composed as follows: 100 ml DMEM-F12, 50 ml Neurobasal, 1ml N2, 1ml B27 w/o RA, 2 mM L-glutamine, 300  $\mu$ l mycozap, 0.1 mM  $\beta$ -mercaptoethanol, 2  $\mu$ M PD0332991, 10  $\mu$ M DAPT, 0.5 mM CaCl<sub>2</sub> (to give 1.8mM total CaCl<sub>2</sub> in final complete medium), 200  $\mu$ M ascorbic acid, 10 ng/mL BDNF, 1  $\mu$ M LM22A4, 10  $\mu$ M Forskolin, 3  $\mu$ M CHIR 99021, 300  $\mu$ M GABA. This was replaced by SCM2 until the end of the experiment, which was composed of: 25 ml DMEM-F12, 25 ml Neurobasal A, 1 ml B27 with RA, 2 mM L-glutamine, 100  $\mu$ l Mycozap, 0.1 mM  $\beta$ -mercaptoethanol, 2  $\mu$ M PD0332991, 3  $\mu$ M CHIR 99021, 0.3 mM CaCl<sub>2</sub>, 200  $\mu$ M ascorbic acid, 10 ng/mL BDNF, 1  $\mu$ M LM22A4.

## 2.2 Cell analysis

### 2.2.1 Immunocytochemical staining

Cultured cells were washed once with PBS and fixed in 3.7% PFA for 15 minutes at room temperature. Fixed cells could be stored up to 2 weeks at 4°C or stained immediately after fixing, as follows. For nuclear stains, fixed cells underwent 5 minute methanol washes of ascending then descending methanol dilutions (33%, 50%, 66% at 4°C, then 100% at -20°C) in PBS. Permeabilisation was achieved by washing with PBS-T (PBS+0.3% Triton-X-100) twice for 10 minutes, then cells were blocked in PBS-T with 2% BSA and 3% donkey serum for 20-30 minutes at room temperature. Primary antibodies were added in PBS-T with 3% donkey serum and left overnight at 4°C. Cells were washed 3 times for 10 minutes with PBS-T before secondary antibodies (1/200, AlexaFluor anti-donkey 488, 555, 594, 647; Life Technologies) were added in PBS-T and left for 1 hour at room temperature. DAPI (1/3000 dilution; Molecular Probes) in PBS was applied for 5 minutes at room temperature. Stained cells were washed 3 times for 10 minutes in PBS before mounting in DAKO fluorescent mounting medium (Life Technologies) either onto glass slides (VWR) or in the culture plate covered with a glass coverslip (VWR). All primary antibodies used are listed in **Table 2.1**.

Stained cells were imaged using Leica DM6000B upright (for slides) or Leica DMI6000B inverted (for plates) fluorescent microscopes. Cell counting for each experiment was carried out on pictures taken from at least 5 random fields of view, manually using ImageJ software, or automatically using Cell Profiler software. Some images were also taken using a Zeiss LSM710 confocal microscope.

## 2.2.2 Quantitative real-time PCR

### 2.2.2.1 RNA extraction

Cultured cells were washed once with PBS and lysed for RNA extraction with 1 ml Tri reagent (Sigma). Cell lysates could be stored at -80°C for up to 1 month before continuing with RNA extraction as detailed in the manufacturer's instructions.

Briefly, samples were thawed and left at room temperature for 5 minutes before adding 200 µl chloroform. They were then shaken vigorously for 15 seconds and allowed to stand for up to 15 minutes at room temperature before centrifugation at 12,000 x g for 15 minutes at 4°C. The aqueous (upper) phase containing RNA was carefully transferred to a new tube. Isopropanol (500 µl) was mixed with the aqueous phase and left to stand for 5 minutes at room temperature. Samples were then centrifuged at 12,000 x g for 10 minutes at 4°C to create an RNA pellet. The supernatant was removed and the pellet washed in 1 ml of 75% ethanol, vortexed and centrifuged at 7,500 x g for 5 minutes at 4°C. The RNA pellet was air dried and resuspended in 20-50 µl of DEPC-treated ddH<sub>2</sub>O.

### 2.2.2.2 DNase treatment

RNA concentration was measured on a BioSpectrometer (Eppendorf) and 10 µg was made up to a 17 µl volume with DEPC-treated ddH<sub>2</sub>O. DNase mastermix containing 2 µl TURBO DNase 10x buffer and 1 µl TURBO DNase (Ambion) per sample was added to the RNA samples. Samples were incubated at 37°C for 20-30 minutes and then 2 µl DNase inactivation reagent was added and samples mixed regularly for 5 minutes at room temperature. Samples were centrifuged for 1.5 minutes at 10,000 x g and supernatant containing DNase-treated RNA was transferred to a fresh tube.

### 2.2.2.3 Reverse transcription PCR

Reverse transcription was carried out as per the manufacturer's instructions (Invitrogen). RNA concentration was measured again and 1 µg added to 1 µl of random primers and 1 µl of dNTP mix, then made up to a final volume of 13 µl with DEPC-treated ddH<sub>2</sub>O. Samples were placed in a Mastercycler (Eppendorf) and heated to 65°C for 5 minutes then cooled to 4°C for 1 minute. A master-mix containing per sample: 4 µl First-Strand buffer, 1 µl 0.1 M DTT, 1 µl RNaseOUT and 2 µl SuperScript III RT were added to each RNA mixture. The Mastercycler program was resumed to include the following steps: 25°C for 5 mins, 55°C for 60 mins and 70°C for 15 mins. cDNA was then diluted 1/10 in ddH<sub>2</sub>O. Three RNA samples were chosen at random to use in a 2<sup>nd</sup> reaction for no reverse transcription controls, without the SuperScript III RT.

### 2.2.2.4 Quantitative real-time PCR (qPCR)

A SYBR MESA green master-mix was used for qPCR, containing per reaction: 10 µl MESA green (Eurogentech), 5 µM of the forward and reverse primers for the gene of interest (10 or 100 µM stock;

custom-made, Sigma) and made up to 18  $\mu$ l with ddH<sub>2</sub>O. The master-mix was distributed into a 96-well-plate (18  $\mu$ l per well; Greiner Bio-One) and 2  $\mu$ l of cDNA from each sample was added to duplicate or triplicate wells. The Bio-Rad CFX Connect Real-Time System was used to run the qPCR program: 94°C for 4 mins, then 40 cycles of [94°C for 30 secs + 60°C for 15 secs + 72°C for 30 secs]. Melting curve analysis was performed from 65-95°C, read every 0.2°C.

Data was collected on CFX Manager software (Bio-Rad) and exported to Microsoft Excel for analysis. All qPCR data was normalised to 2 reference genes – GAPDH and  $\beta$ -ACTIN – and relative quantification was compared to control basal conditions using the  $\Delta\Delta$ -CT method. Error bars represent the SEM of biological replicates ( $n \geq 3$ ).

All primers (**Table 2.2**) had been previously tested for efficiency on human foetal whole brain tissue with serial dilutions and all annealing temperatures were 60°C.

### 2.2.3 Electrophysiological analysis

Neuronal cultures on glass coverlips (days specified with results) were placed in a recording chamber perfused with artificial cerebrospinal fluid (aCSF) at a flow rate of 2-2.5 ml/min, which contained (in mM): 135 NaCl, 5 KCl, 1.2 MgCl<sub>2</sub>, 1.25 CaCl<sub>2</sub>, 10 D-glucose, 5 N-2-265 hydroxyethylpiperazine-N'-2-ethanesulfonic acid (HEPES) (all from Sigma), pH 7.4. Recording pipettes (4-6 M $\Omega$ ) were pulled from borosilicate capillary glass (Sutter Instruments, USA) and filled with internal solution containing (in mM): 117 KCl, 10 NaCl, 11 HEPES, 2 Na<sub>2</sub>-ATP, 2 Na-GTP, 1.2 Na<sub>2</sub>-phosphocreatine, 2 MgCl<sub>2</sub>, 1 CaCl<sub>2</sub> and 11 ethylene-glycol-tetra-acetic acid (EGTA) (all from Sigma), pH 7.2. Cells were visualised using infrared differential interference contrast (DIC) videomicroscopy through a Nikon Eclipse FN1 or Olympus BX51 microscope. Whole-cell patch clamp recordings were acquired at room temperature (20-22°C) using a Multiclamp 700B amplifier and Digidata 1332 or 1550 analogue to digital converter with pClamp 10 software (all Molecular Devices, USA). Cells were recorded in current clamp mode and injected with current steps of 10 or 20 pA between -100 and +100 pA to measure voltage responses. Mean resting membrane potential was calculated using 1 s segments from at least 10 sweeps. Data were analysed with Clampfit software (Molecular Devices) then exported to and plotted using Origin software (OriginLab, USA).

## 2.3 Transplantation of hESC-derived neural progenitors

All animal work was done in compliance with the European Directive 2010/63/EU on the protection of animals used for scientific purposes, under the project licence of Professor Stephen B. Dunnett (PPL 30/3036; PIL IOD92ED42).

### 2.3.1 Transplantation of hPSC-derived MGE progenitors into neonatal rats (with Claire Kelly)

#### 2.3.1.1 *Cell suspension preparation*

Cells cultured to day 20-22 of MGE differentiation (SHH and purmorphamine added day 10-18) were washed with PBS and dissociated with accutase (15 minutes at 37°C). N2B27 medium was added to inactivate the accutase and the cell suspension was counted and then centrifuged at 1150 rpm for 3 minutes. Cells were resuspended in DMEM-F12 to a volume for  $2 \times 10^5$  cells per  $\mu\text{l}$  and transported on ice to the surgery room.

#### 2.3.1.2 *Postnatal care of mother and pups*

Pregnant female Sprague-Dawley rats (Charles River) gave birth to litters and were left 1 day to ensure they had fed and bonded with their pups. To avoid the mothers rejecting their pups after surgery, the mother was removed from her pups before surgery and placed in a separate cage. Once all pups had been injected, the mother was put under isoflurane anaesthesia for 3 minutes and then placed back in her home cage surrounded by her pups.

#### 2.3.1.3 *Transplantation procedure*

All surgical procedures were carried out under isoflurane anaesthesia using a neonatal adaptor on a stereotaxic frame. Post-natal day 2 Sprague Dawley pups were injected with  $2 \times 10^5$  cells in a volume of 1  $\mu\text{l}$  using a syringe. Injection coordinates targeted the right cortex or striatum (0.9 mm anterior and 1.8 mm lateral to bregma, 2.0 mm below the dura; 0.7 mm anterior and 1.9 mm lateral to bregma, 2.9 mm below the dura). Cells were injected over 1 minute and the needle was left in place another 3 minutes before withdrawal. The scalp was glued together using Vetbond (3M) and pups were placed in warm recovery boxes for 10 minutes before being put back in their home cage.

#### 2.3.1.4 *Experimental groups and time points*

Two rounds of transplantation were carried out with two litters per experiment. The first round included 23 pups, sacrificed at 4, 8, 16 and 24 weeks (n=2, 2, 4 and 15). The second round included 31 pups, of which 26 were given daily intraperitoneal Cyclosporine A injections (10 mg/kg; Sandimmun) from weaning onwards, and were sacrificed at 6, 12 and 20 weeks (n=6, 9 and 7; 4 rats had to be sacrificed early due to illness). The remaining 5 animals were not treated with immune suppression and were all sacrificed at 20 weeks.

### 2.3.2 Tissue preparation

Animals were sacrificed by giving a lethal dose of Euthatal (Merial) and were trans-cardially perfused with pre-wash (1.8% di-sodium hydrogen phosphate, 0.9% sodium chloride, in ddH<sub>2</sub>O, pH 7.3) for 2 minutes and PFA (4% diluted in pre-wash) for 5 minutes. The brains were removed and post-fixed in 4% PFA for another 4 hours before being transferred to 25% sucrose (in pre-wash) for storage at 4°C up to 1 week. Coronal sections were cut to 40 µm thickness in 12 series using a microtome (RM2245, Leica) with a freezing stage (BFS-3MP Controller, PhysiTemp). Sections were stored in anti-freeze solution (0.545% di-sodium hydrogen phosphate, 0.157% sodium dihydrogen phosphate, 40% ddH<sub>2</sub>O, pH 7.3; add 30% ethylene glycol, 30% glycerol) at -20°C for up to 6 months before staining.

### 2.3.3 Immunohistochemistry

All steps were performed on a shaker at room temperature. Floating sections were washed 3 times for 10 minutes in TBS (1.2% Trizma base, 0.9% sodium chloride, in ddH<sub>2</sub>O, pH 7.4) and blocked (Triton-X-100-TBS with 3% donkey serum) for 1 hour. Sections were incubated in primary antibody solution (TXTBS + 1% donkey serum + primary antibodies) overnight. Sections were washed 3 times for 10 minutes in TBS before incubation in secondary antibody solution (TBS + secondary antibodies; 1/200, AlexaFluor 488, 555, 594 and 647) overnight. Sections were washed 3 times for 10 minutes in TBS and then put in TNS (0.6% Trizma base in ddH<sub>2</sub>O, pH 7.4) for mounting onto gelatin-coated glass slides. Sections were air dried, cover-slipped with VectaShield hardset antifade mounting medium with DAPI (Vector Labs) and stored at 4°C. All primary antibodies are listed in **Table 2.1**.

### 2.3.4 Section imaging and analysis

Imaging of sections was carried out as described for cells (**Section 2.2.1**). Absolute cell counts were performed for HuNu (human nuclei) and NKX2.1 and corrected using the Abercrombie formula:

$$P=1/F*N*M/(D+M)$$

P = number of cells per graft; N = total raw cell count; F = frequency of sampled sections (1:12); M = section thickness (0.04 mm); D = Mean cell diameter.

NeuN-positive cells were counted as a percentage of GFP and the mean and SEM calculated between subjects. Calretinin and nestin are cytoplasmic markers making reliable counting of cells in clumps using a widefield fluorescent microscope unfeasible. Only cells separate from the clumps were counted for these markers as a percentage of GFP.

### 2.3.5 *Ex vivo* brain slice recording (Michael Laing)

Coronal slices (300 µm) containing the striatum or hippocampus were prepared from 12-week-old rats (12 weeks post-transplantation) in chilled (1-3°C) cutting solution bubbled with carbogen (95% O<sub>2</sub>/5%

CO<sub>2</sub>) (in mM: 60 sucrose, 85 NaCl, 2.5 KCl, 1 CaCl<sub>2</sub>, 2 MgCl<sub>2</sub>, 1.25 NaH<sub>2</sub>PO<sub>4</sub>, 25 NaHCO<sub>3</sub>, 25 D-glucose, 3 kynurenic acid, and 0.045 indomethacin). Slices were stored for 20 min at 35°C in sucrose-containing solution and then maintained at room temperature in aCSF [in mM: 125 NaCl, 2.5 KCl, 1 CaCl<sub>2</sub>, 2 MgCl<sub>2</sub>, 1.25 NaH<sub>2</sub>PO<sub>4</sub>, 25 NaHCO<sub>3</sub>, and 25 D-glucose (305 mOsm)] and used within 4-6 hours. For recording, slices were transferred to a submersion chamber continuously perfused with warmed (35°C) aCSF [in mM: 125 NaCl, 2.5 KCl, 2 CaCl<sub>2</sub>, 1 MgCl<sub>2</sub>, 1.25 NaH<sub>2</sub>PO<sub>4</sub>, 25 NaHCO<sub>3</sub>, and 25 D-glucose (305 mOsm)] at a flow rate of 2-2.5 ml/min. Somatic whole-cell patch-clamp recordings were performed on GFP-positive cells (visually identified by LED fluorescence and infrared DIC videomicroscopy through an Olympus BX51 microscope) using pipettes with resistances of 4–6 MΩ when filled with internal solution containing (in mM): 130 K-gluconate, 20 KCl, 10 HEPES, 0.16 EGTA, 2 Mg-ATP, 2 Na<sub>2</sub>-ATP, and 0.3 Na<sub>2</sub>-GTP, pH 7.3 (295 mOsm). Electrophysiological data were acquired at 20 kHz and filtered at 6 kHz using a Multiclamp 700B patch-clamp amplifier and Digidata 1550 analogue to digital converter with pClamp 10 software (Molecular Devices). Evoked voltage responses were measured by injecting 500 ms current steps from 0-300 pA. Mean resting membrane potential was calculated using 1 s segments from 10 sweeps. Data were analysed with Clampfit software (Molecular Devices) then exported to and plotted using Origin software (OriginLab, USA). These experiments were performed by Michael Laing and the data analysed by myself.

#### 2.4 Statistical analysis

For cell counting analysis, the mean percentage cells and SEM was calculated from the mean of at least 3 independent experiments. A two-way ANOVA was conducted to test for significant differences between groups at different time points, with post-hoc Bonferroni correction for multiple pairwise comparisons. Where only 2 groups were compared, a one-tailed t-test was used to compare means.

For qPCR analysis, technical replicates were averaged to give individual biological replicates. The mean and SEM of 3 biological replicates was calculated and compared between groups by two-way ANOVA with post-hoc Bonferroni correction for multiple pairwise comparisons.

Mean resting membrane potentials and input resistances were calculated from the stated number of cells in **Figures 3.4** and **4.3** in each group of a single experiment. Means were compared by two-way ANOVA with post-hoc Bonferroni correction for multiple pairwise comparisons.



**Table 2.1: List of primary antibodies used for immunostaining.**

Antigen	Species	Supplier	Code	Dilution	
				Cells	Rat tissue
Calbindin	rabbit	Swant	CB-38a	1/500	1/1000
Calretinin	rabbit	Swant	7697	1/500	1/1000
ChAT	goat	Millipore	AB144	1/100	1/200
CTIP2	rat	Abcam	25B6	1/500	
DARPP32	rabbit	Santa Cruz	sc11365	1/200	1/500
Doublecortin	goat	Santa Cruz	sc8067	1/100	1/100
FOXP1	rabbit	Abcam	18259	1/250	
FOXP2	goat	Abcam	ab1307	1/100	
GABA	rabbit	Sigma		1/500	1/1000
GAD67	mouse	Millipore	mab5406	1/500	1/500
GFAP	mouse	Dako		1/100	1/100
GFP	rabbit	Invitrogen		1/500	1/1000
HuNu	mouse	Millipore	mab1281	1/250	1/1000
ISL1	rat	DSHB		1/100	
MAP2	mouse	Sigma		1/500	
ASCL1	mouse	BD	556604	1/500	
MEIS2	goat	Santa Cruz	10600	1/500	
Nestin	mouse	Neuromics		1/300	1/300
Nestin	mouse	BD	611659	1/300	
Nestin	rabbit	Millipore		1/500	
NeuN	mouse	Millipore	mab377	1/250	1/500
NeuN	rabbit	Millipore		1/500	
NKX2.1 (TTF1)	rabbit	Abcam	ab40880	1/1000	1/1000
NOLZ1 (ZNF503)	mouse	Abnova		1/500	
NPY	rabbit	Immunostar	22940	1/200	1/250
Oct4	goat	Santa Cruz	sc8628	1/500	
OLIG2	goat	R&D		1/200	
Parvalbumin	mouse	Sigma	p3088	1/100	1/100
PAX6	mouse	DSHB		1/1000	
Somatostatin	rabbit	Millipore		1/50	
Somatostatin	rat	Millipore		1/50	1/100
STEM121	mouse	Stem Cells Inc			1/3000
TH	rabbit	Pelfreeze	P40101	1/500	
TUJ1	rabbit	Covance		1/1000	

**Table 2.2: List of primers used for qPCR.**

<b>Gene</b>	<b>Forward primer</b>	<b>Reverse primer</b>
GAPDH	ACGACCCCTTCATTGACCTCAACT	ATATTTCTCGTGGTTCACACCCAT
$\beta$ -ACTIN	TCACCACCACGGCCGAGCG	TTCCTTCTGCATCCTGTCTG
CTIP2	CTCCGAGCTCAGGAAAGTGTC	TCATCTTTACCTGCAATGTTCTCC
GSX2	TCACTAGCACGCAACTCCTG	TTTTCACCTGCTTCTCCGAC
DLX2	TCACTAGCACGCAACTCCTG	TTTTCACCTGCTTCTCCGAC
NKX2.1	CGCATCCAATCTCAAGGAAT	TGTGCCCAGAGTGAAGTTTG
PAX6	AATAACCTGCCTATGCAACCC	AACTTGAAGTGGAACTGACACAC

## 3 The role of TGF $\beta$ signalling in hPSC differentiation towards functional MSN fate

### 3.1 Introduction

The generation of MSNs from hPSCs has many potential applications, both scientific and clinical. The use of defined factors to induce an LGE phenotype followed by MSN fate allows modification of conditions to investigate mechanisms that affect MSN differentiation *in vitro* and could therefore have implications for *in vivo* development. This would allow the screening of novel pathways in cell culture before taking studies into animal models, thereby reducing unnecessary use of animals in research. Furthermore, the ability to produce neurons that display functionally mature characteristics would allow unprecedented access to healthy human neurons that could be compared against neurons derived from patient iPSCs. These *in vitro* disease models could then be used for studying both disease mechanisms and therapeutic targets. Finally, transplantation of foetal tissue into the brains of HD patients and animal models has shown promise for the use of cell replacement therapy as a strategy for brain repair and the slowing of disease progression. A self-renewing source of tissue is vital for this type of therapy to become a viable long term option that can be used with many patients. In order to fulfil this potential, a reliable method for generating an enriched population of MSNs from hPSCs is crucial.

Previous work towards differentiating hPSCs into MSNs has focused on ventralising anterior neural progenitors produced from stromal cell co-culture, embryoid body or monolayer neural induction (Aubry *et al.*, 2008; Ma *et al.*, 2012; Carri *et al.*, 2013; Nicoleau *et al.*, 2013). These groups acted on the principle that FOXG1-positive cells in the developing telencephalon are exposed to opposing gradients of the ventralising morphogen SHH and the repressor form of GLI3, which is expressed in dorsal tissues (**Figure 1.3**). BMP and Wnt proteins are also expressed in the cortical hem and their expression is disrupted in GLI3 mutants (Kuschel, R  ther and Theil, 2003). Aubry *et al.* built on the use of SHH by adding DKK1, an endogenous Wnt antagonist that is also released by floor plate cells (Aubry *et al.*, 2008). They later showed that this principle could be applied to the monolayer differentiation model, and DKK1 could be replaced with XAV939, a chemical Wnt inhibitor (Nicoleau *et al.*, 2013). This approach yielded 28% DARPP32-positive neurons in culture, a more efficient protocol than the similar one used by Carri *et al.*, which generated 20% DARPP32-expressing neurons (Carri *et al.*, 2013). Both of these studies faced the challenging trade-off between SHH and XAV939 dosage and the increase in NKX2.1 expression. While they did lead to up-regulated expression of forebrain and pan-GE markers such as FOXG1, OTX2 and GSX2, LGE-specific transcription factor CTIP2 was unaffected at the

progenitor stage. Indeed, even using the optimum concentrations of SHH and XAV939, NKX2.1 showed a 20-fold increase in expression compared to untreated controls (Nicoleau *et al.*, 2013). LGE-specific markers CTIP2, FOXP1 and FOXP2 only appeared alongside DARPP32 expression after neuronal maturation. It is therefore likely that the MSNs generated using SHH and Wnt inhibition resulted from the induction of pan-GE markers rather than a clear instructive effect towards LGE fate.

Recently, our lab discovered that Activin A, a member of the TGF $\beta$  family of ligands, rapidly induces the expression of LGE markers in forebrain progenitors derived from hPSCs (Arber *et al.*, 2015). Phosphorylated Smad2 (pSmad2), which is downstream of Activin and TGF- $\beta$  signalling via the ALK4/5 receptors, was previously detected in the ganglionic eminences, and co-localised with DLX2 throughout. The two proteins were also confirmed to interact *in vivo* by immunoprecipitation, and pSmad2 was found to bind to the *DLX2* gene enhancer by ChIP (Feijen, Goumans and van den Eijnden-van Raaij, 1994; Maira *et al.*, 2010). In line with these findings, we saw a >2-fold increase in *DLX2* and *GSX2* mRNA just 12 hours after Activin treatment began. Furthermore, in contrast to previous attempts at MSN differentiation, we also observed a large increase in *CTIP2* expression. Activin-treated cells were immuno-reactive for other LGE-specific markers, *FOXP2* and *NOLZ1*, at the progenitor stage and matured into 20-40% DARPP32-positive neurons. Despite this robust effect of Activin, there is relatively little evidence of it being essential for forebrain development, making it difficult to decipher a mechanism by which it induces LGE fate. This provides a good example of how this kind of platform can be used to test potential developmentally relevant pathways.

These initial studies showing generation of hPSC-derived MSNs have presented a very basic electrophysiological characterisation of the cells (Ma *et al.*, 2012; Carri *et al.*, 2013; Arber *et al.*, 2015). More in depth analysis of the electrophysiological properties of hPSC-derived cortical neurons throughout differentiation by Kirwan *et al.* demonstrated that if cultured for long periods of time, it is possible for the cells to form functional synapses and develop mature network and membrane properties (Kirwan *et al.*, 2015). Recent advances have been made in enhancing and accelerating the functional maturation of hPSC-derived neurons without the need to leave the cells for several months or co-culture the cells with primary astrocytes or neurons (Talias, Segal and Ben-Yosef, 2014; Telezhkin *et al.*, 2015). These studies used cell cycle inhibitors, neurotrophic factors and increased cAMP levels to achieve accelerated maturation. The Telezhkin protocol also focused on the importance of a higher extracellular calcium concentration to facilitate GABA-dependent depolarisation and voltage-gated Ca<sup>2+</sup> entry, promoting CREB phosphorylation and associated neurogenic gene upregulation. Neither of these studies did any characterisation as to the fate of the cells, but it can be assumed based on their protocols that they produced forebrain neurons. These findings can now be applied to protocols inducing specific neuronal subtypes to see if their effects are universal.

In this chapter, the mechanism by which Activin exerts its LGE-inducing effects *in vitro* and whether other signalling pathways play a role in this have begun to be deciphered. The ability of the cells to become functional neurons *in vitro*, has also been analysed in more depth, with the hope that this could one day progress into forming functional *in vitro* cell models or *in vivo* grafts.

## 3.2 Results

### 3.2.1 Activin acts independently of SHH signalling

Activin and other TGF $\beta$  family members have been shown to exhibit a certain degree of promiscuity between their family of receptors (Hooi and Hearn, 2005). In order to verify that Activin was acting via the ALK4/5 receptors to induce LGE gene upregulation, Activin treatment of forebrain progenitors at day 10 was supplemented with an ALK4/5 inhibitor, SB431542 (SB4) (**Figure 3.1A**). This data forms part of a larger dataset with a higher n number included in a previous lab publication, which supports the conclusions drawn in this section (Arber *et al.*, 2015). Activin-induced expression of *CTIP2* and *GSX2* by day 19 was abolished in the presence of SB4, confirming receptor-specific activity (**Figure 3.1B**).

With the aim of exploring a potential role of SHH signalling in the LGE-inducing effects of Activin, either SHH or its inhibitor, cyclopamine, were added to Activin treatment. Neither molecule had any effect on *CTIP2* or *GSX2* expression levels at day 19, although *DLX2* mRNA was doubled only in the SHH condition. *NKX2.1* expression was also doubled by the presence of SHH while Activin alone actually reduced its mRNA levels. These findings were further corroborated by immunostaining for NKX2.1 and MSN markers CTIP2 and DARPP32 (**Figure 3.1C**). No NKX2.1 staining was observed in Activin only conditions at d18, whereas the addition of SHH caused a visible increase in the number of NKX2.1-positive cells. Although not quantified, MSN marker expression induced by Activin appeared to be unaffected by the addition of SHH both at the progenitor stage (day 23) and in mature neurons (day 35), which was in line with the qPCR data.

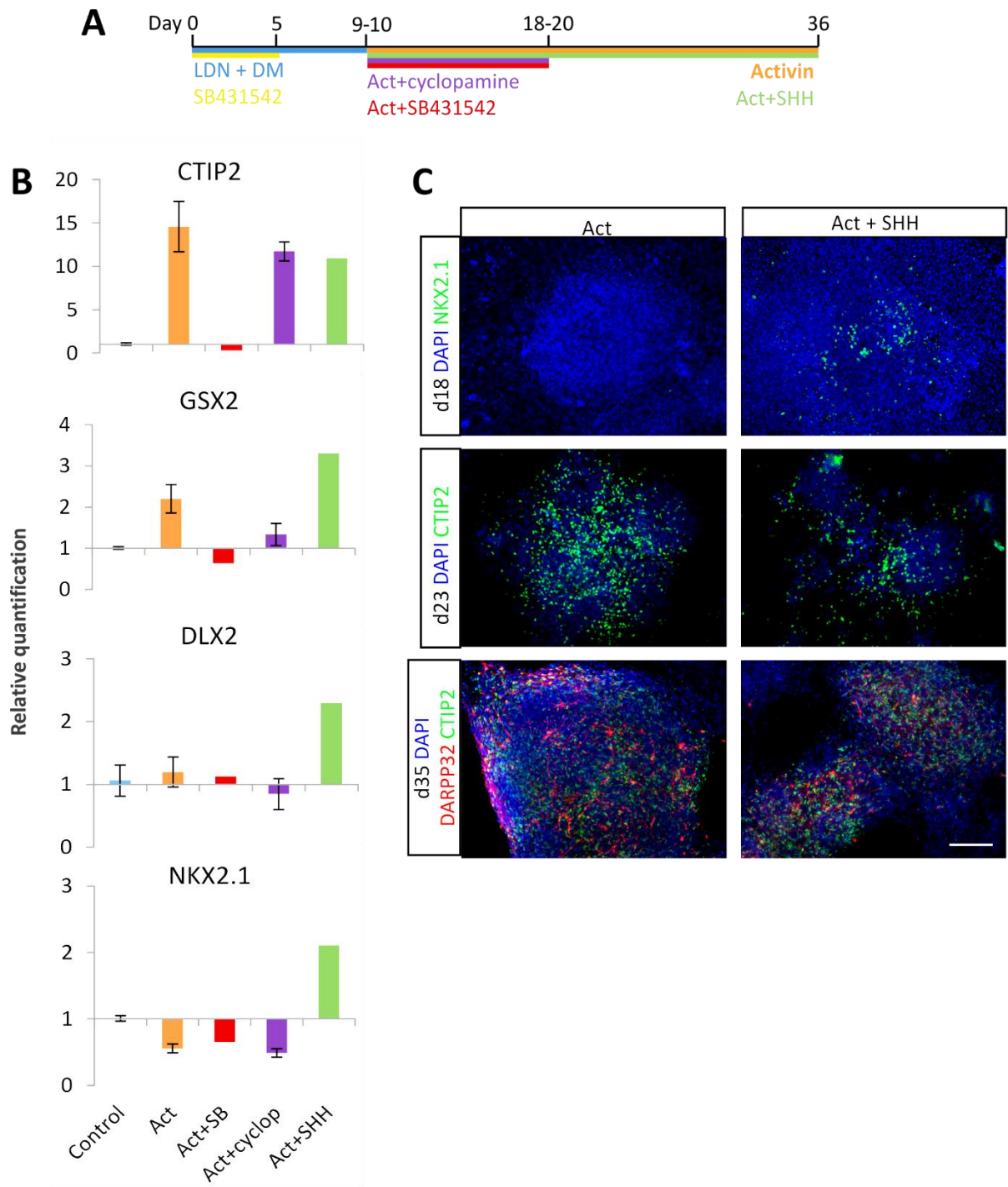


**Figure 3.1: Activin exerts LGE-inducing effects independently of SHH**

A) Schematic timeline of MSN differentiation of H7 cells, with the different conditions colour-coded to the graphs in (B). B) qPCR data from RNA extracted from day 19 samples after treatment with Activin (25 ng/ml) alone or plus SB431542 (10  $\mu$ M), cyclopamine (1  $\mu$ M) or SHH (200 ng/ml) as shown in (A). Data show mean RQ  $\pm$  SEM relative to control (n = 6 (control), 6 (Act), 2 (Act+SB), 4 (Act+cyclop) and 2 (Act+SHH), respectively). C) Immunostaining of day 18, 23 and 35 differentiated cells treated with Activin alone or plus SHH (Scale bar 100  $\mu$ m).

### 3.2.2 Activin acts selectively via ALK5 receptor

With the aim of teasing apart the different TGF $\beta$  pathways that could be activated by treatment of hPSC-derived forebrain progenitors with Activin, a screen of three chemical inhibitors selective for different ALK receptors was given with Activin from day 10. SB525334 (SB5) is an ALK5 inhibitor that also inhibits ALK4 with 4-fold less potency, but is inactive at ALK2/3/6. LY2109761 (LY) is a selective dual ALK5 (TGF $\beta$ -RI)/TGF $\beta$ -RII inhibitor. LDN193189 (LDN) is a selective ALK2/3/6 inhibitor that only affects BMP signalling. Cells were treated with Activin with or without inhibitors from day 10 of differentiation, and then lysed for RNA extraction 1, 3 or 6 days later (**Figure 3.2A,B**). Levels of mRNA from all conditions and time points were normalised to the control condition at 1 day (differentiation day 11).

After 24 hours, Activin alone induced an increase in expression of *CTIP2*, *GSX2* and *NKX2.1* by 2.9, 2.5 and 3.5-fold respectively compared to the untreated control condition (**Figure 3.2B**). This effect was mostly abolished by all of the inhibitors, with LDN consistently showing the least inhibition across all genes. At the 3-day time point, there was very little change in gene expression from control, aside from a small increase in *GSX2* levels in the Activin and control conditions.

At 6 days, the level of *CTIP2* rose by 6-fold in the Activin condition, which was completely inhibited by SB5 and LY, the TGF $\beta$ /Activin pathway inhibitors (**Figure 3.2B**). Surprisingly the addition of LDN to Activin caused an 18-fold increase in *CTIP2* mRNA levels, although this was also completely abolished by the further addition of both SB5 and LY. *GSX2* expression increased 11-fold in the control condition, whereas Activin alone only led to a 7.6-fold increase. Again, Activin plus LDN saw a modest increase in *GSX2* compared to the control, of 13.2. *NKX2.1* mRNA levels dropped to nearly undetectable levels in all conditions. *PAX6* expression was consistently higher than the subpallial markers from the first time point, but remained constant in all conditions across all time points.

The unexpected result from the Activin plus LDN condition was verified using a second qPCR experiment repeating the control, Activin and Activin plus LDN conditions at 1 and 6 days after starting treatment (**Figure 3.2C**). Activin caused a 3-fold upregulation of *CTIP2*, which was found to not be significantly different from the control condition at either time point. The addition of LDN, however, caused a significant 5.8-fold increase in *CTIP2* mRNA compared to all conditions after 1 day and the control condition at 6 days. Again, there was a large and significant upregulation of *GSX2* in the control condition (39.6-fold), which was closely matched by the Activin treatment. Activin plus LDN caused a further increase (56.7-fold), which was significantly different from both control and Activin alone.

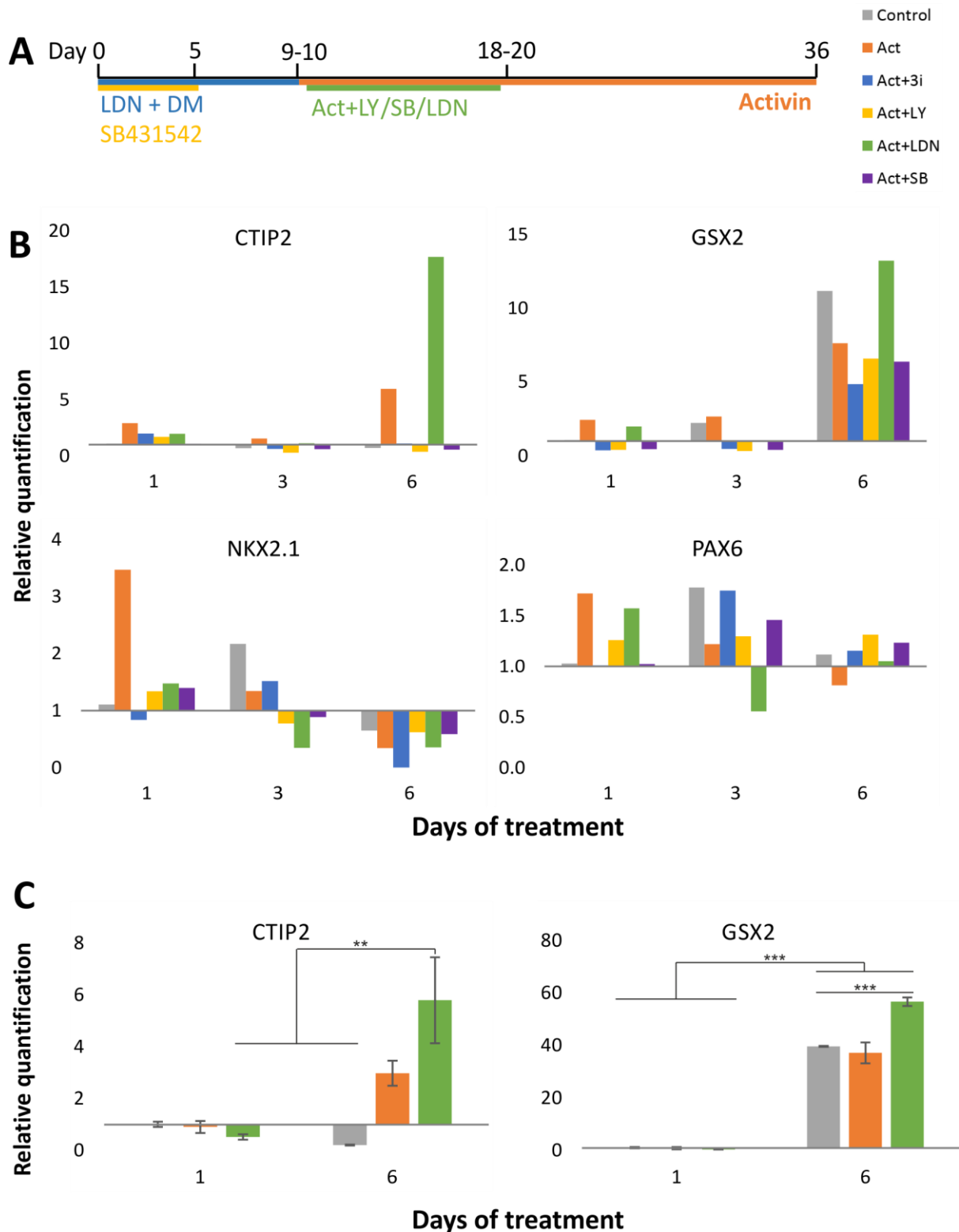


**Figure 3.2: Activin exerts its effects selectively via the ALK5 receptor.**

A) Schematic timeline of MSN differentiation of H7 cells, with the legend of the different conditions used in (B) and (C). B) qPCR data from RNA extracted 1, 3 or 6 days after treatment that began on day 10 of differentiation. Cells were untreated (control) or treated with Activin (25 ng/ml), or Activin plus SB525334 (1  $\mu$ M), LY2109761 (5  $\mu$ M) or LDN193189 (100 nM). Data show mean RQ relative to the 1 day control ( $n = 2$ ). C) A repeat of the experiment in (B) with just control, Activin and Activin plus LDN conditions to confirm the LDN effects on CTIP2 and GSX2 upregulation. Data show mean RQ  $\pm$  SEM relative to the 1 day control ( $n = 3$ ; \*\* $P < 0.01$ , \*\*\* $P < 0.001$ ; two-way ANOVA with post-hoc Bonferroni).



### 3.2.3 Inhibition of BMP signalling accelerates Activin effects

The unexpected finding that inhibition of BMP signalling by LDN could enhance LGE gene upregulation by Activin prompted further enquiry into its effects on protein expression at the MSN stage of differentiation. Day 10 differentiated H7 hESCs and i900 human iPSCs cells were treated with Activin with or without LDN (100 nM). Activin treatment in both conditions continued throughout the experiment, while addition of LDN was stopped at day 20 based on a preliminary experiment. Cells were fixed for immunostaining at days 20, 25, 30, 35 and 40 (**Figure 3.3A**) and cell fate markers were counted as a proportion of DAPI (**Figure 3.3B,C,D**).

The percentage of NeuN-positive cells increased between days 30 and 40 in all conditions, from around 60% to 80%. There was no significant difference in the number of neurons between any of the groups at any time (**Figure 3.3B**). In H7 cells, there was no difference in the percentage of CTIP2 or DARPP32-positive cells between the conditions at days 20, 25 and 40 (**Figure 3.3C**). However, at days 30 and 35 there was a significant 10% increase in the number of CTIP2-positive cells with LDN compared to Activin alone. This was also seen in the number of DARPP32-positive cells, which was more than doubled at day 30. There was a final increase in CTIP2 and DARPP32 numbers in the final 5 days of differentiation in both conditions, causing the Activin cultures to catch up in the number of cells expressing both markers.

In contrast to these findings, the number of CTIP2 and DARPP32-positive neurons from the i900 cell line remained equal between the conditions from day 20 to 30 (**Figure 3.3C**). At day 40, however, while the proportion of CTIP2 in the Activin condition appeared to plateau, LDN caused a 17% increase in the number of positive cells. Although there were 5% more DARPP32-positive cells with LDN at day 40, this was not significant.

There was no effect on other markers that were looked at with immunostaining, including *Islet1*, *Meis2*, *FOXP2* and *NOLZ1*, nor other neuronal fate markers such as *TH*, *SST* or *PV*. The only marker that did seem to change was the proportion of calretinin-positive cells. The Activin protocol routinely produces around 3% calretinin neurons, but the H7 LDN condition saw this proportion double to 6% by day 40 (**Figure 3.3D**). In the i900 cultures, the number of calretinin cells was much higher in Activin than with LDN at day 30 (8 and 3% respectively), but this had equalised by day 40 at around 7% for both conditions.

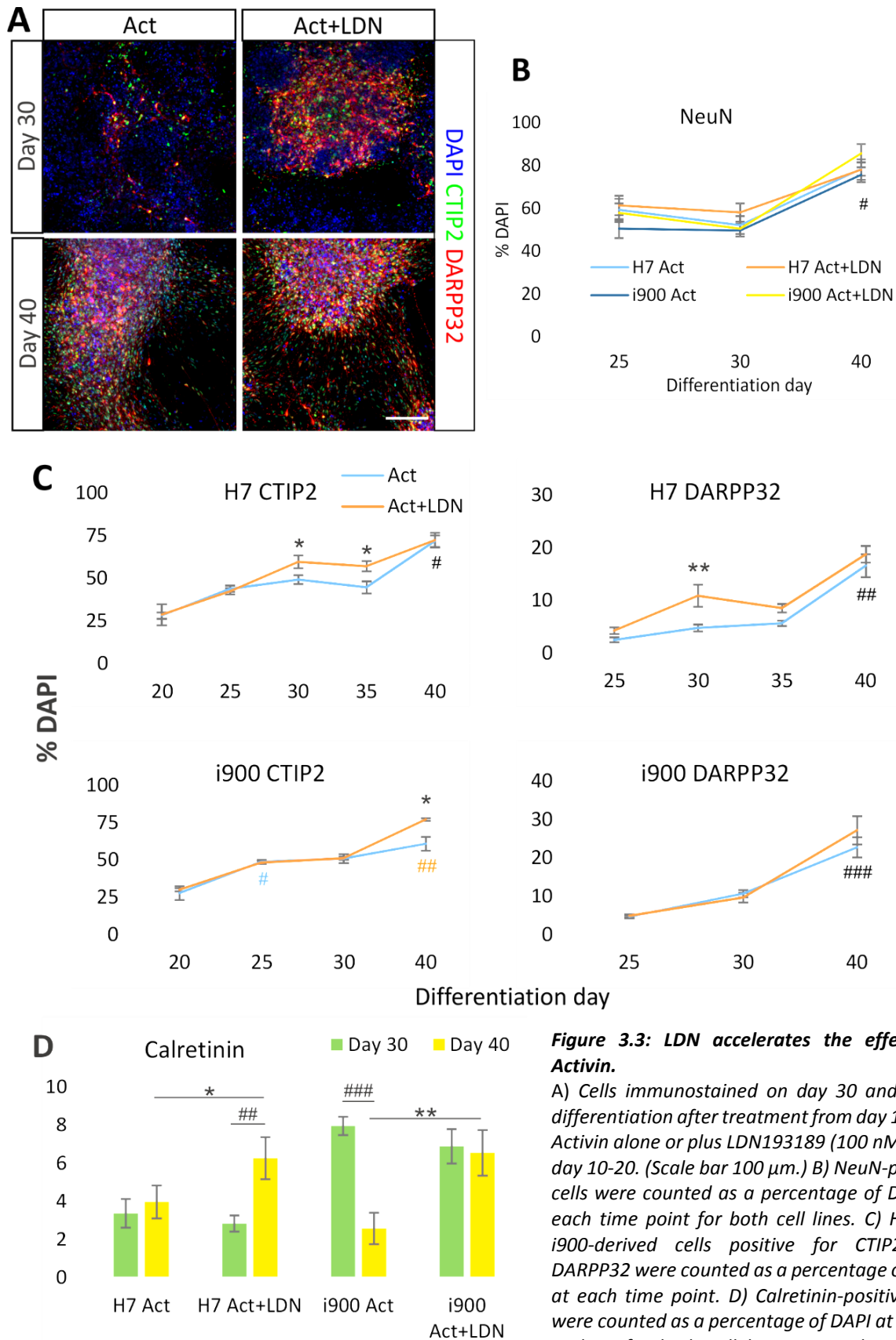


**Figure 3.3: LDN accelerates the effects of Activin.**

A) Cells immunostained on day 30 and 40 of differentiation after treatment from day 10 with Activin alone or plus LDN193189 (100 nM) from day 10-20. (Scale bar 100  $\mu$ m.) B) NeuN-positive cells were counted as a percentage of DAPI at each time point for both cell lines. C) H7 and i900-derived cells positive for CTIP2 and DARPP32 were counted as a percentage of DAPI at each time point. D) Calretinin-positive cells were counted as a percentage of DAPI at day 30 and 40 for both cell lines. Data show mean

percentage  $\pm$  SEM of positive cells from 3 independent experiments (\* and # denote significant differences between the conditions and the time points, respectively, with the coloured # indicating where just one condition has changed. \* $P$ <0.05, \*\* $P$ <0.01, \*\*\* $P$ <0.001; two-way ANOVA with post-hoc Bonferroni).

### 3.2.4 Electrophysiological characterisation of hESC-derived MSNs *in vitro*

It has been shown recently that the addition of a combination of small molecules and factors can help to enhance maturation of hPSC-derived neurons *in vitro*, by mimicking the supportive effects of astrocytes (Telezhkin *et al.*, 2015). In order to demonstrate the potential of hESC-derived DARPP32-positive cells to become functional neurons that can be used to model synaptic or network properties of MSNs, the cells were plated at low density on day 30 of the MSN differentiation protocol. Immature neurons were given SCM1 medium for 8 days, followed by SCM2 medium for the remainder of the culture time. A control group was also given the usual basal N2B27 medium with BDNF and GDNF. Electrophysiological properties were recorded by whole cell patch clamp recordings from neurons at days 45 and 90 of differentiation (**Figure 3.4A**). Cells did not show any obvious reduction in expression of DARPP32 or CTIP2 in response to the SCM media, meaning that approximately 30% of cells patched should be DARPP32-positive (**Figure 3.4B**).

The mean resting membrane potential (RMP) was the same between basal and SCM at day 45 (-31.5 mV and -29.1 mV respectively). At day 90 however, the SCM group had an average of -37.9 mV, significantly lower than -30 mV in the basal medium (**Figure 3.4C**). Having observed that a subset of the cells recorded fired induced action potentials (APs) upon current injection (iAP) while others showed no activity at all (nAP), the groups were split into iAP and nAP to look at whether this would alter the mean RMP (**Figure 3.4D**). Indeed, there was an overall significant difference between iAP and nAP cells at all time point and in both basal and SCM conditions. Interestingly, the SCM groups at day 90 had the same mean RMP regardless of whether they fired APs or not. At day 45, there was no difference in mean input resistance between basal and SCM (580 m $\Omega$  and 586 m $\Omega$  respectively) (**Figure 3.4E**). By day 90, the mean input resistance of cells in the basal medium had reduced to 342 m $\Omega$ , while SCM cells showed a further significant decrease to 195 m $\Omega$ .

Cells were recorded in current clamp and injected with current steps of 10 or 20 pA between -100 and +100 pA. At day 45 only 1 cell in each condition fired any spontaneous APs, and 3 cells fired at least 1 AP following current injection (**Figure 3.5A**). Two cells in each condition responded with trains of more than 2 APs (**Figure 3.5B**). At day 90, cells in the basal condition had lost all spontaneous activity and only 1 cell fired a full AP upon stimulation. In the SCM condition, more spontaneous activity was observed than at day 45, with 2 cells firing full APs, 2 attempting APs and 2 cells showing evidence of synaptic activity in the form of post-synaptic potentials (PSPs). All but 3 cells fired APs upon current injection, however the majority of APs occurred as “rebound spikes” following the negative current steps (**Figure 3.5B**). Having observed the increase in activity when depolarising back to RMP from a negative current step, each SCM cell was held at -60 mV and the current step protocol repeated to detect any changes in activity. Cells displayed more spontaneous activity, with 2 cells showing

repetitive firing and 6 cells firing sporadic APs. There was also increased activity during the current steps, with only 1 cell failing to fire a full AP, and the majority at least attempting to fire a train of APs (Figure 3.5B,C).

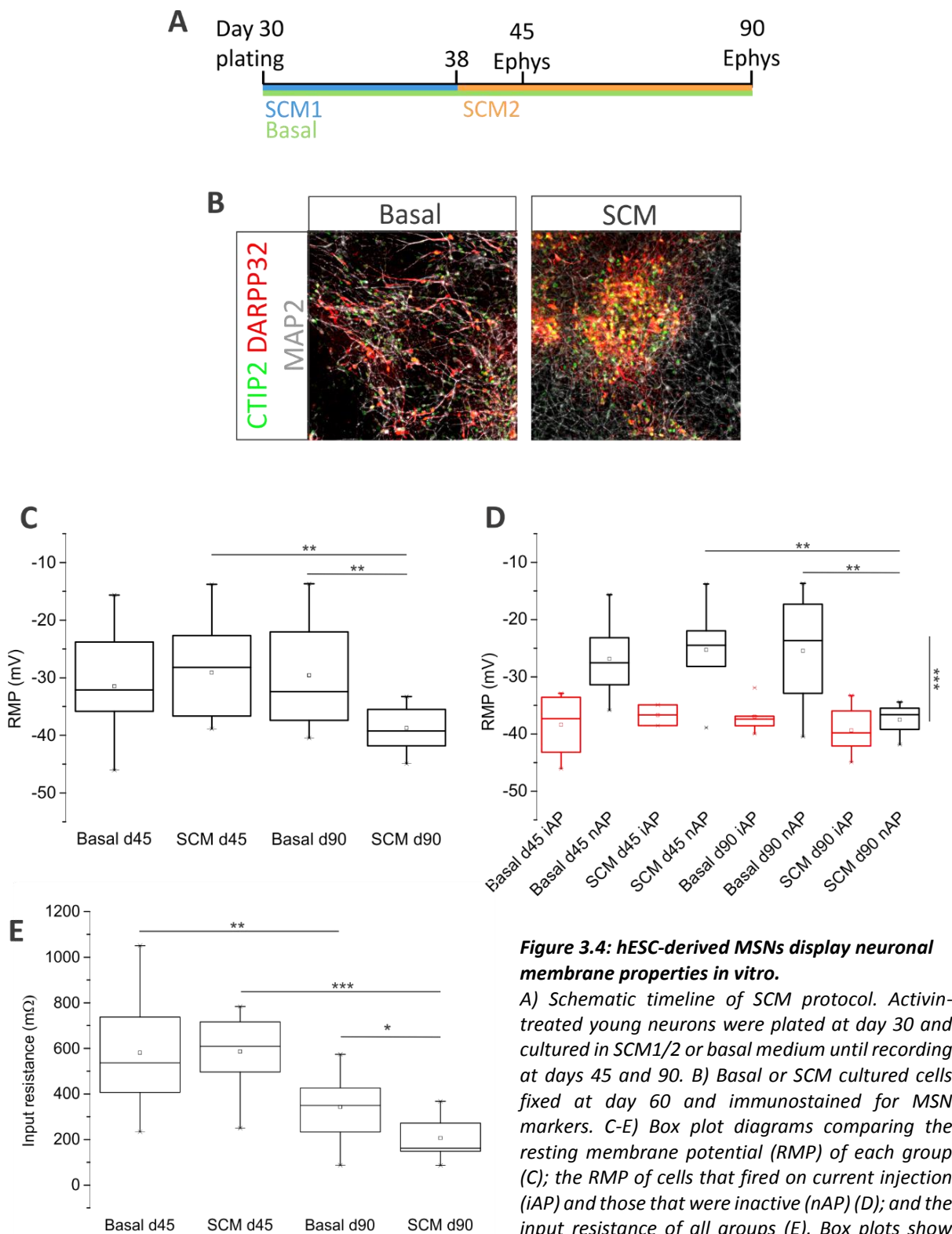


**Figure 3.4: hESC-derived MSNs display neuronal membrane properties in vitro.**

A) Schematic timeline of SCM protocol. Activin-treated young neurons were plated at day 30 and cultured in SCM1/2 or basal medium until recording at days 45 and 90. B) Basal or SCM cultured cells fixed at day 60 and immunostained for MSN markers. C-E) Box plot diagrams comparing the resting membrane potential (RMP) of each group (C); the RMP of cells that fired on current injection (iAP) and those that were inactive (nAP) (D); and the input resistance of all groups (E). Box plots show median with 25<sup>th</sup> and 75<sup>th</sup> percentiles (box) and outliers (whiskers), as well as the mean (square) (n cells = 10 (Basal d45), 9 (SCM d45), 14 (Basal d90) and 15 (SCM d90)). Two-way ANOVA with post-hoc Bonferroni; \*P<0.05, \*\*P<0.01, \*\*\*P<0.001).

Two-way ANOVA with post-hoc Bonferroni; \*P<0.05, \*\*P<0.01, \*\*\*P<0.001).

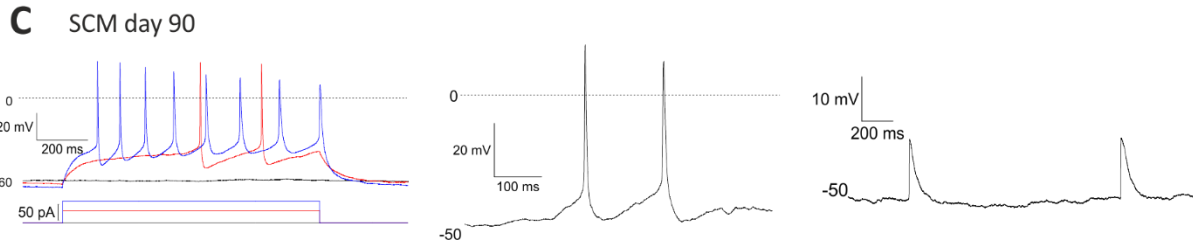
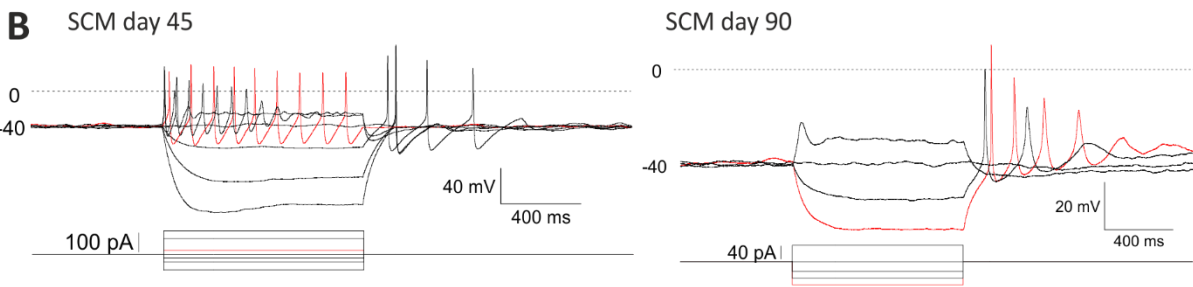
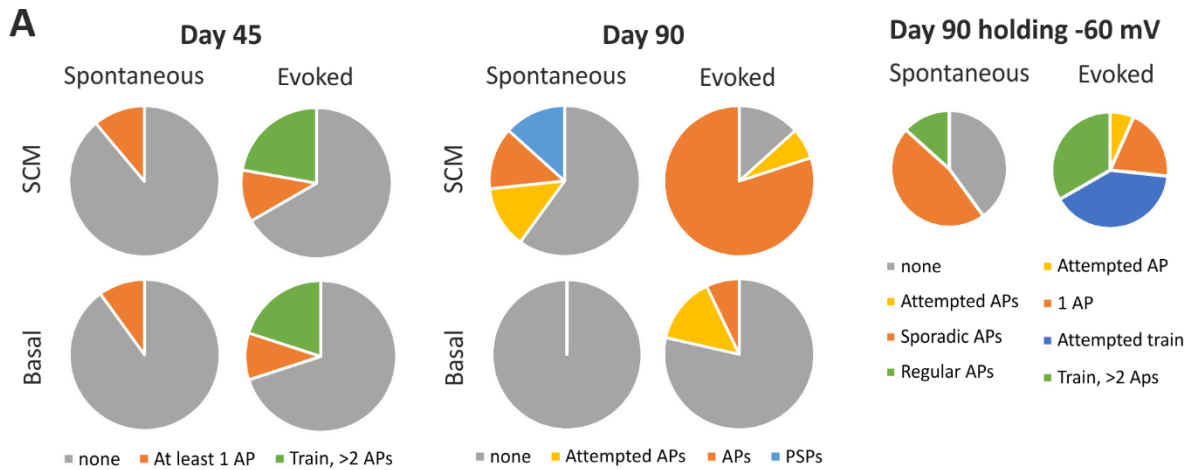


**Figure 3.5: hESC-derived MSNs display spontaneous and evoked neuronal activity in vitro.**  
 A) Pie charts showing the proportion of cells in SCM and basal conditions that displayed spontaneous or evoked activity at days 45 and 90 from their RMP (left and middle), and SCM at day 90 from a holding potential of -60 mV (right). Basal n=10 (d45), 14 (d90); SCM n=9 (d45), 15(d90). B) Representative traces of SCM cells at days 45 and 90, showing voltage responses to consecutive current steps. C) Example traces of SCM day 90 cells displaying repetitive firing when held at -60 mV (left); spontaneous AP firing from resting (middle); and spontaneous post-synaptic potentials (PSPs) while held at -60 mV (right).

### 3.3 Discussion

In this chapter I have begun to dissect the different components that could be contributing to the mechanism by which Activin induces LGE characteristics in hPSC-derived forebrain progenitors. Activation of SHH signalling has typically been the approach taken for the generation of MSNs from hPSCs, however the data presented here, which is included in a larger dataset that has been published, depicts Activin as a distinct pathway completely independent of SHH (Arber *et al.*, 2015). Neither blockade of SHH signalling, nor addition of SHH, had any impact on the increased expression of LGE-specific genes induced by Activin treatment. Indeed, *Shh* knockout mouse embryos retain expression of LGE markers *Dlx2* and *Gsx2*, albeit displaced ventrally in the absence of an *Nkx2.1*-expressing MGE (Rallu *et al.*, 2002). This shows that LGE formation is possible in the absence of *Shh* activation and indicates an alternative pathway by which LGE induction can still occur. Conversely, a study using a zebrafish model of development demonstrated that the presence of Nodal, a TGF $\beta$  family member that shares receptors with Activin, is necessary for *Shh* expression across the CNS and likely acts upstream of *Shh* to establish dorso-ventral patterning of the telencephalon (Rohr *et al.*, 2001). Ventral expression of the zebrafish *NKX2.1* homologue, *nk2.1b*, was abolished in Nodal signalling-deficient embryos, but could be partially restored through ectopic *Shh* expression. Another group more recently showed that *Smad3*, an intracellular effector of TGF $\beta$ , Nodal and Activin signalling, is highly expressed in the subpallium throughout development, further highlighting the importance of these signalling pathways (Casari *et al.*, 2014). It would be worth looking at whether SHH or any component of its downstream signalling pathway is upregulated in Activin-treated cultures.

The use of two TGF $\beta$ -RI (ALK5) inhibitors with slightly differing selectivity for other ALK receptors indicated that Activin exerts its effects via both ALK5 and ALK4, as SB5, which inhibits both ALKs, was consistently more effective at inhibiting LGE marker up-regulation than LY. Furthermore, SB4 in earlier experiments demonstrated a complete abolishment of LGE marker expression, both at the mRNA and protein levels. This is in agreement with the fact that Activin binds to both receptors *in vivo* and that they have the same intracellular effector proteins, *Smad2/3*, which should have the same transcriptional targets (Piek, Heldin and Ten Dijke, 1999).

Through the screening of 3 TGF $\beta$  family inhibitors, it was found that blocking BMP signalling could enhance Activin-induced upregulation of LGE markers CTIP2 and GSX2. While the bulk of the CTIP2 increase occurred at the later time point, with LDN comfortably doubling the effect of Activin, GSX2 levels increased earlier in Activin and appeared to be caught up by the control around day 3. LDN maintained higher levels of GSX2 by day 6. These differences in gene expression could be put down to either LDN improving the differentiation of the cells towards the LGE lineage and potentially increasing the final number of MSNs, or simply that the LDN changed the kinetics of the differentiation causing

gene expression levels to increase and decrease at different times between the conditions. This was tested by looking at MSN markers at different time points in 2 cell lines. Our MSN differentiation protocol is extremely robust and has been repeated many times in the H7 cell line (Arber *et al.*, 2015). From this, we know that the peak of DARPP32 expression is by day 40, so this was the last time point in this experiment. Indeed, in H7 cells, the increase in CTIP2 and DARPP32 in the middle time points suggests that blockade of BMP signalling accelerates the MSN differentiation, but cannot improve the final outcome. It is important to note that there was no effect of LDN on the number of NeuN-positive cells, showing that it is not simply an improvement of neural induction by Smad inhibition. The results from the i900 cells contrast with these findings, the level of CTIP2 remained equal up until day 40, when they diverged. It is unknown whether this would have plateaued, as in the H7 cell line, or continued to rise further. It would be interesting to verify this result, as it would mean that the addition of LDN until day 20 could cause a difference in CTIP2 expression 20 days after treatment had ended. It is not surprising that LDN also had an effect on the number of calretinin-positive neurons, as we previously showed that late treatment of forebrain progenitors with Activin produces CGE-derived calretinin interneurons (Cambray *et al.*, 2012).

BMPs are heavily involved in dorsal neural tube development, but are specifically expressed in the dorsal midline of the forebrain (Hu *et al.*, 2008). It is therefore possible that the enhancement of Activin-induced CTIP2 and GSX2 expression by BMP receptor inhibition is down to the suppression of a dorso-medial telencephalic fate, encouraging the cells more ventro-lateral towards an LGE fate. The default fate for the dual Smad inhibition neural induction protocol is dorsal forebrain fate, with high PAX6 expression and eventually the expression of mature cortical layer markers (Chambers *et al.*, 2009). Neither treatment with Activin alone or with LDN appeared to affect the expression of PAX6, although there is some PAX6 expression in the LGE so other dorsal markers would need to be analysed to test this theory. It is likely that inhibition of BMP signalling could simply reduce the lineage options for neural progenitors to take, leading to an increase in CTIP2-positive LGE progenitors.

As Activins and BMPs share some common Type II receptors (ActR-II and ActR-IIB), it is also possible that LDN, which inhibits BMP Type I receptors ALK1/2/3/6, causes more Type II receptors to be available for Activin to bind and increase Smad2/3 phosphorylation (Piek, Heldin and Ten Dijke, 1999). Indeed Smad2 has been shown to directly interact with the GSX2 gene, supporting the result that LDN increased GSX2 expression (Maira *et al.*, 2010). Previous unpublished work in our lab into the dose response of Activin showed that increasing the concentration of Activin could further increase the expression of LGE markers. So increasing receptor availability or non-specific binding is another likely explanation for this effect.

It is worth noting that we have shown previously that adding Activin from differentiation day 10 to 20 is crucial for obtaining a high proportion of DARPP32-expressing neurons in the H9 hESC line; any longer than this continues to increase the proportion of CTIP2-positive cells but has no effect on DARPP32 expression (Arber *et al.*, 2015). The data from the H7 cells support this, as increased expression can be seen in the middle of the differentiation, but there appears to be a maximum possible proportion of both CTIP2 and DARPP32. The i900 cells did show a higher proportion of CTIP2-positive cells in the LDN condition at day 40, which may indicate that their differentiation kinetics are different from H7, taking longer for the effects to be detected. However, from observing the cells in culture they actually appeared to mature faster than their H7 counterparts, and tended to express mature MSN markers in higher proportions, so it is unclear what led to these differences. These findings require further clarification by testing firstly whether Activin increases the phosphorylation of Smad2/3 in these cultures, and if so, whether LDN further upregulates this phosphorylation.

We have provided much evidence that Activin robustly generates neurons from hESCs that express the correct proteins and mRNA to be defined as striatal MSN-like (Arber *et al.*, 2015). Moving forward, if these cells are to be used as a source of tissue for transplantation or *in vitro* modelling of disease or striatal function, they must also become electrophysiologically active and mimic certain characteristics of real MSNs. Patch clamp recordings from rat MSNs in acute brain slices show that they have a relatively hyperpolarised RMP of around -80 mV and an average input resistance of 193 M $\Omega$  (Kawaguchi, 1993). However, human foetal neurons from 20-22 weeks gestation have shown RMPs of -45-55 mV and input resistances of 0.9-2.5 G $\Omega$ , which may be more indicative of what can be expected of hPSC-derived neurons (Moore *et al.*, 2011; Nicholas *et al.*, 2013). There has been very little work done on hPSC-derived MSN electrophysiology, with focus being on developing methods for their production (Carri *et al.*, 2013; Arber *et al.*, 2015). The HD iPSC consortium described some deficits in action potential firing in iPSC-derived neurons from HD patients, but the proportion of DARPP32-expressing MSNs in the cultures was very low (The HD iPSC Consortium, 2012). SCM media described by Telezhkin *et al.* had no effect on hESC-derived MSNs at day 45 of differentiation compared to the usual basal differentiation medium. This is in contrast to their findings, which demonstrated significant improvements in membrane properties by day 36 (Telezhkin *et al.*, 2015). However, individual cell lines have distinct differentiation and maturation kinetics, so cells were recorded from again at day 90. At this later time point, cells in the basal condition had lost most of their functionality, perhaps indicating a decline in the health of the cells. Neurons in the SCM medium were almost all able to fire action potentials either from resting or after being held at -60 mV. Cells from either condition that were able to fire action potentials had a RMP of around -40 mV, with the most hyperpolarised cell resting at -45 mV. This is in line with the kinds of values observed by Telezhkin *et al.*, whereas Song *et*



*al.* managed to produce neurons with RMPs of -70 mV after just 3 weeks in culture (Song *et al.*, 2013; Telezhkin *et al.*, 2015). Interestingly, Kirwan *et al.* showed that 4 different hPSC lines differentiated in exactly the same way could have very different RMPs, ranging from -40 mV to -55 mV, while also exhibiting very similar firing properties (Kirwan *et al.*, 2015). A key finding in the data presented here is that despite the inability of positive current injection to stimulate an action potential, in returning to baseline from a negative current step the majority of cells fired at least one action potential. This is likely due to the inactivation of voltage-gated sodium channels held at depolarised membrane potentials of -40 mV or above (Bean, 2007). This means that when the cell is hyperpolarised by negative current injection the channels can reactivate, then as the current step ends the membrane potential returns to its RMP allowing the channels to open as the membrane reaches the action potential threshold. This also means that action potentials fired in these conditions often had a larger amplitude as they were able to recruit more sodium channels. Artificially holding the membrane potential in a hyperpolarised state by injecting negative current may be a good way to observe some of the more interesting properties of the neurons, such as synaptic events and spontaneous activity. Input resistance in our cells was relatively low compared to other studies, and it decreased over time and further with addition of SCM media. Even Telezhkin *et al.* showed an average input resistance of around 800 M $\Omega$ , while others consistently observed measurements of more than 2 G $\Omega$ . This could be another difference between cell lines or represent neuronal subtype-specific differences in ion channel expression.

The desire to obtain homogeneous cultures may be holding back this particular aspect of neuron differentiation from hPSCs, as this completely ignores the heterogeneity of the developing brain. The motivation behind the Telezhkin *et al.* study was to design a fully-defined medium that could enhance maturation of hPSC-derived neurons by mimicking the positive effects of astrocyte conditioned medium (Rushton *et al.*, 2013; Telezhkin *et al.*, 2015). However, while achieving a homogeneous culture of functional neurons in a matter of weeks may be beneficial for high throughput analysis of different cell lines or drug screening, it may not be useful for more complex studies modelling brain function due to the absence of astrocytes and the tripartite synapse. The opportunity to observe the activity of human neurons *in vitro* is certainly worth maximising and more work must be done to devise optimal culture paradigms by which to study their function. This should include high throughput methods such as this one, as well as more complex co-culture systems involving all the relevant cell types for a certain brain region or circuit.

Data presented in this chapter have shown that Activin selectively activates ALK4/5 receptors, sufficient to upregulate CTIP2 and GSX2 expression independently of SHH signalling. Evidence is also shown suggesting that this effect may be marginally enhanced by inhibiting BMP Type I receptors.

Basic electrophysiological characterisation of the cells has demonstrated that they can become functional enough to study membrane and synaptic properties, but further analysis will show whether the cells have MSN-specific characteristics such as the response to dopamine release or susceptibility to excitotoxicity.

## 4 Characterisation of hPSC-derived MGE-like interneurons

### 4.1 Introduction

Striatal interneurons are often ignored when discussing striatal function or the impact of HD. Most of our knowledge comes from studies in rodents, whose interneurons comprise only 5% of neurons in the striatum. In contrast, human and primate interneurons make up 23% of striatal neurons (Graveland and Difiglia, 1985; Wu and Parent, 2000). This is a large disparity, and indicates a more important role for primate interneurons compared to rodents'. It would be useful to generate human striatal interneurons from hPSCs for the ability to study them *in vitro* and transplanted in rodent striatum for a direct comparison between species. The more cell types we can produce *in vitro*, the more complex culture systems we may be able to exploit for modelling either striatal function alone or in networks with other neuronal subtypes such as cortical, pallidal or nigral neurons. Striatal interneurons originate in the MGE, along with cortical and hippocampal interneurons, and neurons of the globus pallidus, septum, pre-optic area, amygdala and basal forebrain (Marin, Anderson and Rubenstein, 2000; Flandin, Kimura and Rubenstein, 2010). Distinct mature markers define the different subtypes of interneurons and projection neurons produced in the MGE, of which ChAT, PV and SST are the main subpopulation identifiers (**Figure 1.3**). A small proportion of CR interneurons are also produced in the MGE, some co-expressing SST, but the majority are born in the nearby CGE. Before their migration away from the MGE, progenitors can be identified by their combinatorial expression of NKX2.1, OLIG2, ASCL1 and DLX1/2, followed by post-mitotic expression of LHX6 or LHX7 for GABAergic or cholinergic neurons respectively (Marin, Anderson and Rubenstein, 2000; Nóbrega-Pereira *et al.*, 2010).

Although loss of striatal MSNs represents the most marked cell loss in HD, PV interneurons are also diminished by up to 80% in symptomatic HD patients (Reiner *et al.*, 2013). Other interneuron subtypes, such as SST, NPY, CR and cholinergic, are spared, although CR and ChAT expression are lost in surviving large cholinergic interneurons, causing previous confusion as to their fate (Massouh *et al.*, 2008). There is uncertainty as to which interneuron subtypes survive the quinolinic acid (QA) lesion, used to produce the majority of non-transgenic rodent HD models. Previous work demonstrated that PV interneurons were spared 2 months after intrastriatal QA injection while SST interneurons were lost (Figueredo-Cardenas *et al.*, 1998). Conversely, a more recent study showed that both PV and SST/NPY interneurons were severely reduced, while CR and ChAT interneurons were spared (Feng *et al.*, 2014). It has been shown that the age of the rats receiving the QA lesion can affect the survival or loss of SST interneurons, which may also extend to PV interneurons, potentially explaining the different findings between studies (Figueredo-Cardenas, Chen and Reiner, 1997). Despite this ambiguity in the QA

rodent HD model, the huge difference in proportion of striatal interneurons between rodents and humans suggests that such a reduction in parvalbumin interneurons in HD patients will play a big part in symptom progression. This is particularly relevant to the dystonia associated with HD, as loss of PV striatal interneurons in rodent models has been shown to cause dystonia (Reiner *et al.*, 2013). It is therefore likely that replacement of all cell types will be required to restore striatal function in HD patients, even if this is not necessary for animal models of HD.

Indeed, transplantation of hESC-derived MSNs alone has so far yielded little functional improvement in HD rodent models (Carri *et al.*, 2013; Nicoleau *et al.*, 2013; Arber *et al.*, 2015). The only study that has shown substantial functional improvement was by Ma *et al.*, in which 4% of cells in 4-month-old grafts were interneurons that expressed ChAT (1.5%), PV (1%), CR (1%) and SST (0.5%), due to their use of SHH as a patterning factor (Ma *et al.*, 2012). This is remarkably close to the real percentage of interneurons present in the rat striatum (Wu and Parent, 2000). This may have contributed to the significant motor improvement seen in the QA-lesioned mice, either by replacing both MSNs and interneurons into the lesioned striatum, or by providing the grafted MSNs with target cell types such as interneurons or globus pallidus projection neurons, which are also derived from MGE cells. These are possible mechanisms that could be further explored by achieving differentiation of both MSNs and interneurons from hPSCs as separate, defined populations, then studying their behaviour when cultured or grafted separately and together.

In addition to striatal interneuron changes in HD, there is also evidence of their dysfunction in PD. Mice over-expressing human  $\alpha$ -synuclein experienced early loss of the ability to induce long term potentiation of cholinergic interneurons, but this was fully restored with 3 days of L-DOPA treatment (Tozzi *et al.*, 2015). Similarly, 3 days of dopamine depletion in mice led to a doubling of connectivity between fast-spiking PV interneurons and indirect pathway MSNs. Computational modelling of the striatal micro-circuit revealed that this increase in feed-forward inhibition could result in increased synchrony in indirect pathway output (Gittis *et al.*, 2011). This may explain the increased synchrony and oscillations seen in the subthalamic nucleus and globus pallidus of PD patients.

Dysfunction or imbalance of MGE-derived cortical interneurons is heavily implicated in neurodevelopmental disorders such as epilepsy, schizophrenia and autism, instigating extensive research into their derivation from hPSCs (Maroof *et al.*, 2013; Nicholas *et al.*, 2013; Cunningham *et al.*, 2014; Tyson *et al.*, 2015). However, no one has yet tried to use these same MGE-like progenitors generated from hPSCs to produce striatal interneurons. The typical markers used to distinguish between interneuron subtypes are almost useless in informing whether cultured interneurons are cortical, hippocampal or striatal in nature. PV, SST and CR interneurons are all found in these regions.

Cholinergic interneurons are solely striatal, and derived from the MGE, but distinguishing these from basal forebrain cholinergic projection neurons with any confidence would also be a challenge. The studies described in **Section 1.2.4** named some guidance molecules that are differentially expressed in each population, however the antibodies they used are not commercially available (Villar-Cerviño *et al.*, 2015). Immunohistochemistry performed on brain sections from human foetuses confirmed that migrating interneurons lose NKX2.1 expression by the time they have migrated through the LGE, and switch on the post-mitotic MGE marker LHX6. Meanwhile, interneurons that settle in the striatum appear to maintain expression of both transcription factors, which would be one way to distinguish between cortical and striatal interneurons, but we have been unable to find a LHX6 antibody that works in our hands (Hansen *et al.*, 2013).

*In vitro*, without target brain regions to migrate to, it is difficult to identify the true fate of the MGE-like cells derived from hPSCs. Hence, transplantation into the neonatal brain is one good way to assess the capacity of the cells to differentiate and integrate into appropriate brain regions *in vivo*, which will be addressed in **Chapter 5**. Hypothesising that hPSC-derived MGE progenitors would differentiate into striatal as well as cortical interneurons, the aim of the experiments described in this chapter was to adapt a monolayer differentiation protocol for cortical interneurons published by Maroof *et al.* to our culture conditions and characterise it using qPCR, immunocytochemistry and electrophysiology (Maroof *et al.*, 2013).

## 4.2 Results

### 4.2.1 Activation of SHH signalling induces MGE fate in hPSCs

Human ESCs were differentiated using the protocol described by Maroof *et al.* adapted to our neural induction method by Smad inhibitors LDN193189 and SB431542 in N2B27-defined medium. The addition of XAV939, a Wnt inhibitor, from day 0-9 has been shown to effectively promote forebrain identity and FOXP1 expression (Maroof *et al.*, 2013). SHH and purmorphamine, a SHH agonist, were added following the first passage from day 10 to 18 (**Figure 4.1A**). This induced very strong expression of the MGE marker NKX2.1 – almost 9000-fold higher mRNA levels were detected in SHH-treated versus untreated controls and 63% of cells were immuno-reactive for NKX2.1 (**Figure 4.1B,D,E**). Pan-GE marker *DLX2* mRNA was also substantially increased by 60-fold, whereas the LGE marker *CTIP2* was only increased 3-fold. FOXP1 was expressed in 42% of cells at day 20, while MGE-enriched transcription factors OLIG2 and ASCL1 were expressed by around 20% of cells (**Figure 4.1C,E**). The majority of cells were also Nestin positive, a marker for neural progenitors.

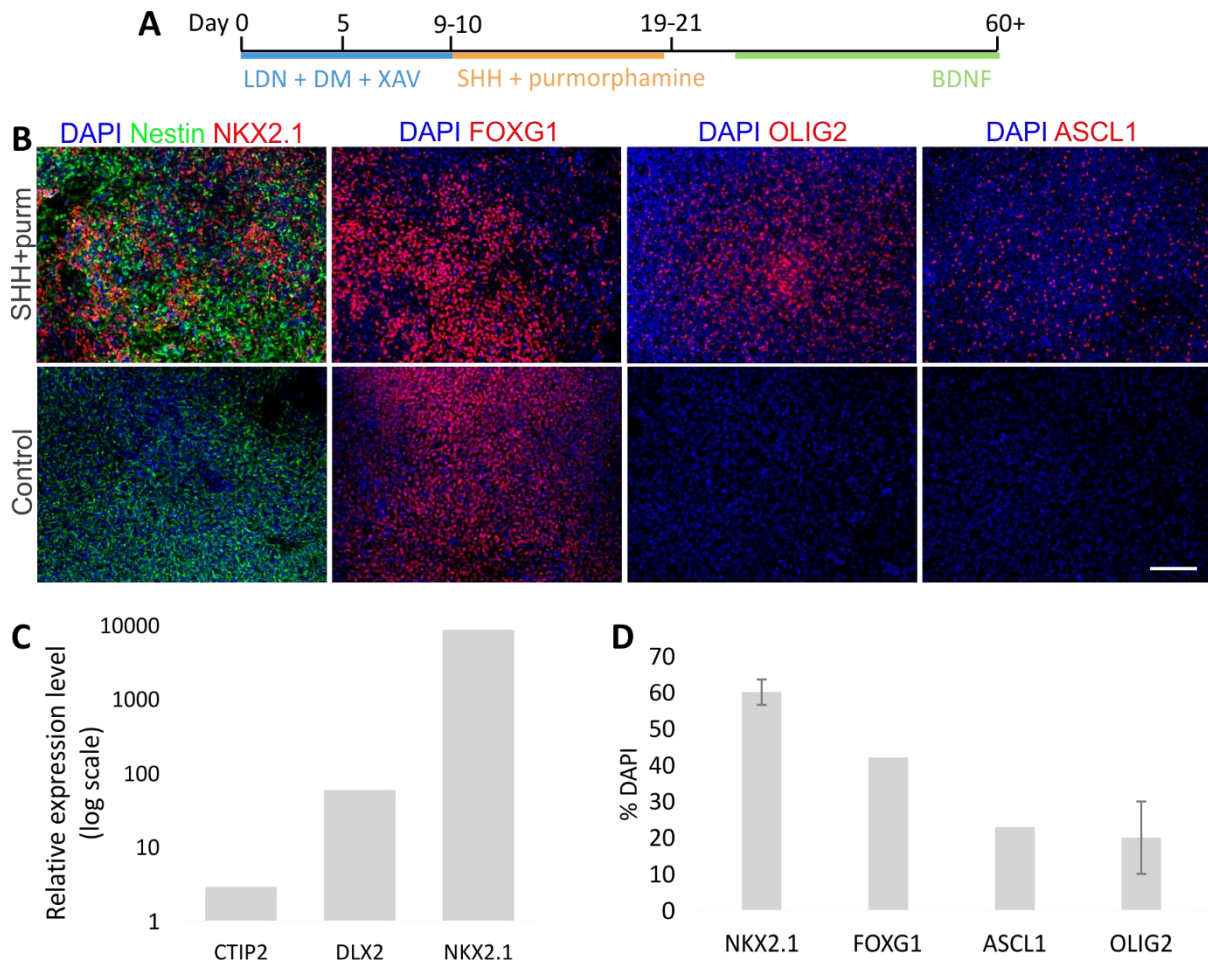


**Figure 4.1: SHH activation induces MGE fate in hESCs**

A) Schematic timeline of MGE differentiation of hESCs. SHH (200 ng/ml) and purmorphamine (1  $\mu$ M) were applied from day 10-18 and BDNF (10 ng/ml) from day 25 onwards. B) Cells immunostained on day 20 of differentiation with NKX2.1, Nestin, FOXG1, OLIG2 and ASCL1 in SHH and control conditions. C) qPCR data from cells lysed on day 18 of differentiation following 8 days of SHH+purm treatment, relative to control. Data show mean RQ (n=2). D) Day 20 cells that stained positive for MGE markers were counted as a percentage of DAPI. Data show mean  $\pm$  SEM from n = 4 (NKX2.1), 1 (FOXG1 and ASCL1) and 3 (OLIG2) independent experiments. Scale bars: white, 200  $\mu$ m; yellow, 100  $\mu$ m; green, 20  $\mu$ m.

4.2.2 MGE progenitors mature into cortical and striatal interneurons

MGE progenitors were kept in culture until day 60 and immunostained for several interneuron subtype markers. At this stage, all of the main mature markers of MGE-derived cortical and striatal interneurons were present (**Figure 4.2A-C**). Somatostatin and parvalbumin are the most abundant types of MGE-derived interneurons, and were found in 7.3 and 5.5% of cells, respectively (**Figure 4.2A,C**). Calretinin interneurons are another common subtype found in the cortex and striatum, the majority of which are born in the CGE, but made up 3% of cells in these cultures (**Figure 4.2B,C**). ChAT is a cholinergic neuron marker found to be expressed in a small number of cells at day 60, which identifies an important striatal interneuron subtype as well as basal forebrain projection neurons. Calbindin is another GABAergic interneuron marker that was abundantly expressed. MAP2, a mature

neuronal marker, was highly expressed throughout the cultures, as was GAD67, a protein specific to GABAergic neurons (**Figure 4.2B**). NKX2.1 expression still appeared to be very high, but had fallen by more than 20% compared to differentiation day 20 (**Figure 4.2D**).

These results show that hPSCs can be efficiently patterned towards MGE progenitor identity and mature into the various neuronal subtypes that derive from the MGE.

#### 4.2.3 hESC-derived MGE progenitors can become functional GABAergic neurons

MGE progenitors differentiated under normoxic conditions were seeded onto coverslips and placed in a hypoxic incubator (2% O<sub>2</sub>) for the remainder of the experiment, due to observed improvements in cell adherence and survival compared to normoxic conditions. They were fed with SCM1 medium from day 22-30, then SCM2 until day 70, when their activity was recorded. Spontaneous and evoked activity was recorded from cells in current clamp mode, once with the cells at their normal resting membrane potential, and once more while holding the cells at -60 mV. Cells were filled with Alexa594 and post-hoc stained for GAD67.

The mean RMP for all cells was -30 mV (**Figure 4.3A**). Cells were divided into two groups based on whether they fired evoked APs from resting (iAP) or not (nAP). However, no difference was seen in mean RMP between the 2 groups. Input resistance also did not differ significantly between iAP and nAP cells, and averaged at 255 MΩ (**Figure 4.3B**). At rest, only 1 cell fired spontaneous APs as well as small PSPs, shown in **Figure 4.3** (C,D). Four other cells did not fire APs but did receive synaptic stimulation evidenced by PSPs. When holding these same cells at a membrane potential of -60 mV, however, all but one began firing full APs, often triggered directly by PSPs, which were also larger in amplitude.

All cells were injected with current steps of 10 or 20 pA between -100 and +100 pA. From resting, half of cells fired at least 1 AP, the majority of which were “rebound spikes” triggered by hyperpolarising negative current. Two cells fired trains of more than 2 APs in succession. When cells were held at -60 mV, only 2 cells did not fire an AP. Three cells fired AP trains, and 2 more attempted to fire trains. The same cell can be seen firing a short train from resting compared to 2 trains of at least 5 APs when held at -60 mV (**Figure 4.3E**).

Of the 12 cells filled with Alexa594 during recording, only 3 were successfully relocated after staining for GAD67. This was likely due to rupturing of the cell membrane during removal of the patch pipette, which would have allowed the dye to leak out. However, all 3 cells that were found were stained positive for GAD67 (**Figure 4.3F**).



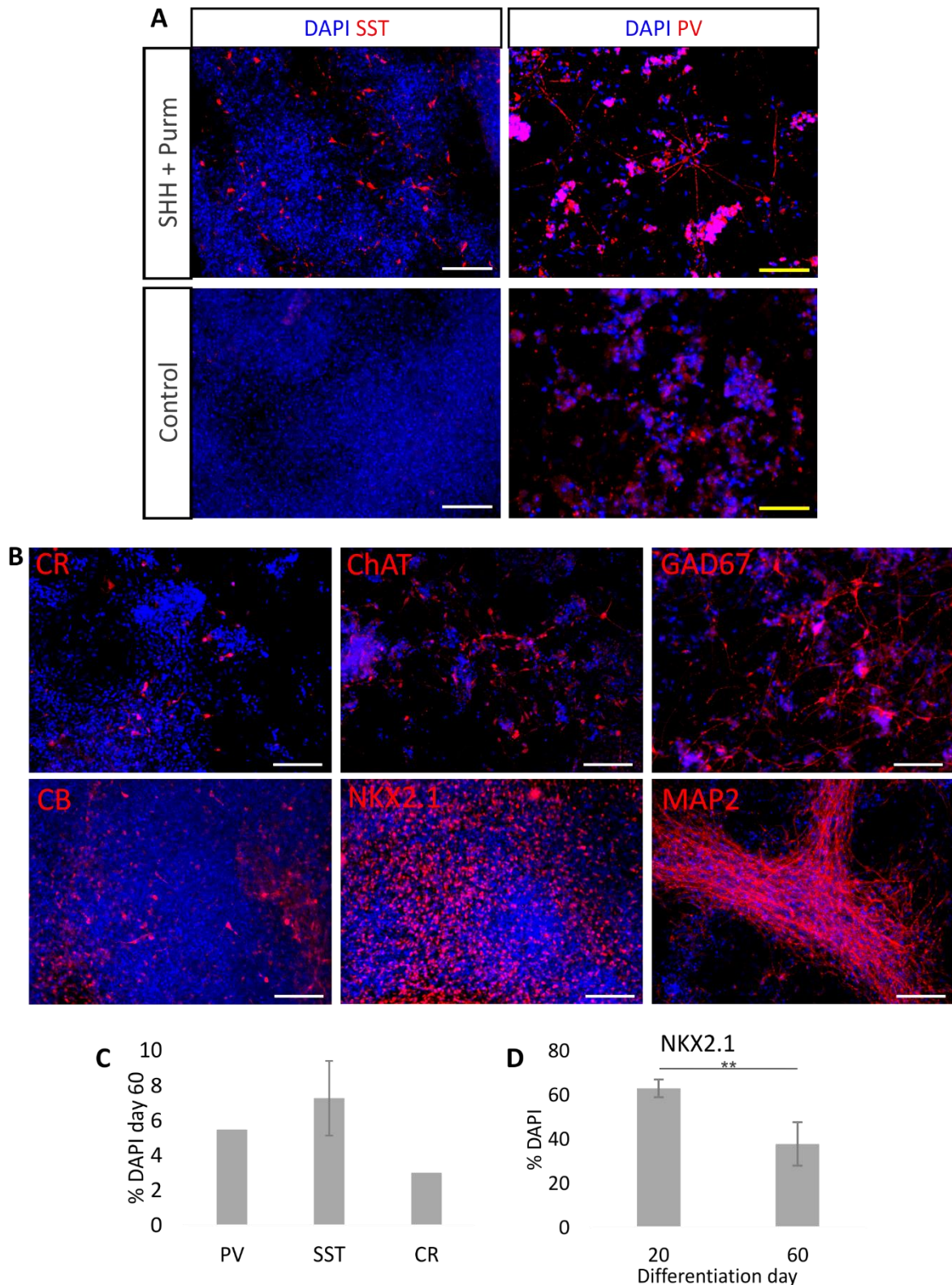


**Figure 4.2: MGE progenitors mature into cortical and striatal interneurons.**

A) Cells were fixed on day 60 of MGE and control (no SHH or purmorphamine) differentiation and immunostained for somatostatin (SST) and parvalbumin (PV). B) Day 60 MGE differentiated cells were immunostained for calretinin (CR), choline acetyltransferase (ChAT), GAD67, Calbindin (CB), NKX2.1 and MAP2. Scale bars: white, 100  $\mu$ m; yellow, 20  $\mu$ m. C) Cells that stained positive for interneuron markers were counted as a percentage of DAPI. D) A bar graph comparing the percentage of cells that stained positive for NKX2.1 at days 20 and 60 (\*\*P < 0.01, 1-tailed t-test). Bar graph data show mean  $\pm$  SEM from n = 2 (PV), 3 (SST), 2 (CR), 3 (NKX2.1 d20), 4 (NKX2.1 d60) independent experiments respectively.



### 4.3 Discussion

This chapter has depicted the cell-types generated using an adapted version of the MGE differentiation protocol from Maroof *et al.* (2013). These data have confirmed that hESCs can be differentiated to MGE progenitors via Wnt inhibition and SHH activation, and that these can be left to mature into GABAergic and cholinergic interneuron subtypes. In medium designed to enhance functional maturation of neurons, the cells can begin to show neuronal activity including action potentials and post-synaptic potentials.

At the progenitor stage, a high proportion of cells expressed FOXG1 and NKX2.1 indicating a ventral forebrain identity. This was followed by a long *in vitro* maturation period up to at least day 45, by which time some cells had begun to express subtype-specific markers GAD67, somatostatin and calretinin. Around day 60, a small proportion of cells also began to express parvalbumin, and the proportion of cells expressing NKX2.1 had significantly reduced. This suggests that some cells down-regulate NKX2.1 expression and are therefore likely to be programmed for cortical interneuron fate. The remaining NKX2.1+ cells in the cultures could either be of striatal identity, or simply still be at the progenitor stage of differentiation, although the high levels of MAP2 expression would oppose this. Maroof *et al.* used a NKX2.1/GFP reporter hESC line for their study, and so were able to sort GFP-positive cells on day 32 and plate them onto a mouse cortical feeder layer (Maroof *et al.*, 2013). At day 18, around 50% of cells were GFP-positive, slightly less than shown here at day 20. Following 30 days of co-culture with mouse cortical neurons however, approximately 40% of cells each were SST and PV-positive. They did an interesting comparison of the electrophysiology of interneurons cultured on mouse cortical feeders versus hESC-derived cortical feeders. With this they showed that the cells became more mature at earlier time points on the mouse feeders, perhaps indicating that the speed of the mouse neuron maturation may aid in maturing the human interneurons. While the electrophysiological data in this chapter shows modest functionality in the absence of feeder cells, their cells achieved resting membrane potentials of -66 mV and -45 mV on mouse and human feeders, respectively. They also demonstrated the ability to generate fast and long trains of action potentials. This shows that the presence of mature neurons and glia may be crucial for achieving useful levels of functionality in hPSC-derived neurons.

Nicholas *et al.* performed a detailed long term study of the differentiation timeline of their hPSC-derived interneurons, which they generated using embryoid bodies, the Wnt inhibitor DKK1 and purmorphamine (Nicholas *et al.*, 2013). They also made use of a NKX2.1/GFP reporter line, and so sorted the cells on day 35 and co-cultured them with mouse glial cells. They obtained 10% PV neurons at 15 weeks, but this reduced to 1.5% by 30 weeks and was replaced by SST (40%) and CR-expressing

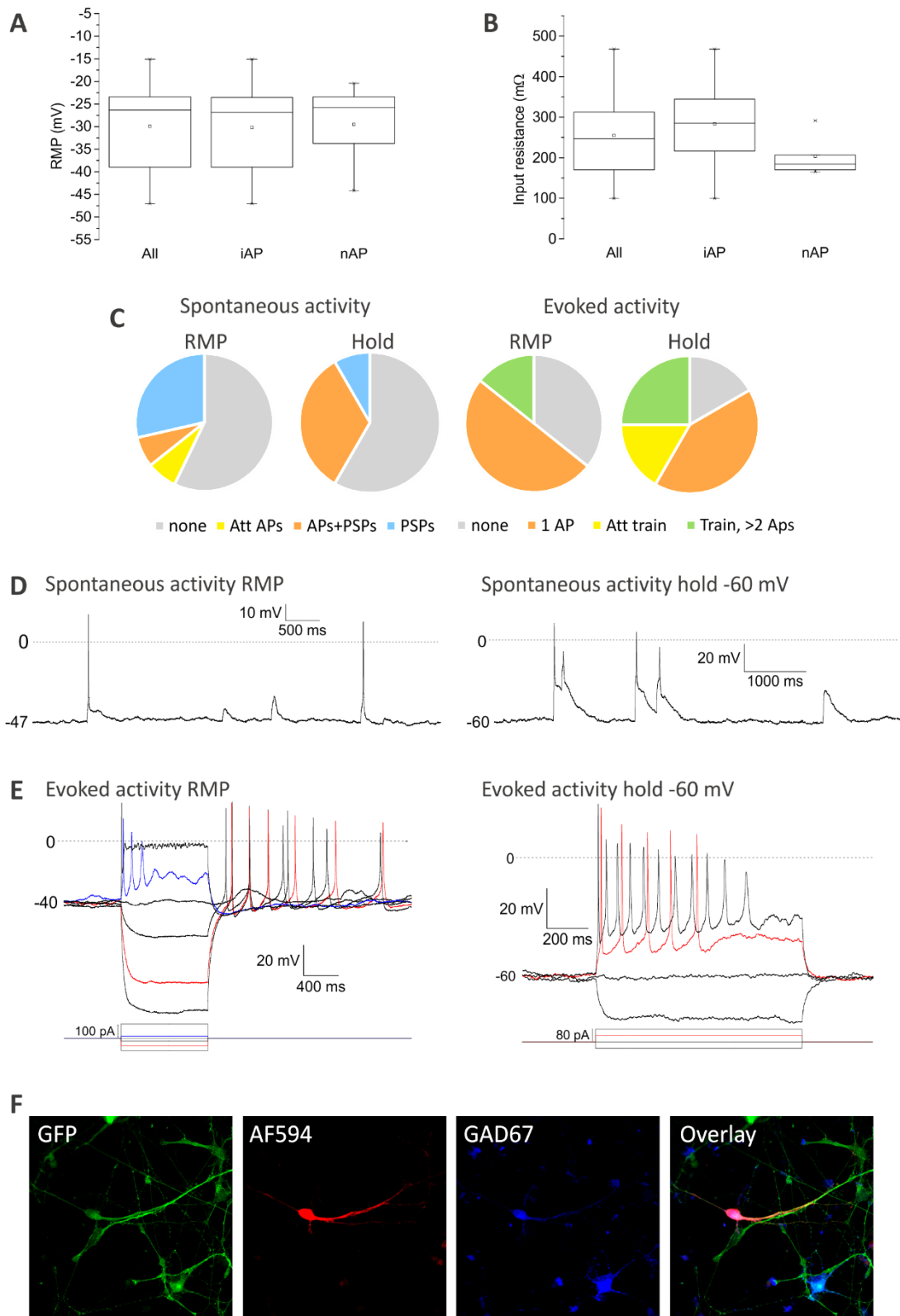


**Figure 4.3: hESC-derived MGE progenitors become functional GABAergic neurons.**

A-B) Box plot diagrams comparing the RMP (A) and input resistance (B) of all cells against iAP or nAP cells only. Box plots show median with 25<sup>th</sup> and 75<sup>th</sup> percentiles (box) and outliers (whiskers), as well as the mean (square) from  $n$  cells = 14 (all), 9 (iAP) and 5 (nAP) from a single experiment. C) Pie charts showing the proportion of cells that displayed spontaneous or evoked activity from their RMP ( $n=14$ ) or from a holding potential of -60 mV ( $n=12$ ). "Att" = attempted. D-E) Example traces of spontaneous APs and PSPs (D), and voltage responses to consecutive current steps (E) each from RMP or -60 mV. F) Representative image of a cell filled with Alexa594 and post-hoc immunostained for GAD67.

cells (77%). Immunostaining for LHX6 allowed them to observe both co-expression with NKX2.1 and LHX6+/NKX2.1- cells, which should represent striatal and cortical interneurons respectively, as cortical interneurons downregulate NKX2.1 before LHX6 is upregulated on their way to the cortex. This would be the easiest way to confirm the presence of striatal interneurons in our cultures, but we have been unable to find an antibody that works in our hands. The electrophysiology of the neurons co-cultured with mouse glial cells matured dramatically from 8 to 30 weeks of differentiation, with the resting membrane potential decreasing from -42 mV to -57 mV and the input resistance reducing from 2 G $\Omega$  to 0.2 G $\Omega$ . The frequency and amplitude of evoked action potentials increased, while the kinetics of individual action potentials also became more refined and resembled that of a mature neuron.

In terms of input resistance, the neurons in this study appear relatively mature compared to those presented previously (Maroof *et al.*, 2013; Nicholas *et al.*, 2013), suggesting that they are expressing the necessary ion channels to initiate action potentials and respond to synaptic input. However, their actual firing patterns are much less mature. This is likely down to the homogeneous nature of these cultures, in contrast to co-culture systems, which contain much faster-maturing mouse neurons and glia. It would appear from their data that the cells Maroof *et al.* co-cultured with mouse neurons and glia matured more quickly than those Nicholas *et al.* co-cultured only with glia. This may signify the importance of the presence of cortical glutamatergic neurons as well as glia during the maturation of cortical interneurons. This theory would also apply to striatal interneurons, which receive glutamatergic input from the cortex as well as GABAergic input from striatal MSNs. The cocktail of factors and small molecules in the SCM medium devised by Telezhkin *et al.* for enhanced maturation of hPSC-derived neurons may substitute part of what astrocytes provide in terms of what they would secrete, but it cannot replace the physical contact that forms the third component of the tripartite synapse (Perea, Navarrete and Araque, 2009; Telezhkin *et al.*, 2015). Together, these findings suggest that co-culture of hPSC-derived neurons with more mature neurons and glia may be crucial for future electrophysiology studies.

It is interesting that Nicholas *et al.* showed an initial increase in PV cells followed by almost a complete loss of expression (Nicholas *et al.*, 2013). This implies that the PV interneurons may have been lacking some form of support to survive, which happened to be present in the cultures of Maroof *et al.* (2013). It would seem logical that PV interneurons are more difficult to produce compared to SST or CR, as they appear only postnatally in both the human and rodent brain (Nicholas *et al.*, 2013). However, Anderson's group recently conducted another study in mouse ESCs that has confirmed the possibility to enrich for one subtype over another (Tyson *et al.*, 2015). They showed that SST-positive cells are derived from MGE progenitors exposed to higher levels of SHH and born early in the differentiation, while PV-positive cells are generated later and require lower levels of SHH. Mouse ESCs are known to

produce higher levels of endogenous SHH than hESCs, and this was enough to promote differentiation into PV interneurons. Translation of this finding into hESC-derived interneurons will require some optimisation of SHH concentrations. Furthermore, FACS was used on the mESC-derived MGE progenitors to obtain a pure population of Lhx6-positive post-mitotic neural precursors, or NKX2.1-positive neural progenitors, which produced higher proportions of SST or PV interneurons respectively. Use of reporter cell lines for obtaining a pure cell population is suitable for research applications, but is not a realistic source of neurons for transplantation therapy. This line of research will be of great importance to the field of cell therapy, as PV interneurons appear to play a greater role in neurological and psychiatric diseases compared to other subtypes (Hu, Gan and Jonas, 2014).

This chapter has demonstrated the limited ability of hESCs to differentiate into interneurons in a monoculture *in vitro*. As the intention is to have a source of MGE cells for transplantation as well as co-culture systems, the next chapter will describe the outcome of the same cells following transplantation into neonatal rat striatum.

## 5 Transplantation of hPSC-derived MGE progenitors into neonatal rat striatum

### 5.1 Introduction

As explained in **Chapter 4**, the MGE gives rise to both cortical and striatal interneurons, as well as other forebrain projection neurons. Despite being able to show the generation of MGE-derived interneurons from hESCs *in vitro*, all *in vivo* studies so far have involved MGE progenitor transplantation into cortex or hippocampus (Liu *et al.*, 2013; Maroof *et al.*, 2013). One way to test their ability to become striatal interneurons is to transplant the cells as progenitors, directly into the striatum of an animal and observe whether they differentiate into relevant interneuron subtypes.

Use of a GFP-expressing cell line is useful for transplantation studies as a way of easily identifying the human cells within host tissue without the need to always use a human-specific antibody. Another benefit is the ability to visualise the cells in living tissue, enabling targeted patch clamp recording from transplanted neurons to observe their functional properties. Maroof *et al.* used a NKX2.1/GFP reporter hESC line for their study, in which they transplanted MGE progenitors into neonatal mice (Maroof *et al.*, 2013). Although they observed minimal GFP down-regulation in their cells and concluded they had not matured into PV or SST-expressing interneurons by 8 weeks, they did address that due to the natural down-regulation of NKX2.1 in cortical interneurons they would have lost some GFP expression over a longer time span, which would have impeded any efforts to easily locate the cells for electrophysiology or immunohistochemistry. Denham *et al.* used a constitutive GFP-expressing hESC line and transplanted dorsal forebrain progenitors into neonatal rat striatum (Denham *et al.*, 2012). They were able to demonstrate that over 10 weeks, their cells extended long projections through white matter tracts and adopted a variety of neuronal morphologies. In addition, they conducted patch clamp recording of the cells and showed that 2 out of 4 cells displayed relatively mature neuronal firing, both spontaneous and evoked, with evidence of excitatory post-synaptic potentials suggesting at least some functional integration. Furthermore, future co-culture or co-transplantation of striatal interneurons with MSNs could benefit from distinguishing the 2 cell types by one expressing GFP and the other not.

Allografting studies have provided strong evidence that fate committed neural progenitors can be used to replace neurons lost in neurodegenerative disorders such as Parkinson's and Huntington's disease (Björklund and Stenevi, 1979; Graybiel, Liu and Dunnett, 1989; Klein, Lane and Dunnett, 2012). However, for this method to translate to clinical trials, a reliable method of xenografting human tissue into animal models for the long term study of its survival, differentiation and functional integration

has been vital. Transplantation into neonates is a simple way of observing the capacity of transplanted cells to survive, migrate and differentiate in a host brain, and the immaturity of the host immune system reduces graft rejection (Rosser, Tyers and Dunnett, 2000; Englund *et al.*, 2002; Eriksson, Björklund and Victorin, 2003; Kallur *et al.*, 2006). As the field has evolved towards trying to generate foetal-like tissue from hPSCs, researchers have continued to use neonatal transplantation to demonstrate the differentiation and integration potential of cells (Denham *et al.*, 2012; Maroof *et al.*, 2013). For studies into using cell transplantation as a therapy, graft recipients must be adult disease models. Immune suppression of host animals with Cyclosporine A (CsA) was found to highly increase xenograft survival and allowed study of human foetal tissue transplants in HD rat models (Brundin *et al.*, 1985; Grasbon-Frodl *et al.*, 1997), but over time CsA causes nephrotoxicity that limits the length of experiments in rats to around 20 weeks post-transplantation. This may be sufficient to observe neuronal survival and differentiation, but real functional integration of human cells is likely to take much longer (Espuny-Camacho *et al.*, 2013; Nicholas *et al.*, 2013). The use of immune-deficient animals (Nude or SCID), has also become more popular, abolishing the risk of graft rejection by the immune system (Samata *et al.*, 2015). However, immune-deficient rodents have a much higher susceptibility to infection and must be kept in a pathogen-free environment at all times, making facilities more expensive and behavioural studies more difficult to perform. A more recent finding has shown that recipient rats can be desensitised to foreign tissue by injecting them with donor cells peripherally as neonates (Kelly *et al.*, 2009). Although this technique encountered some initial criticism, further research has shown that neonatal desensitisation does not work well in mice, but is successful in allowing good survival of human foetal brain-derived cells or hESC-derived neural progenitors transplanted into rats until 40 weeks (Janowski *et al.*, 2012; Robertson *et al.*, 2013; Heuer *et al.*, 2016). This is much longer than with CsA treatment and leaves the animals in good health for the entire experiment.

The aim of this chapter is to address whether hESC-derived MGE progenitors can become striatal interneurons following transplantation into the striatum of neonatal rats. A hESC line that constitutively expresses a tau-GFP fusion protein was generated to easily identify the transplanted cells during histology and in *ex vivo* brain slices for electrophysiological recordings.

## 5.2 Results

### 5.2.1 Generation of a tau-GFP-expressing hESC line

The TG4 hESC line was generated as explained in **Section 2.1.3**. H7 hESCs were transfected with a plasmid containing a construct for tau-GFP fusion protein expression and a puromycin resistance cassette driven by a constitutive CAG promoter (**Figure 5.1A**). TG4 (Tau-GFP cell line 4) cells displayed homogeneous GFP expression from the hESC stage and throughout neuronal differentiation (**Figure 5.1B,C**). Co-culture of TG4 cells with normal H7 cells allowed for the visualisation of individual cell morphology in culture. At day 9 of neuronal differentiation neural rosettes were clearly formed and regularly interspaced, by day 21 neural progenitors were migrating out from the rosette core and extending longer processes. By day 39, cells were more multipolar and forming structured networks of neurons. This cell line was used for all transplantation studies.

### 5.2.2 Neonatal transplantation does not avoid immune response to xenograft

Two separate rounds of transplantation were carried out. For both rounds, cells were dissociated on day 20 of MGE differentiation and approximately 200,000 cells injected in 1  $\mu$ l into the right striatum of 2-day-old Sprague Dawley pups (**Figure 5.2A,D**). Pups were placed back with their mothers and weaned at around 4 weeks of age. Animals were not given immunosuppressant for the first round, as it was thought that transplanting into neonates would avoid immune rejection of the graft. At 4 and 8 weeks, graft survival was 100% and 50%, respectively (n=2). Maintenance of GFP expression in transplanted cells was verified using the human nucleus-specific antibody HuNu. All GFP-positive cells stained positive for HuNu, and vice versa (**Figure 5.2B**). At 16 and 24 weeks, no surviving grafts were found.

There was a strong suspicion that grafts from the first round did not survive due to immune rejection of the human cells, therefore a second round of transplantation was carried out with the immunosuppressant CsA administered daily (i.p. 10 mg/kg) from weaning onwards. Brains were taken at 6, 12 and 20 weeks for histology, and 3 brains were taken at 12 weeks for electrophysiology (**Figure 5.2D**). While grafts survived in 3 out of 7 immune suppressed animals at 20 weeks, none of the 5 untreated rats had surviving grafts, confirming the need for immune suppression in transplantation studies using hPSCs. Despite the increased survival rate in the immune suppressed animals, there was still a gradual decline in the number of surviving cells as a percentage of the 200,000 transplanted cells. At 6 weeks, there was an average of 4.3% cell survival, while at 12 and 20 weeks this had reduced to 2.6 and 1.15% respectively (**Figure 5.2E**).

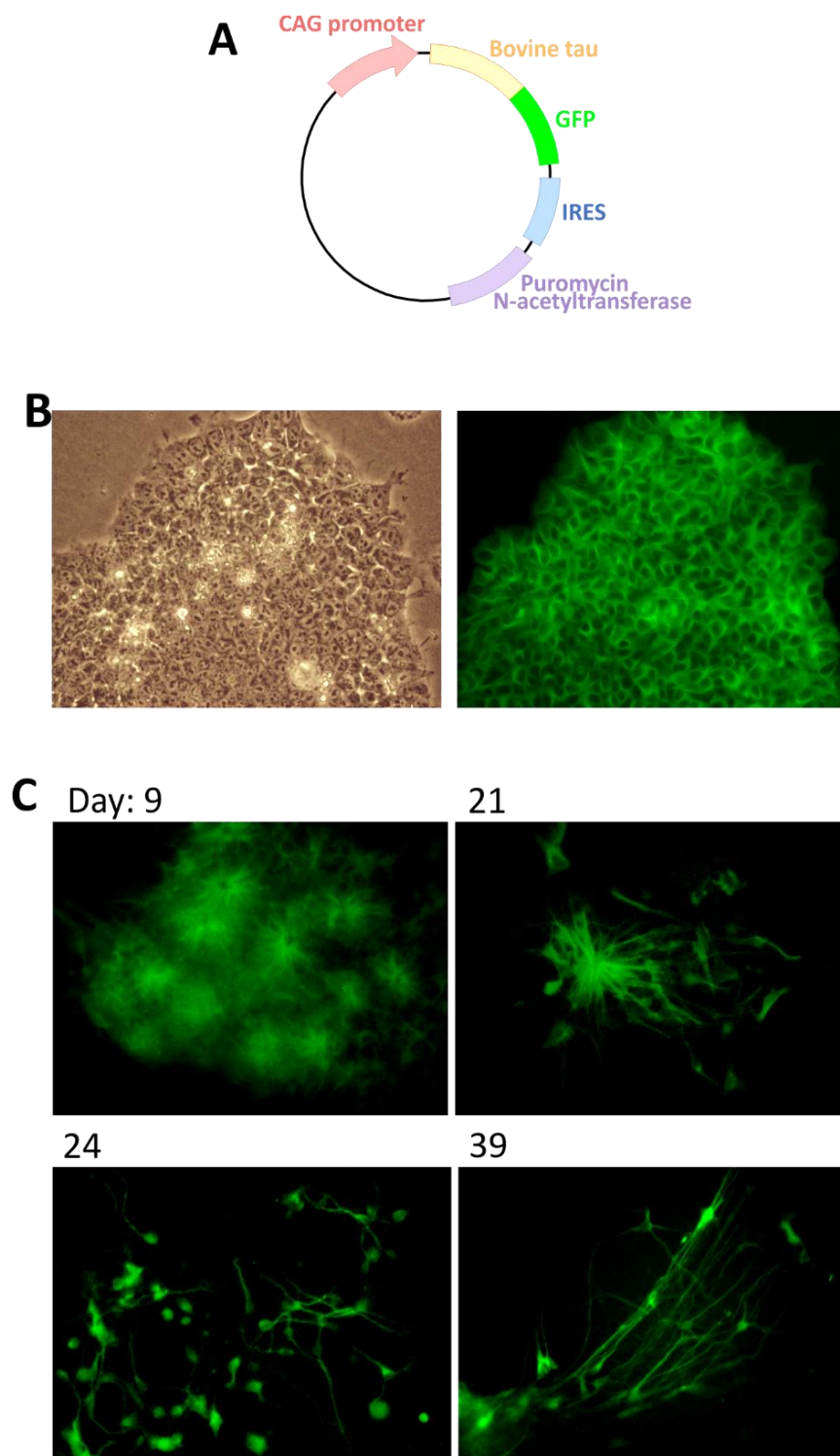


**Figure 5.1: Generation of tau-GFP hESC line TG4**

A) Schematic of plasmid used to transfect cells. B) Brightfield and fluorescent image of TG4 hESCs showing ubiquitous GFP expression. C) TG4 cells differentiated in co-culture with H7 show cell morphology throughout neuronal differentiation.



Microglia staining with IBA1 showed a huge increase in the number of microglia in the right, transplanted hemisphere of a rat with a rejected graft compared to the left striatum (**Figure 5.2C**). These data show that immune rejection of hESC-derived neural progenitors remains a possibility despite transplanting into neonates and administering CsA.

### 5.2.3 Transplanted hESC-derived MGE progenitors migrate within the first 6 weeks of transplantation

Within the first 6 weeks, cells had migrated from the striatum to the septum and hippocampus in 4 of 6 animals. It was difficult to know the exact injection site due to brain growth and repair since the surgery, so the section in which the majority of cells were found in the striatum, was taken as the point of reference for cell migration (**Figure 5.3A**). By 6 weeks, cells had migrated at least 2.88 mm away from the graft core in both anterior and posterior directions, although there was a trend towards a greater number of cells migrating posteriorly to the hippocampus. Over time, it appeared that a decline in surviving cells lead to a higher proportion of cells close to the graft core and fewer cells surviving on their own, especially anteriorly. Although, there were still surviving cells in the septum and hippocampus in the majority of animals at 12 and 20 weeks (**Figure 5.3B,C**).

Interestingly, cells very rarely entered the cortex, occasionally settling just dorsally to the corpus callosum close to the graft core. They did, however, appear to migrate to the dorso-lateral SVZ and across to the lateral septum, or ventrally along the SVZ through the pallidum and into the septum, from which they could migrate caudally towards the hippocampus (**Figure 5.3B**). Once in the hippocampus, cells concentrated around the CA3 region in the stratum oriens layer, which is home to many of the host GABAergic interneurons.

These data show that transplanted hPSC-derived MGE progenitors can migrate to their normal final destination within 6 weeks and settle thereafter.

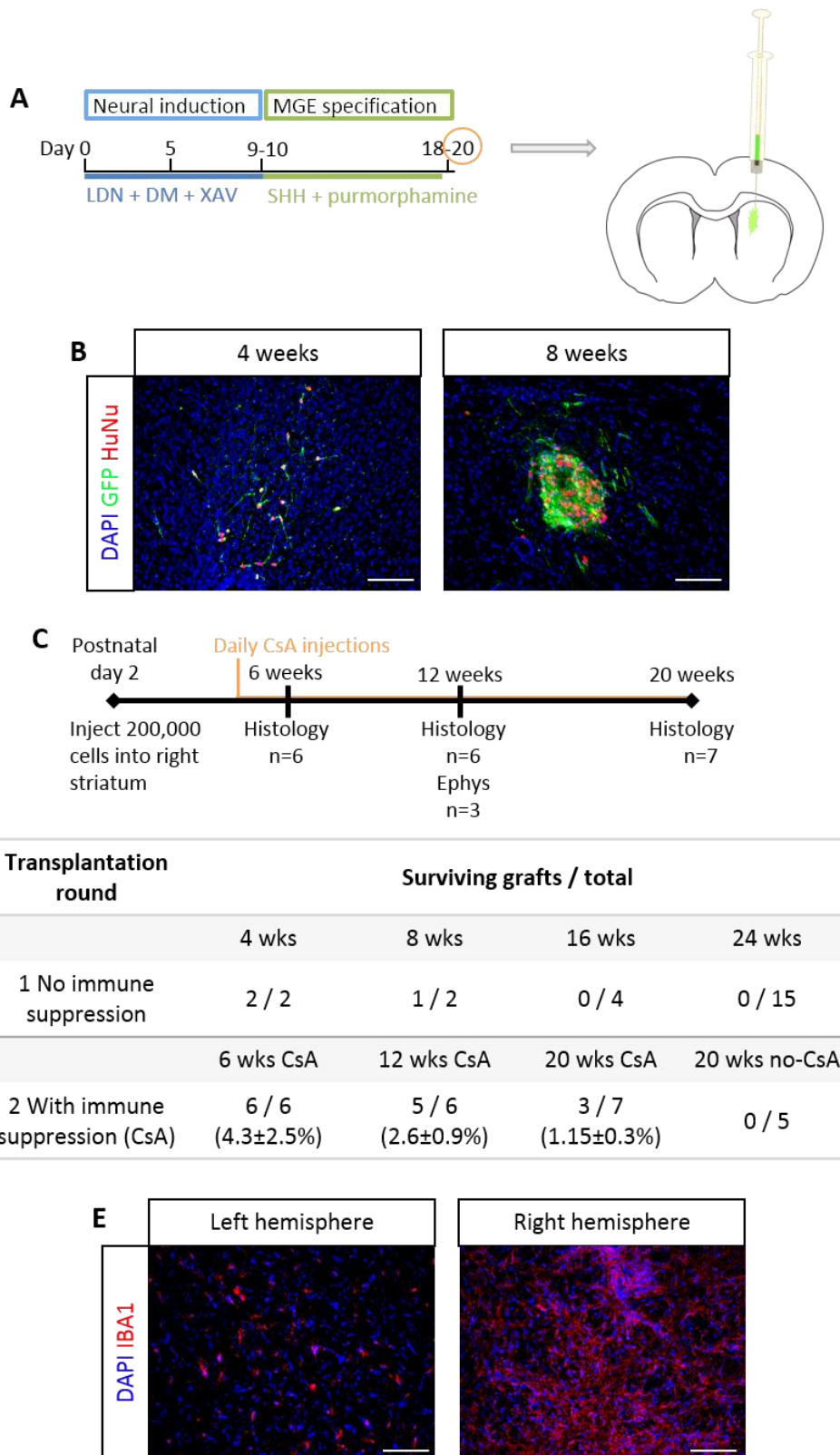


**Figure 5.2: Neonatal transplantation does not avoid host immune response and graft rejection**

A) Schematic timeline of MGE differentiation for transplantation, with cells dissociated for grafting on day 20 and injected into the striatum of neonatal rats. B) Immunostaining for HuNu 4 and 8 weeks post-transplantation, showing co-localisation with GFP. C) Timeline for the second round of transplantation, showing the number of animals taken for histology or electrophysiology (ephys). D) Table showing the graft survival for each timepoint and experiment. E) Immunostaining of brain from 20 weeks with a rejected graft for microglia (IBA1), showing left (ungrafted) and right (grafted) striatum. All scale bars = 100  $\mu$ m.

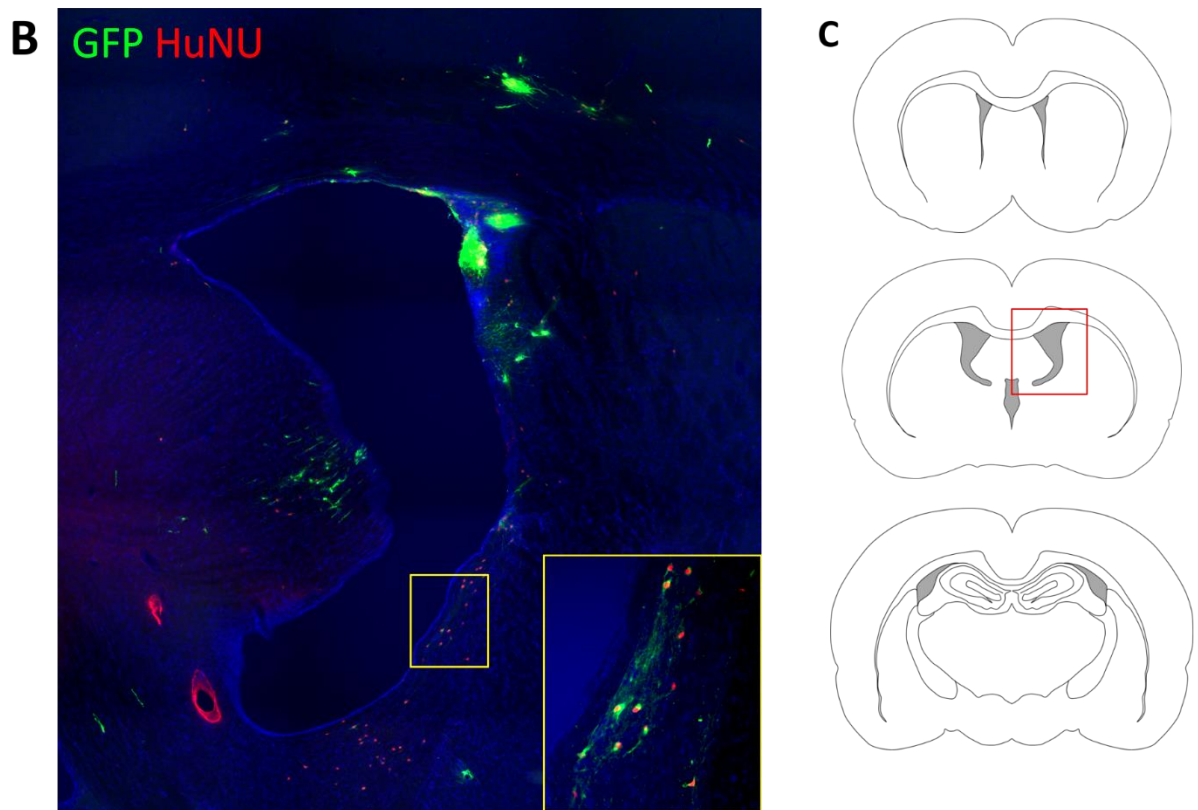
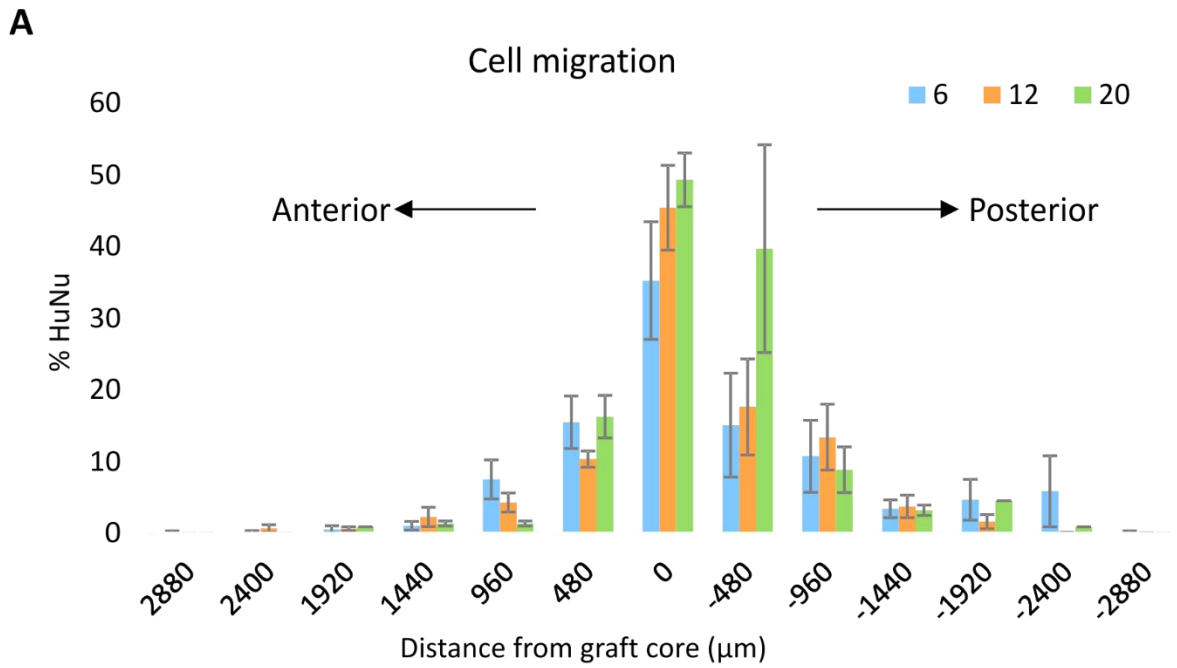


**Figure 5.3: Transplanted cells migrate within the first 6 weeks of transplantation.**

A) HuNu-positive cells were counted in each section (1/12) as a percentage of total HuNu-positive cells, and plotted to show the distribution of cells at each time point – 6 (blue), 12 (orange) and 20 (green) weeks. The data show mean percentage  $\pm$  SEM,  $n = 6, 5$  and  $3$  respectively. B) Tilescan image of a brain section from 12 week old rat showing distribution of GFP/HuNu+ cells, including higher magnification of migrating cells (yellow box). C) Schematic diagrams of rat brain sections showing the area imaged in (B, red box) and other usual locations of GFP/HuNu+ cells in all grafts: striatum, septum, corpus callosum, SVZ and hippocampus.

#### 5.2.4 Transplanted hESC-derived MGE progenitors become striatal interneurons

Brain sections were stained by fluorescent immunohistochemistry to assess the expression of interneuron markers by transplanted cells. NKX2.1 was the most abundantly expressed MGE marker in the transplanted progenitor population (approximately 80%). Due to the crucial role it plays in interneuron migration to either striatum or cortex (and hippocampus), it was hypothesised that NKX2.1 expression may differ between cells that had settled in the different brain regions. However, NKX2.1 was expressed in 30-36% of HuNu-positive cells at each time point (**Figure 5.4A-D**), and this did not differ significantly between cells in the striatum, septum or hippocampus (data not shown). As the proportion of NKX2.1-positive cells did not decrease over the time points, the initial reduction from 80% in the transplanted population must have occurred in the first 6 weeks following transplantation.

NeuN, a neuronal marker, was expressed by 50% of cells 6 weeks post-transplantation, and by 49% and 56% after 12 and 20 weeks respectively (**Figure 5.4A,B,D**). These differences were not significant, suggesting that by 6 weeks all neural progenitors had differentiated into post-mitotic neurons. Despite this, at 20 weeks 44% of cells in one graft still expressed nestin, a neural progenitor marker, indicating the maintenance of a progenitor pool that may account for the remaining 44-51% of NeuN-negative cells at each time point (**Figure 5.4A,D**). A good proportion of cells appeared to express GABA or GAD67, both GABAergic markers, from 6 weeks onwards, however due to the high positive staining of the surrounding striatum and septum, it was not feasible to properly quantify this (**Figure 5.4C**).

ChAT, a cholinergic neuron marker, was found to be expressed in a few GFP-positive cells in the striatum at 12 and 20 weeks in 3 different grafts, but this was not enough to quantify (**Figure 5.4B,C**). It is worth noting that adjacent sections immunostained for NKX2.1 saw positive staining in cells with similar morphology and level of GFP expression to those expressing ChAT. This suggests that the GFP/ChAT-positive cells could also be NKX2.1-positive, which would confirm their striatal interneuron identity. Surprisingly CR, the subtype marker showing the lowest expression *in vitro*, was expressed in 41% and 26% of GFP-positive cells at 12 and 20 weeks respectively (**Figure 5.4B-D**). CR was widely expressed in all brain regions, and actually showed slightly higher expression in the septum and hippocampus than in the striatum when the data were separated (data not shown). This is likely to be due to the cells in the septum and hippocampus being mature neurons, compared to the graft core in the striatum. PV, SST and NPY were not found to be expressed in any GFP-positive cells in any animals. There was also no expression of GFAP, a glial marker, in any GFP-positive cells. These data show that hESC-derived MGE progenitors can differentiate into CR-expressing or cholinergic striatal, septal and hippocampal interneurons *in vivo*.

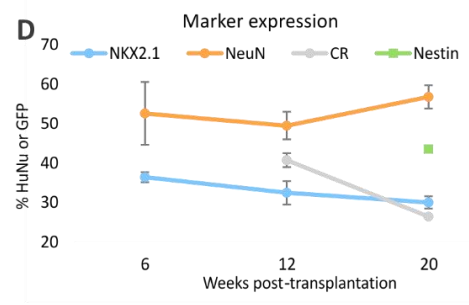
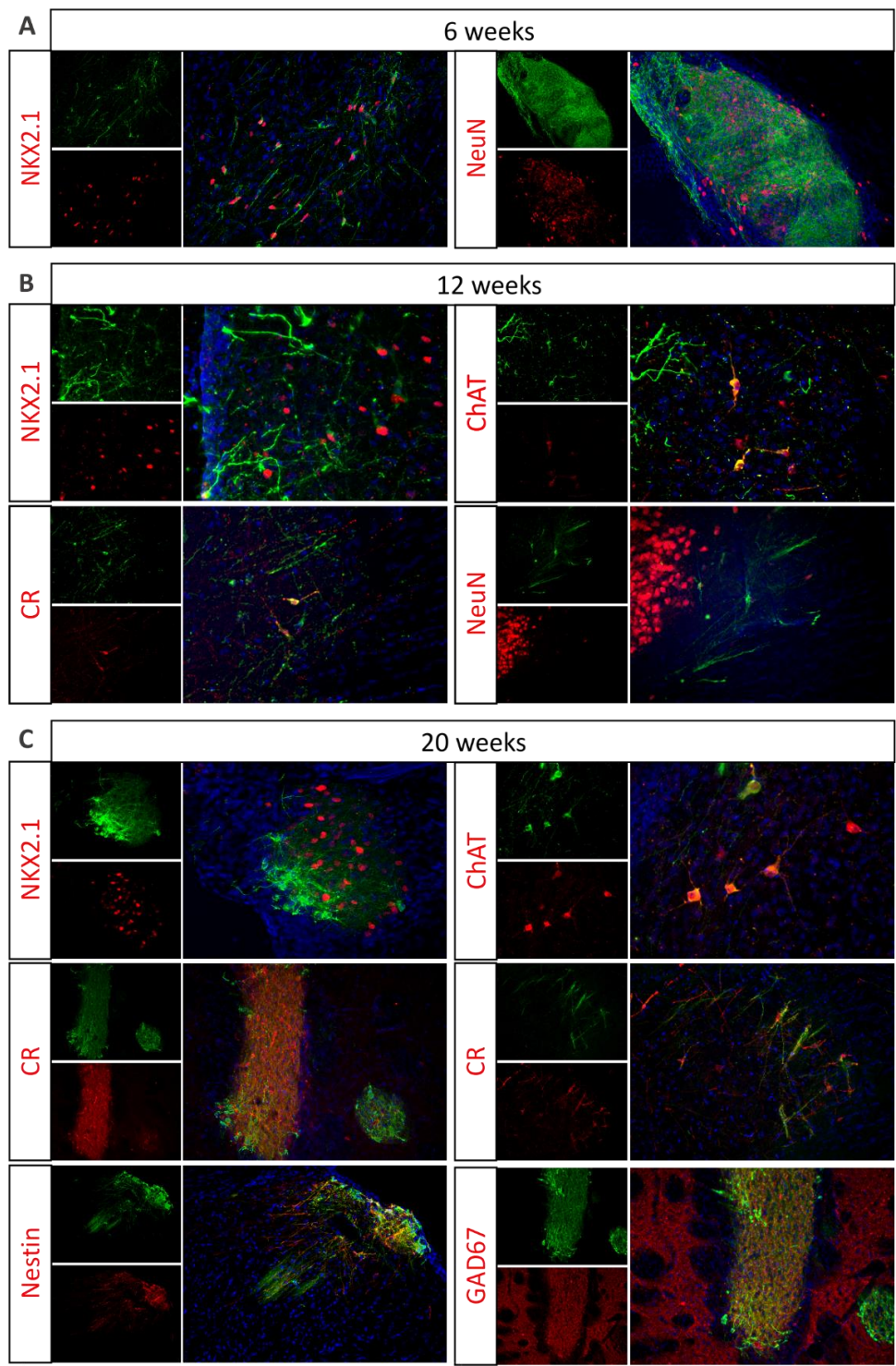


**Figure 5.4: Transplanted MGE progenitors differentiate into striatal interneurons.**

A) Graph of quantified markers from immunostaining as a percentage of HuNu or GFP-positive cells. B-D) Representative images of immunostaining of brain sections from 6 (B), 12 (C) and 20 (D) weeks post-transplantation, with GFP-positive (green) transplanted cells and DAPI (blue). The brain regions depicted are as follows: B) NKX2.1 – striatum, NeuN – SVZ/striatum; C) NKX2.1 – striatum, ChAT – striatum, CR – hippocampus, NeuN – hippocampus; D) NKX2.1 – SVZ, ChAT – striatum, CR – striatum and hippocampus, Nestin – septum, GAD67 – striatum.

### 5.2.5 Transplanted cells adopt region-specific morphologies

All GFP-positive cells with a visible morphology (i.e. not in clumps) were classified as unipolar, bipolar or multipolar and their location recorded (**Figure 5.5A**). It was hypothesised that neuronal morphology would mature over time until the majority or all of the neurons were multipolar but that the rate might differ between brain regions.

Indeed, in the striatum and septum, GFP-positive cells became increasingly complex over time, with almost a 1:1:1 ratio at 6 weeks, but more than 73% multipolar cells by 20 weeks and almost no unipolar cells present (**Figure 5.5B,C**). In contrast, the hippocampus had a majority of bipolar cells from 6 weeks, which was maintained up to 20 weeks, with 78% bipolar cells and only 19% multipolar cells.

The data show a clear tendency for neurons to develop a multipolar morphology in the striatum and septum, whereas a bipolar morphology is maintained in the hippocampus. However, looking at images of the cells it is clear that there are other differences between the morphologies of cells that settled in different brain regions (**Figure 5.5C**). Cells in the striatum showed clear maturation between 6 and 12 weeks from bipolar to multipolar morphology, but the majority still only had 3-5 visible processes. In the septum, however, the morphology of the multipolar cells at 12 and 20 weeks was very different from those in the striatum, with many processes coming from each soma and a relatively dense dendritic tree. The morphology of neurons in the hippocampus appeared to change very little between 6 and 20 weeks, with very straight, bipolar cells positioned in two strict orientations parallel or perpendicular to the adjacent pyramidal cell layer.

This shows that transplanted cells that settle in different brain regions adopt distinct morphologies, however it cannot be discerned whether this is cell autonomous or dependent on the surrounding environment.

### 5.2.6 Patch clamping of transplanted hESC-derived neurons

At 12 weeks post-transplantation, brain slices were prepared from 3 rats for whole cell patch clamp recording of GFP+ cells. Distinct GFP+ cell bodies were found in only one of the brains, from which 3 cells were patched successfully. Cells were filled with biocytin during recording and post-hoc analysis confirmed that all 3 cells were also GFP+ (**Figure 5.6A**).

All 3 cells had polarised resting membrane potentials of around -70 mV, however 2 of the cells were unresponsive to current injection and showed no spontaneous activity. The third cell had an unstable resting membrane potential that averaged at -75 mV ( $\pm 13$  mV), but displayed robust action potential



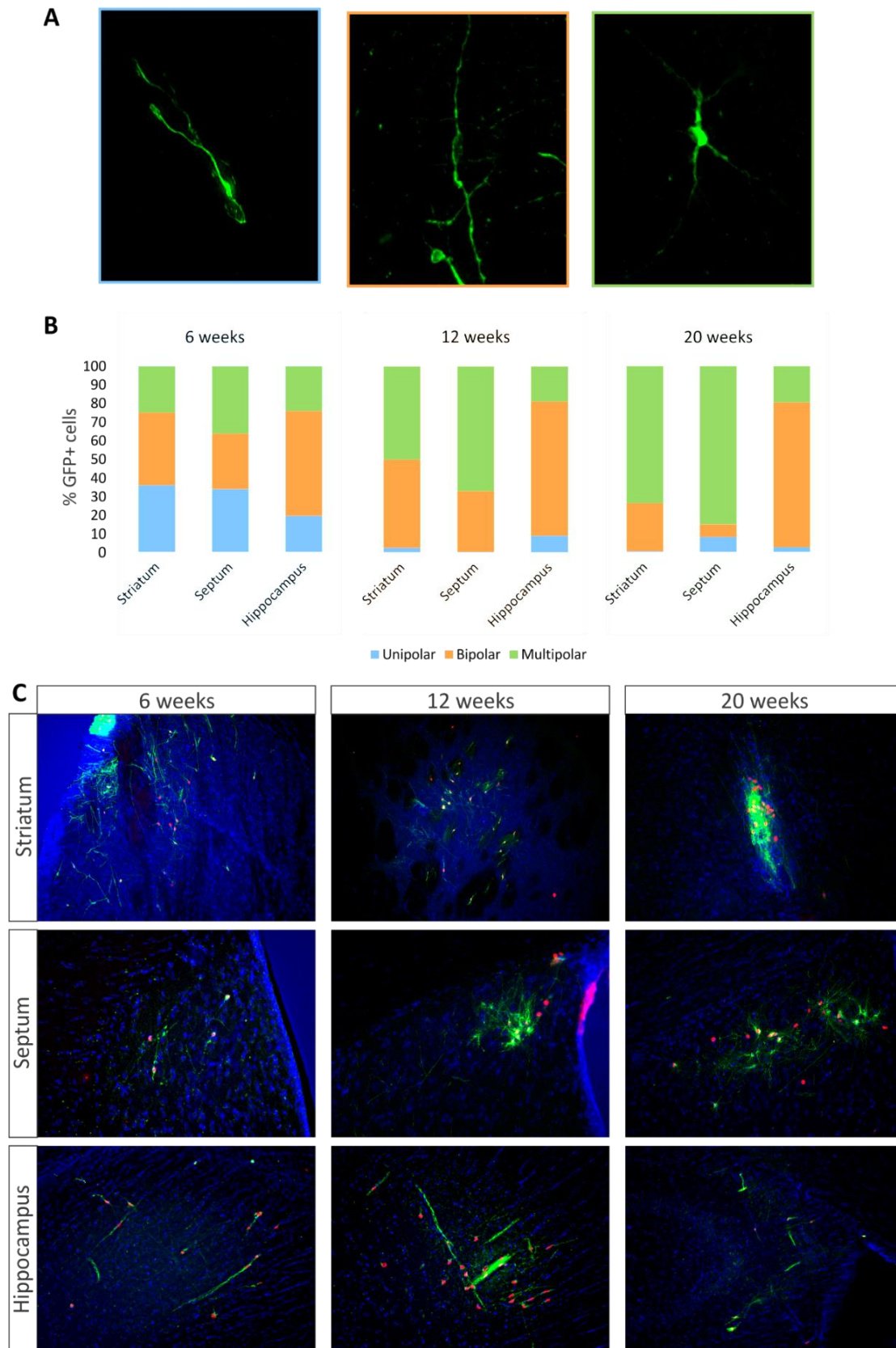


**Figure 5.5: Transplanted MGE progenitors adopt region-specific morphologies.**

A) Examples of unipolar (blue), bipolar (orange) and multipolar (green) GFP-positive cells counted in each region. B) Quantification of GFP-positive cells classified as in (A) in the striatum, septum and hippocampus at each time point. Data shown are the mean percentage of GFP-positive cells in each category. C) Immunofluorescent images of GFP/HuNu-positive (green/red) cells in each region at each time point, with DAPI (blue).

firing upon current injection of at least 80 pA, with 120 pA injection triggering a train of action potentials (**Figure 5.6C,E**). Occasional spontaneous firing was also detected, as well as what looked like an excitatory post-synaptic current, demonstrating synaptic responsiveness of the cell (**Figure 5.6D**).

Biocytin filling allowed for post-hoc staining with Streptavidin Cy3 conjugate and morphological analysis of the functional cell. Partial 3D reconstruction using NeuroLucida software showed that the cell had a typical neuronal morphology and Sholl profile (**Figure 5.6Figure 5.6B**).

### 5.3 Discussion

In this chapter, I have shown that MGE-like progenitors derived from GFP-expressing hESCs can be transplanted into neonatal rats' brains to produce functional neurons with molecular profiles resembling certain striatal interneuron subtypes. I have also presented findings that conflict with the general consensus of the underdeveloped neonatal immune system providing a cover behind which human cells can hide indefinitely. For my second transplantation experiment, I administered daily immunosuppressant CsA in order to get a higher graft survival rate.

Firstly, generation of a hESC-line expressing tau-GFP was vital for the post-transplantation identification of the transplanted cells, particularly because of the migratory nature of both MGE progenitors and neonatal grafts (Wichterle *et al.*, 1999). Silencing of transgenes is very common, especially in hPSCs and throughout differentiation, so it was important to screen all 4 clones that were picked and expanded following transfection and puromycin selection. Of the 4 clones, only one maintained GFP expression throughout neuronal differentiation (TG4), and indeed maintained expression when transplanted into rat brain. The CAG promoter used here is a constitutive promoter that has been shown to drive strong expression in transfected mouse ESCs, increasing at later stages of differentiation (Hong *et al.*, 2007). Even within one graft it was clear that some cells were much brighter, expressing higher levels of GFP, than others. This shows the importance of screening transgenic clones both during routine culture and after differentiation.

There have been many studies showing long-term survival of human neural tissue transplanted into neonatal rats (Englund *et al.*, 2002; Kallur *et al.*, 2006; Zietlow *et al.*, 2012). However, all these studies used expanded neural stem cells from human foetal primary tissue. Studies using hPSC-derived neural progenitors for transplantation have typically used SCID mice, for both neonatal and adult transplants (Liu *et al.*, 2013; Maroof *et al.*, 2013; Nicholas *et al.*, 2013; Cunningham *et al.*, 2014). However, SCID mice and their rat counterparts, the athymic nude rat,



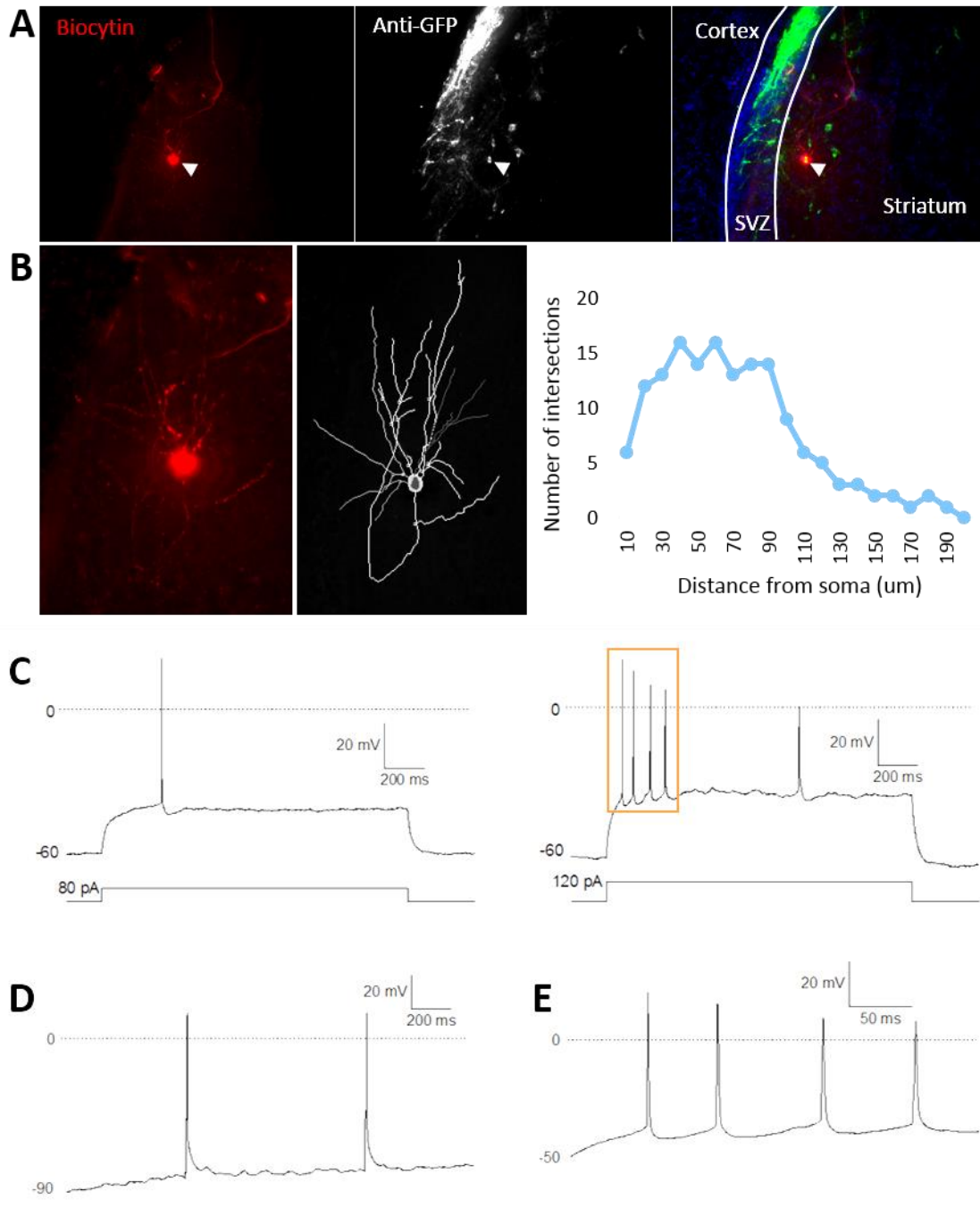


**Figure 5.6: Transplanted hESC-derived MGE progenitors can mature into functional neurons.**

A) Immunostaining of the biocytin-filled cell double-labelled with GFP and located in the anterior dorsomedial striatum. B) Biocytin filling allowed for partial reconstruction of the neuron with NeuroLucida software and Sholl analysis. C) Current injection of 80 pA was sufficient to drive single action potential firing, and 120 pA triggered a train of 4 action potentials. D) Spontaneous action potentials were fired in the absence of current injection. E) Larger scale version of the action potential train shown in (C), showing the kinetics of the action potentials.

are extremely prone to infection and have specific housing requirements that are not always feasible to meet. One other study used neonatal Sprague-Dawley rats as recipients for hESC-derived neuron transplantation, but only left the grafts for 10 weeks post-transplantation (Denham *et al.*, 2012). The authors saw surviving grafts in 13 out of 20 animals transplanted, so it is also possible that over a longer time scale the grafts would have been fully rejected. It is very possible that the GFP expression causes the cells to be even more immunogenic than the typical foetal tissue grafts. A study showed that GFP-positive haematopoietic stem cell (HSC) grafts were rejected far more quickly than HSCs from mice with the same genetic background that did not express GFP (Bubnic, Nagy and Keating, 2005). Furthermore, a study showed that hESCs (expressing GFP) were rejected from the leg muscle of immunocompetent mice within 1 week, and that their survival was extended to 10 days when the mice were treated with a rapamycin inhibitor (Swijnenburg *et al.*, 2008). The calcineurin inhibitor, the group to which CsA also belongs, did not prolong graft survival past 7 days, although in combination with the rapamycin inhibitor it did prolong survival to 14 days. The blood brain barrier makes the brain immune-privileged, however the act of transplanting the cells and the neuroinflammatory response was found to cause the blood brain barrier to leak for the first 7 days following mouse tissue transplantation into rat striatum, allowing entry of peripheral T-lymphocytes (Brundin *et al.*, 1989). The dose of CsA used here (10 mg/kg), has typically been enough to keep these T cells at bay and prevent xenograft rejection, but on this occasion there was still over 50% loss of grafts at 20 weeks. It is likely that human to rat grafts could cause a bigger insult to the blood brain barrier than mouse tissue, and it takes longer to develop and express all antigens, prolonging the potential immune response. This means that transplanting into neonates may not bypass the immune response as this begins to mature after 7-10 days, which is not long enough for the human cells to integrate and the blood brain barrier to restore itself (Brundin *et al.*, 1989). As CsA was only given from 4 weeks onwards, this also may not be early enough to prevent the immune response from initiating. The IBA1 staining presented here was from a CsA-treated rat with a rejected graft, showing that the CsA treatment was not sufficient to inactivate the microglia. A big challenge in the transplantation field appears to be the variation between findings in different studies, even within the same lab (Brundin *et al.*, 1989). Perhaps moving towards the use of immune-deficient mice or rats will be the only way to study the true integration and functional potential of hPSC-derived neurons.

The high level of migration of these MGE-like cells is very similar to that seen previously when transplanting foetal MGE tissue into neonatal rat striatum (Wichterle *et al.*, 1999; Englund *et al.*, 2002). The protocol used for generating MGE-like progenitors in this study was established by Maroof *et al.* and characterised *in vitro* in the previous chapter (Maroof *et al.*, 2013). In their paper, Maroof *et al.* transplanted cells at differentiation day 32 into mouse neonates and found that after 2 months,

cells were still immature, expressing doublecortin and exhibiting uni- or bipolar morphology. In contrast, this study transplanted cells after just 20 days of differentiation, at which point there was no more expression of pluripotency marker, OCT4, and the vast majority of cells were Nestin and NKX2.1-positive. Although there was still a lot of nestin expression at 20 weeks, more than half of transplanted cells were NeuN-positive from 6 weeks onwards, and more than 25% of cells (half of neurons) had undergone subtype specification by 12 weeks to express calretinin. By 12 weeks there were also a few cells that had differentiated into cholinergic striatal interneurons. Furthermore, by 6 weeks, the NKX2.1-positive population had dropped from 80% at transplantation to 36%. This is in stark contrast to the previous study, which found that all transplanted cells were still expressing NKX2.1 and GFP, and that none of them had differentiated into any interneuron subtype (Maroof *et al.*, 2013). Curiously, very few transplanted cells settled in the cortex, and in many subjects only cell debris could be seen in the cortex, likely from cells being deposited along the needle tract, compared to healthy-looking cells in the striatum, septum and hippocampus. This finding cannot really be explained, as many groups have reported successful transplantation of MGE foetal tissue or hPSC-derived either directly into the cortex or that has actually migrated there from the striatum or lateral ventricle (Wichterle *et al.*, 1999; Nicholas *et al.*, 2013; Wang *et al.*, 2016). Despite this, the finding that more than a quarter of transplanted cells differentiated into CR interneurons is promising, as these are an important interneuron subtype. The majority of CR-expressing interneurons are thought to derive from the CGE, the caudal neighbour to the MGE, which does not express NKX2.1 at progenitor stage and is instead identified by COUP-TFII expression (Kanatani *et al.*, 2008). Nonetheless, Marin *et al.* reported that 94% of CR cells in the striatum of adult mice co-expressed NKX2.1, and that NKX2.1 mutants saw a six fold reduction in the number of CR interneurons (Marin, Anderson and Rubenstein, 2000). It is possible, then, that the majority of CGE-derived CR interneurons migrate to the cortex, while MGE-derived CR interneurons settle in the striatum. Indeed, it was recently shown that in human and primate striatum, nearly all striatal interneurons originate from the MGE and express NKX2.1 (Wang *et al.*, 2014). Crucially, primate CR interneurons form a much higher proportion of striatal neurons as a whole, as well as within the interneuron population, than in rodents. Rat GABAergic interneurons comprise only 4-5% of striatal neurons, with predominantly PV interneurons in comparison to CR or SST. In contrast, human and primate GABAergic interneurons make up 23% of striatal neurons, with around three times more CR interneurons than PV or SST (Wu and Parent, 2000). This difference cannot be overstated, and indeed is often overlooked when discussing striatal interneuron research conducted in rodents for the purposes of understanding human biology.

Perhaps the cells at day 20 of differentiation are plastic enough that their subtype specification is still undecided. Sister cultures left to mature *in vitro* produced more PV and SST cells than CR (**Chapter 4**),

but when transplanted into neonatal rat striatum the only subtype to appear was CR. As 40% of transplanted cells became CR interneurons, whereas only approximately 16% of cells *in vitro* matured into any specific interneuron subtype, it would appear that the cells maturing *in vitro* may be lacking environmental cues to fully differentiate that were present in the neonatal rat brain. Future studies of this nature should address transplantation of more mature cells at later differentiation points to see if this changes their subtype specification *in vivo*. Another key factor may be the age and level of neurodegeneration of the recipient brain. Transplanting the same cells into the adult rat lesioned striatum may bias them towards a different interneuron subtype or encourage outgrowth and integration. Indeed, hESC-derived neuronal maturation has been shown to be accelerated in lesioned striatum compared with intact neonatal transplantation (Joannides *et al.*, 2007). Furthermore, migration of transplanted MGE-like cells was less extensive in intact adults compared to neonatal recipients in the Maroof *et al.* study, and mesencephalic stem cells have been shown to differentiate faster in 6-OHDA lesioned than intact striatum (Nishino *et al.*, 2000; Maroof *et al.*, 2013). These differences could prove crucial for clinical transplantation and will need thorough assessment before progression towards trials in humans.

The transplanted cells acquired very distinct morphologies depending on the brain region in which they settled. NKX2.1 is the only known migratory regulator whose expression was analysed in the different brain regions, but there was no difference in its expression between cells in the striatum, septum or hippocampus. This means that we cannot conclude whether the cells migrated purposefully to their destinations and acquired, for example, a hippocampal CR interneuron morphology because they were intrinsically programmed to do so, or whether this occurred as a result of exogenous cues after finding themselves in the hippocampus. In normal mammalian development, MGE progenitors destined for the hippocampus would down-regulate NKX2.1 before migrating through the cortex to end up in the hippocampus (Marin, Anderson and Rubenstein, 2000). In this study, however, they appear to have migrated either through the septum or the globus pallidus to reach the hippocampus, many maintaining NKX2.1 expression. Many of the cells that settled in the lateral septal nucleus had a very unique morphology that differed from any other GFP-positive cells seen in the brain. They had a very complex stellate shape, were mostly NeuN-positive and all GFAP-negative. None of the molecular markers apart from NKX2.1 or NeuN were expressed in these cells, so despite their specific morphology they did not adopt the fate of the majority of septal neurons, which is a GABAergic CR fate (Zhao, Eisinger and Gammie, 2013). Further characterisation will be necessary to identify these cells.

Finally, the constitutive GFP expression in the transplanted cells allowed for visualisation in *ex vivo* brain slices for whole cell patch clamp analysis of the cells' membrane properties and firing

characteristics. Although GFP expression alone was sufficient to see the cells following fixation and immunohistochemical staining of 40  $\mu\text{m}$  thick sections, in 300  $\mu\text{m}$  sections used for electrophysiology, it was apparently much more difficult to see the GFP. This meant that of three brains taken for electrophysiology at 12 weeks, only three cells were found in two sections of one of the brains. However, one of these cells did show some promising characteristics, in that it had a polarised resting membrane potential and fired large action potentials both spontaneously and when stimulated. This is a similar level of functionality to what Denham *et al.* saw in their study at 10 weeks post-transplantation (Denham *et al.*, 2012). Nicholas *et al.* left their cells to mature for 7 months in SCID-mice cortices, and saw a much more mature electrophysiological profile, suggesting that the maturation of hPSC-derived neurons resembles that of neurons developing in the human brain (Nicholas *et al.*, 2013). The thickness of the section used for electrophysiology allowed for a more comprehensive view of the cell's morphology compared to the sections made for histology. Biocytin filling of the cell therefore allowed for a partial reconstruction of the cell, which was relatively complex possessing 7 primary processes.

In this chapter, the data presented have shown that hESC-derived MGE progenitors can differentiate and mature *in vivo* into striatal, septal and hippocampal interneurons. Although they appear to be limited to a CR fate when transplanted into the striatum, the cells appear to be adaptable to their environment and it may be possible to push them towards a more PV or SST fate by altering the time windows for transplantation or the age of the animals. It will be important for future transplantation studies to achieve a standard procedure to enable long term maturation of hPSC-derived neuron grafts if these cells are ever to be taken into clinical trials.

## 6 General discussion

### 6.1 Summary

This thesis has reported findings that demonstrate the possibility of generating functional striatal neurons *in vitro* from hPSCs. Two published protocols were used, one to produce striatal projection neurons, or MSNs, developed in our lab, and another to derive GABAergic and cholinergic striatal interneurons (Maroof *et al.*, 2013; Arber *et al.*, 2015). Investigation into the mechanism of the MSN differentiation uncovered a potential novel role for BMP signalling in MSN development, and it has been shown for the first time that hPSC-derived MGE progenitors can produce striatal-specific interneurons rather than cortical or hippocampal interneurons, which have already been heavily studied (Liu *et al.*, 2013; Maroof *et al.*, 2013; Nicholas *et al.*, 2013; Cunningham *et al.*, 2014). In addition, the advantages of deriving and using a hESC-line with constitutive GFP expression for transplantation studies have been highlighted.

In the process of working towards the aim of generating functional striatal neurons, many of the applications for which hPSCs can be useful have been portrayed. By investigating the mechanism via which Activin induces LGE and MSN fate, a potential novel pathway in MSN specification has been discovered, showing how directed differentiation of hPSCs can aid in studying human development. Secondly, electrophysiological data from both types of striatal neurons has been presented, showing that their functionality can be improved by culturing them in more physiologically and developmentally relevant media (Telezhkin *et al.*, 2015). This will be crucial in future studies aiming to model functional development of the striatum as well as analysing disease cell models for changes in their membrane and synaptic properties. Finally, the last chapter has established that transplantation of the hPSC-derived MGE progenitors into neonatal rat striatum could push the cells to favour a calretinin interneuron fate when compared to the sister cultures *in vitro*. This highlights the importance of transplantation studies in this field for the purpose of observing the differentiation potential of hPSC-derived neurons. It also shows the possibility of transplanting GFP-expressing cells for electrophysiological analysis, which will be crucial for proving true functional integration of transplanted neurons in a host brain.

### 6.2 Implications for the study of human development

There are many stages to striatal development that can be clearly defined and modelled through hPSC differentiation. The procedure for generating both striatal cell types exploited the dual Smad inhibition monolayer neural induction method proposed by Chambers *et al.* (2009). This is a reliable and straight forward technique of efficiently pushing hPSCs towards a forebrain lineage within 10 days. Our lab has a wealth of experience working on directed monolayer differentiation of mouse and human ESCs

towards neurons of diverse subtypes (Jaeger *et al.*, 2011; Cambray *et al.*, 2012; Arber *et al.*, 2015). The monolayer method has several advantages over 3D differentiation methods, such as embryoid bodies or organoids, in that all cells are uniformly exposed to the culture medium and patterning factors, resulting in a more synchronised and therefore homogeneous neuronal population. There is no need for mechanical selection, and the entire process can be done in a fully defined and xeno-free environment making it easier to scale up for future clinical purposes.

The next stage involves patterning of the neural progenitors towards a particular neuronal lineage, namely striatal neurons. This is the step represented by the Activin or SHH treatment, which aims to produce as high a proportion of the desired cell type as possible (Maroof *et al.*, 2013; Arber *et al.*, 2015). At this stage, much work has already been done to optimise the concentration and timing of patterning factors to produce a homogeneous population, but more research could be done to enrich them further. In addition, the mechanism of induction is not always well-defined, and while the presence of Smads and Activins in the developing striatum was previously known, the developmental mechanism by which Activin induces LGE fate remains unclear (Maira *et al.*, 2010). In this thesis, I have presented evidence showing that Activin exerts its effects independently of the SHH pathway, which was the pathway previously exploited for the production of MSNs (Aubry *et al.*, 2008; Ma *et al.*, 2012; Carri *et al.*, 2013; Nicoleau *et al.*, 2013). Furthermore, in an attempt to elucidate the mechanism of Activin, I have discovered a novel pathway that appears to play a role in MSN differentiation, BMP receptor inhibition. Future experiments in this area will focus on the actions of phosphorylated Smad2/3, Activin's intracellular effector, and its effects on gene transcription. Another logical next step would be to look *in vivo*, and whether Activin and BMP signalling play an instructive role in MSN fate specification in rodent striatal development. In this way, preliminary studies and high throughput screening on hPSC differentiation allow more hypothesis-driven *in vivo* experiments, reducing the number of animals used in research.

In contrast, the mechanism by which SHH induces MGE fate by NKX2.1 upregulation is somewhat better understood (Gulacsi and Anderson, 2006). NKX2.1 is expressed throughout the entire ventral neural tube, though co-expression with the forebrain marker FOXG1 is vital for MGE specification. Stewart Anderson's group have done much work to optimise the timing of Wnt inhibition for forebrain promotion, and SHH activation, showing that earlier SHH treatment encourages a more caudal fate resulting in hypothalamic-like progenitors, while later addition of SHH promotes a GABAergic interneuron fate (Maroof *et al.*, 2013). This work also demonstrates how research on hPSCs has a mutually beneficial relationship with *in vivo* developmental research, as hPSCs provide a more easily manipulable model on which to test different conditions, while *in vivo* studies give an insight into the brain developing as a whole within an organism. Crucially, hPSCs, unlike mouse ESCs, offer an

unprecedented bridge between rodent studies and live human development, as human brain tissue is sparse and difficult to standardise.

The final stage of *in vitro* differentiation is neuronal maturation – the cells have been patterned towards the cell type of choice, then they are typically left to mature in a basal differentiation medium containing neurotrophic factors. This is now a stage that can begin to be optimised and used as a model of development and function for the specific brain region being studied. In other words, the organisation, physiology and synaptic connectivity of hPSC-derived MSNs and striatal interneurons can be studied as they mature as a model of striatal development. For this, it is likely that novel culture systems will need to be devised for co-culturing MSNs, interneurons and glial cells, as well as innervating cells such as cortical pyramidal and midbrain dopaminergic neurons or target cells such as pallidal projection neurons. Studies using mouse embryonic neurons have demonstrated the importance of co-cultures including cortical neurons in co-culture with MSNs in order to achieve an *in vivo*-like morphology with mature dendritic spines (Penrod *et al.*, 2011). Reporter cell lines would also be invaluable to this line of research, not only to distinguish between, for example, hPSC-derived interneurons that are co-cultured with MSNs, but also to be able to identify interneuron subtypes within the heterogeneous population of cells produced using the MGE protocol. This would allow much more targeted experiments, particularly for electrophysiology, without the need to analyse undesired cell types and retrospectively identify them using post-hoc staining.

### 6.3 Implications for disease modelling

Just as each differentiation step can model the stages of development in physiological conditions. There are many neurological and neuropsychiatric conditions that carry a developmental component. Indeed, there is evidence that HD affects foetal and childhood brain development, despite not typically becoming symptomatic until middle age (Nopoulos *et al.*, 2011; Lee *et al.*, 2012). Previous work on HD iPSCs have been carried out using heterogeneous cell populations with a relatively low proportion of DARPP32-positive MSNs, but have already found HD-induced changes in cell metabolism, adhesion and death (Zhang *et al.*, 2010; The HD iPSC Consortium, 2012). ASD and schizophrenia are known neurodevelopmental disorders caused by a complex interaction between genes and the environment. Despite a huge amount of research into cortical and hippocampal dysfunction in these disorders, there is also strong evidence for a striatal role in the cognitive and repetitive behavioural deficits experienced (Simpson, Kellendonk and Kandel, 2010; Fuccillo, 2016). Having devised a robust protocol for generating MSNs, and here shown that we can also produce striatal interneurons from hPSCs, our future research plan is to apply these methods to HD, ASD or schizophrenia patient-derived iPSCs to look at more striatal-relevant phenotypes. Perhaps an ultimate test of the authenticity of hPSC-derived MSNs would be their relative vulnerability compared to neurons of other types derived from



HD patient iPSCs. Again, hPSCs provide a bridge between *in vivo* studies or work done on rodent *in vitro* models and human disease.

Induced neurons are another source of living human neurons that may hold greater promise for patient-specific studies, such as personalised medicine. They provide a fast and effective way of obtaining a high proportion of MSNs or interneurons from patient fibroblast biopsies, which would allow screening of potential drugs for a specific patient (Victor *et al.*, 2014; Colasante *et al.*, 2015). However, the direct conversion of the fibroblasts into neurons avoids the neural progenitor stage missing the opportunity for expansion and limiting the yield considerably. Human PSC-derived LGE and MGE progenitors can be easily frozen in bulk and then thawed as needed, generating MSNs or interneurons within 3 or 6 weeks respectively. Furthermore, hPSCs allow genetic manipulation of potential downstream targets of HD, such as CTIP2 (Desplats, Lambert and Thomas, 2008). Our lab has recently established multiple cell lines either with tamoxifen-inducible overexpression or heterozygous or homozygous knockout of CTIP2. Studies like this aid in the dissection of disease mechanisms, and are also being applied for candidate genes in schizophrenia and ASD discovered in genome-wide association studies. As these are polygenic diseases with no single cause, specific genes can be manipulated in hPSCs to investigate their cellular function and therefore how they cause a disease phenotype (Williams *et al.*, 2011; Chen *et al.*, 2015). The ability to specify the hPSCs towards a particular cell type widens the opportunities for complex co-culture systems with which to model these diseases.

#### 6.4 Implications for regenerative medicine

The findings presented here do not directly address the issue of cell replacement therapy, as transplantation was only carried out in intact neonatal rats as opposed to an adult disease model. However, they did highlight some technical obstacles delaying progress in the field. Firstly, transplantation of hPSC-derived neural progenitors into neonatal rats does not appear to prevent immune rejection of the graft, nor does daily immunosuppressant administration guarantee it. In addition, 20 weeks is not sufficient time for all human cells to mature into neurons, nor for those that do to become fully functionally integrated (Nicholas *et al.*, 2013). The workload and timeline for these experiments is very heavy, and so a more reliable method must be considered for future studies. Nude rats may provide the necessary incubation time for neonatal or intact animal experiments to observe the differentiation and integration potential of cells, but their susceptibility to infection and illness makes behavioural experiments very difficult to conduct. Instead, neonatal desensitisation may be a more viable option for disease models and behavioural studies, as no immune suppression is required and can allow graft survival to at least 40 weeks (Kelly *et al.*, 2009; Heuer *et al.*, 2016). Another important consideration when transplanting hPSC-derived neural progenitors is their level of fate

commitment and the extent to which the host brain environment may influence and fine tune their differentiation. This was made clear in the experiment presented here, where sister cultures left to mature *in vitro* produced quite different interneuron subtypes than those in the grafts, although they could all be considered of MGE identity.

## 6.5 Conclusions

The findings presented in this thesis support the use of hPSCs in the generation of specific neuronal subtypes for studying neural development, disease modelling and transplantation studies for cell replacement therapy. These types of studies have gained a lot of momentum over the recent years, and the ability to produce functional striatal neurons allows much more directed experiments into striatal development and function, rather than studying undefined heterogeneous populations of neurons. The ability to generate iPSCs from patient somatic cells also opens up a wealth of possibilities for personalised research and medicine in the future.

## 7 References

- Anderson, R. M., Lawrence, A. R., Stottmann, R. W., Bachiller, D. and Klingensmith, J. (2002) 'Chordin and noggin promote organizing centers of forebrain development in the mouse.', *Development*, 129(21), pp. 4975–4987. doi: 10.1006/bbrc.1998.9170.
- Anderson, S. A., Qiu, M., Bulfone, A., Eisenstat, D. D., Meneses, J., Pedersen, R. and Rubenstein, J. L. R. (1997) 'Mutations of the homeobox genes *Dlx-1* and *Dlx-2* disrupt the striatal subventricular zone and differentiation of late born striatal neurons', *Neuron*, 19(1), pp. 27–37. doi: 10.1016/S0896-6273(00)80345-1.
- Andoniadou, C. L. and Martinez-Barbera, J. P. (2013) 'Developmental mechanisms directing early anterior forebrain specification in vertebrates', *Cellular and Molecular Life Sciences*, 70(20), pp. 3739–3752. doi: 10.1007/s00018-013-1269-5.
- Andrew, S. E., Goldberg, Y. P., Kremer, B., Telenius, H., Theilmann, J., Adam, S., Starr, E., Squitieri, F., Lin, B. and Kalchman, M. a (1993) 'The relationship between trinucleotide (CAG) repeat length and clinical features of Huntington's disease.', *Nature Genetics*, 4(4), pp. 398–403. doi: 10.1038/ng0893-398.
- Arber, C., Precious, S. V, Cambray, S., Risner-Janiczek, J. R., Kelly, C., Noakes, Z., Fjodorova, M., Heuer, A., Ungless, M. A., Rodr, T. A., Rosser, A. E., Dunnett, S. B. and Li, M. (2015) 'Activin A directs striatal projection neuron differentiation of human pluripotent stem cells', *Development*, 142(7), pp. 1375–1386. doi: 10.1242/dev.117093.
- Arlotta, P., Molyneaux, B. J., Chen, J., Inoue, J., Kominami, R. and MacKlis, J. D. (2005) 'Neuronal subtype-specific genes that control corticospinal motor neuron development in vivo', *Neuron*, 45(2), pp. 207–221. doi: 10.1016/j.neuron.2004.12.036.
- Arlotta, P., Molyneaux, B. J., Jabaudon, D., Yoshida, Y. and Macklis, J. D. (2008) 'Ctip2 controls the differentiation of medium spiny neurons and the establishment of the cellular architecture of the striatum.', *Journal of Neuroscience*, 28(3), pp. 622–632. doi: 10.1523/JNEUROSCI.2986-07.2008.
- Aubry, L., Bugi, A., Lefort, N., Rousseau, F., Peschanski, M. and Perrier, A. L. (2008) 'Striatal progenitors derived from human ES cells mature into DARPP32 neurons in vitro and in quinolinic acid-lesioned rats.', *Proceedings of the National Academy of Sciences of the United States of America*, 105(43), pp. 16707–16712. doi: 10.1073/pnas.0808488105.
- Bachiller, D., Klingensmith, J., Kemp, C., Belo, J. A., Anderson, R. M., May, S. R., McMahon, J. A., McMahon, A. P., Harland, R. M., Rossant, J. and De Robertis, E. M. (2000) 'The organizer factors Chordin and Noggin are required for mouse forebrain development.', *Nature*, 403(6770), pp. 658–661. doi: 10.1038/35001072.
- Bachoud-Lévi, A., Bourdet, C., Brugières, P., Nguyen, J. P., Grandmougin, T., Haddad, B., Jény, R., Bartolomeo, P., Boissé, M. F., Barba, G. D., Degos, J. D., Ergis, A. M., Lefaucheur, J. P., Lisovoski, F., Pailhous, E., Rémy, P., Palfi, S., Defer, G. L., Cesaro, P., Hantraye, P. and Peschanski, M. (2000) 'Safety and tolerability assessment of intrastriatal neural allografts in five patients with Huntington's disease.', *Experimental Neurology*, 161(1), pp. 194–202. doi: 10.1006/exnr.1999.7239.
- Bachoud-Lévi, A. C., Gaura, V., Brugières, P., Lefaucheur, J. P., Boissé, M. F., Maison, P., Baudic, S., Ribeiro, M. J., Bourdet, C., Remy, P., Cesaro, P., Hantraye, P. and Peschanski, M. (2006) 'Effect of fetal neural transplants in patients with Huntington's disease 6 years after surgery: A long-term follow-up study', *Lancet Neurology*, 5(4), pp. 303–309. doi: 10.1016/S1474-4422(06)70381-7.
- Backman, M., Machon, O., Mygland, L., Van Den Bout, C. J., Zhong, W., Taketo, M. M. and Krauss, S.

- (2005) 'Effects of canonical Wnt signaling on dorso-ventral specification of the mouse telencephalon', *Developmental Biology*, 279(1), pp. 155–168. doi: 10.1016/j.ydbio.2004.12.010.
- Barker, R. a, Mason, S. L., Harrower, T. P., Swain, R. a, Ho, A. K., Sahakian, B. J., Mathur, R., Elneil, S., Thornton, S., Hurrelbrink, C., Armstrong, R. J., Tyers, P., Smith, E., Carpenter, A., Piccini, P., Tai, Y. F., Brooks, D. J., Pavese, N., Watts, C., Pickard, J. D., Rosser, A. E. and Dunnett, S. B. (2013) 'The long-term safety and efficacy of bilateral transplantation of human fetal striatal tissue in patients with mild to moderate Huntington's disease.', *Journal of Neurology, Neurosurgery and Psychiatry*, 84(6), pp. 657–665. doi: 10.1136/jnnp-2012-302441.
- Bean, B. P. (2007) 'The action potential in mammalian central neurons', *Nature Reviews Neuroscience*, 8(6), pp. 451–465. doi: 10.1038/nrn2148.
- Beaulieu, J.-M. and Gainetdinov, R. R. (2011) 'The physiology, signaling, and pharmacology of dopamine receptors.', *Pharmacological Reviews*, 63(1), pp. 182–217. doi: 10.1124/pr.110.002642.182.
- Björklund, A., Dunnett, S. B., Brundin, P., Stoessl, A. J., Freed, C. R., Breeze, R. E., Levivier, M., Peschanski, M., Studer, L. and Barker, R. (2003) 'Neural transplantation for the treatment of Parkinson's disease', *Lancet Neurology*, 2(7), pp. 437–445. doi: 10.1016/S1474-4422(03)00442-3.
- Björklund, A. and Stenevi, U. (1979) 'Reconstruction of the nigrostriatal dopamine pathway by intracerebral nigral transplants', *Brain Research*, 177(3), pp. 555–560. doi: 10.1016/0006-8993(79)90472-4.
- Björkqvist, M., Wild, E. J., Thiele, J., Silvestroni, A., Andre, R., Lahiri, N., Raibon, E., Lee, R. V, Benn, C. L., Soulet, D., Magnusson, A., Woodman, B., Landles, C., Pouladi, M. A., Hayden, M. R., Khalili-Shirazi, A., Lowdell, M. W., Brundin, P., Bates, G. P., Leavitt, B. R., Möller, T. and Tabrizi, S. J. (2008) 'A novel pathogenic pathway of immune activation detectable before clinical onset in Huntington's disease.', *Journal of Experimental Medicine*, 205(8), pp. 1869–77. doi: 10.1084/jem.20080178.
- Bloch, J., Bachoud-Levi, A. C., Deglon, N., Lefaucheur, J. P., Winkel, L., Palfi, S., Nguyen, J. P., Bourdet, C., Gaura, V., Remy, P., Brugieres, P., Boisse, M. F., Baudic, S., Cesaro, P., Hantraye, P., Aebischer, P. and Peschanski, M. (2004) 'Neuroprotective gene therapy for Huntington's disease, using polymer-encapsulated cells engineered to secrete human ciliary neurotrophic factor: results of a phase I study', *Human Gene Therapy*, 15(10), pp. 968–975. doi: 10.1089/hum.2004.15.968.
- Boergermann, J. H., Kopf, J., Yu, P. B. and Knaus, P. (2010) 'Dorsomorphin and LDN-193189 inhibit BMP-mediated Smad, p38 and Akt signalling in C2C12 cells', *International Journal of Biochemistry and Cell Biology*, 42(11), pp. 1802–1807. doi: 10.1016/j.biocel.2010.07.018.
- Bolam, J. P., Hanley, J. J., Booth, P. a and Bevan, M. D. (2000) 'Synaptic organisation of the basal ganglia.', *Journal of Anatomy*, 196 ( Pt 4), pp. 527–542. doi: 10.1046/j.1469-7580.2000.19640527.x.
- Brennand, K., Simone, A., Jou, J., Gelboin-Burkhart, C., Tran, N., Sangar, S., Li, Y., Mu, Y., Chen, G., Yu, D., McCarthy, S., Sebat, J. and Gage, F. H. (2011) 'Modelling schizophrenia using human induced pluripotent stem cells', *Nature*. Nature Publishing Group, 473, pp. 221–225. doi: 10.1038/nature09915.
- Bronner-Fraser, M. and Fraser, S. E. (1997) 'Differentiation of the vertebrate neural tube', *Current Opinion in Cell Biology*, 9(6), pp. 885–891. doi: 10.1016/S0955-0674(97)80092-0.
- Brundin, P., Nilsson, O. G., Gage, F. H. and Björklund, A. (1985) 'Cyclosporin A increases survival of cross-species intrastriatal grafts of embryonic dopamine-containing neurons', *Experimental Brain Research*, 60(1), pp. 204–208. doi: 10.1007/BF00237035.
- Brundin, P., Widner, H., Nilsson, O. G., Strecker, R. E. and Björklund, A. (1989) 'Intracerebral xenografts

of dopamine neurons: the role of immunosuppression and the blood-brain barrier', *Experimental Brain Research*, 75(1), pp. 195–207. doi: 10.1007/BF00248542.

Bubnic, S. J., Nagy, A. and Keating, A. (2005) 'Donor hematopoietic cells from transgenic mice that express GFP are immunogenic in immunocompetent recipients.', *Hematology*, 10(August), pp. 289–295. doi: 10.1080/10245330500093468.

Calabresi, P., Picconi, B., Tozzi, A., Ghiglieri, V. and Di Filippo, M. (2014) 'Direct and indirect pathways of basal ganglia: a critical reappraisal', *Nature Neuroscience*. Nature Publishing Group, 17(8), pp. 1022–1030. doi: 10.1038/nn.3743.

Cambray, S., Arber, C., Little, G., Dougalis, A. G., de Paola, V., Ungless, M. a., Li, M. and Rodríguez, T. a. (2012) 'Activin induces cortical interneuron identity and differentiation in embryonic stem cell-derived telencephalic neural precursors', *Nature Communications*, 3(May), p. 841. doi: 10.1038/ncomms1817.

Capetian, P., Knoth, R., Maciaczyk, J., Pantazis, G., Ditter, M., Bokla, L., Landwehrmeyer, G. B., Volk, B. and Nikkhah, G. (2009) 'Histological findings on fetal striatal grafts in a Huntington's disease patient early after transplantation', *Neuroscience*, 160(3), pp. 661–675. doi: 10.1016/j.neuroscience.2009.02.035.

Capetian, P., Pauly, M. G., Azmita, L. M. and Klein, C. (2014) 'Striatal cholinergic interneurons in isolated generalized dystonia Rationale and perspectives for stem cell-derived cellular models', *Frontiers in Cellular Neuroscience*, 8, pp. 1–9. doi: 10.3389/fncel.2014.00205.

Carr, A.-J. F., Smart, M. J. K., Ramsden, C. M., Powner, M. B., da Cruz, L. and Coffey, P. J. (2013) 'Development of human embryonic stem cell therapies for age-related macular degeneration.', *Trends in Neurosciences*, 36(7), pp. 385–95. doi: 10.1016/j.tins.2013.03.006.

Carri, A. D., Onorati, M., Lelos, M. J., Castiglioni, V., Faedo, A., Menon, R., Camnasio, S., Vuono, R., Spaiardi, P., Talpo, F., Toselli, M., Martino, G., Barker, R. A., Dunnett, S. B., Biella, G. and Cattaneo, E. (2013) 'Developmentally coordinated extrinsic signals drive human pluripotent stem cell differentiation toward authentic DARPP-32+ medium-sized spiny neurons.', *Development*, 140(2), pp. 301–12. doi: 10.1242/dev.084608.

Casari, A., Schiavone, M., Facchinello, N., Vettori, A., Meyer, D., Tiso, N., Moro, E. and Argenton, F. (2014) 'A Smad3 transgenic reporter reveals TGF-beta control of zebrafish spinal cord development', *Developmental Biology*. Elsevier, 396(1), pp. 81–93. doi: 10.1016/j.ydbio.2014.09.025.

Chambers, S. M., Fasano, C. A., Papapetrou, E. P., Tomishima, M., Sadelain, M. and Studer, L. (2009) 'Highly efficient neural conversion of human ES and iPS cells by dual inhibition of SMAD signaling.', *Nature Biotechnology*, 27(3), pp. 275–280. doi: 10.1038/nbt0509-485a.

Chatzi, C., Brade, T. and Duester, G. (2011) 'Retinoic acid functions as a key GABAergic differentiation signal in the basal ganglia', *PLoS Biology*, 9(4). doi: 10.1371/journal.pbio.1000609.

Chen, J. K., Taipale, J., Cooper, M. K. and Beachy, P. A. (2002) 'Inhibition of Hedgehog signaling by direct binding of cyclopamine to Smoothed service Inhibition of Hedgehog signaling by direct binding of cyclopamine to Smoothed', *Genes and Development*, 16, pp. 2743–2748. doi: 10.1101/gad.1025302.

Chen, J., Lin, M., Hrabovsky, A., Pedrosa, E., Dean, J., Jain, S., Zheng, D. and Lachman, H. M. (2015) 'ZNF804A transcriptional networks in differentiating neurons derived from induced pluripotent stem cells of human origin', *PLoS ONE*, 10(4), pp. 1–23. doi: 10.1371/journal.pone.0124597.

Cicchetti, F., Saporta, S., Hauser, R. a, Parent, M., Saint-Pierre, M., Sanberg, P. R., Li, X. J., Parker, J. R., Chu, Y., Mufson, E. J., Kordower, J. H. and Freeman, T. B. (2009) 'Neural transplants in patients with

Huntington's disease undergo disease-like neuronal degeneration.', *Proceedings of the National Academy of Sciences of the United States of America*, 106(30), pp. 12483–12488. doi: 10.1073/pnas.0904239106.

Cisbani, G., Freeman, T. B., Soulet, D., Saint-Pierre, M., Gagnon, D., Parent, M., Hauser, R. A., Barker, R. A. and Cicchetti, F. (2013) 'Striatal allografts in patients with Huntington's disease: Impact of diminished astrocytes and vascularization on graft viability', *Brain*, 136(2), pp. 433–443. doi: 10.1093/brain/aws359.

Colasante, G., Lignani, G., Rubio, A., Medrihan, L., Yekhelef, L., Sessa, A., Massimino, L., Giannelli, S. G., Sacchetti, S., Caiazzo, M., Leo, D., Alexopoulou, D., Dell'Anno, M. T., Ciabatti, E., Orlando, M., Studer, M., Dahl, A., Gainetdinov, R. R., Taverna, S., Benfenati, F. and Broccoli, V. (2015) 'Rapid conversion of fibroblasts into functional forebrain GABAergic interneurons by direct genetic reprogramming', *Cell Stem Cell*. Elsevier Inc., 17(6), pp. 719–734. doi: 10.1016/j.stem.2015.09.002.

Crompton, L. A., Byrne, M. L., Taylor, H., Kerrigan, T. L., Bru-Mercier, G., Badger, J. L., Barbuti, P. A., Jo, J., Tyler, S. J., Allen, S. J., Kunath, T., Cho, K. and Caldwell, M. A. (2013) 'Stepwise, non-adherent differentiation of human pluripotent stem cells to generate basal forebrain cholinergic neurons via hedgehog signaling', *Stem Cell Research*. Elsevier B.V., 11(3), pp. 1206–1221. doi: DOI 10.1016/j.scr.2013.08.002.

Cunningham, M., Cho, J.-H., Leung, A., Savvidis, G., Ahn, S., Moon, M., Lee, P. K. J., Han, J. J., Azimi, N., Kim, K.-S., Bolshakov, V. Y. and Chung, S. (2014) 'hPSC-derived maturing GABAergic interneurons ameliorate seizures and abnormal behavior in epileptic mice', *Cell Stem Cell*. Elsevier Inc., 15(5), pp. 559–573. doi: 10.1016/j.stem.2014.10.006.

Danjo, T., Eiraku, M., Muguruma, K., Watanabe, K., Kawada, M., Yanagawa, Y., Rubenstein, J. L. R. and Sasai, Y. (2011) 'Subregional specification of embryonic stem cell-derived ventral telencephalic tissues by timed and combinatory treatment with extrinsic signals.', *Journal of Neuroscience*, 31(5), pp. 1919–1933. doi: 10.1523/JNEUROSCI.5128-10.2011.

Davis, M. I. and Puhl, H. L. (2011) 'Nr4a1-eGFP is a marker of striosome-matrix architecture, development and activity in the extended striatum', *PLoS ONE*, 6(1). doi: 10.1371/journal.pone.0016619.

Deng, P., Torrest, A., Pollock, K., Dahlenburg, H., Annett, G., Nolte, J. and Fink, K. (2016) 'Clinical trial perspective for adult and juvenile Huntington's disease using genetically-engineered mesenchymal stem cells', *Neural Regeneration Research*, 11(5). doi: 10.4103/1.

Deng, Y. P., Albin, R. L., Penney, J. B., Young, A. B., Anderson, K. D. and Reiner, A. (2004) 'Differential loss of striatal projection systems in Huntington's disease: A quantitative immunohistochemical study', *Journal of Chemical Neuroanatomy*, 27(3), pp. 143–164. doi: 10.1016/j.jchemneu.2004.02.005.

Denham, M., Parish, C. L., Leaw, B., Wright, J., Reid, C. A., Petrou, S., Dottori, M. and Thompson, L. H. (2012) 'Neurons derived from human embryonic stem cells extend long-distance axonal projections through growth along host white matter tracts after intra-cerebral transplantation', *Frontiers in Cellular Neuroscience*, 6(March), pp. 1–14. doi: 10.3389/fncel.2012.00011.

Desplats, P. A., Lambert, J. R. and Thomas, E. A. (2008) 'Functional roles for the striatal-enriched transcription factor, Bcl11b, in the control of striatal gene expression and transcriptional dysregulation in Huntington's disease', *Neurobiology of Disease*, 31(3), pp. 298–308. doi: 10.1016/j.nbd.2008.05.005.

Döbrössy, M. D. and Dunnett, S. B. (2005) 'Training specificity, graft development and graft-mediated functional recovery in a rodent model of Huntington's disease', *Neuroscience*, 132(3), pp. 543–552. doi: 10.1016/j.neuroscience.2005.01.016.

- Echelard, Y., Epstein, D. J., St-Jacques, B., Shen, L., Mohler, J., McMahon, J. A. and McMahon, A. P. (1993) 'Sonic hedgehog, a member of a family of putative signaling molecules, is implicated in the regulation of CNS polarity', *Cell*, 75(7), pp. 1417–1430. doi: 10.1016/0092-8674(93)90627-3.
- Englund, U., Fricker-Gates, R. a, Lundberg, C., Björklund, A. and Wictorin, K. (2002) 'Transplantation of human neural progenitor cells into the neonatal rat brain: extensive migration and differentiation with long-distance axonal projections.', *Experimental Neurology*, 173(1), pp. 1–21. doi: 10.1006/exnr.2001.7750.
- Eriksson, C., Björklund, A. and Wictorin, K. (2003) 'Neuronal differentiation following transplantation of expanded mouse neurosphere cultures derived from different embryonic forebrain regions', *Experimental Neurology*, 184(2), pp. 615–635. doi: 10.1016/S0014-4886(03)00271-1.
- Espuny-Camacho, I., Michelsen, K. a., Gall, D., Linaro, D., Hasche, A., Bonnefont, J., Bali, C., Orduz, D., Bilheu, A., Herpoel, A., Lambert, N., Gaspard, N., Péron, S., Schiffmann, S. N., Giugliano, M., Gaillard, A. and Vanderhaeghen, P. (2013) 'Pyramidal Neurons Derived from Human Pluripotent Stem Cells Integrate Efficiently into Mouse Brain Circuits In Vivo', *Neuron*, 77(3), pp. 440–456. doi: 10.1016/j.neuron.2012.12.011.
- Evans, J. R., Mason, S. L. and Barker, R. A. (2012) 'Current status of clinical trials of neural transplantation in Parkinson's disease', *Progress in Brain Research*. 1st edn. Elsevier B.V., 200, pp. 169–198. doi: 10.1016/B978-0-444-59575-1.00008-9.
- Feijen, A., Goumans, M. J. and van den Eijnden-van Raaij, A. J. (1994) 'Expression of activin subunits, activin receptors and follistatin in postimplantation mouse embryos suggests specific developmental functions for different activins.', *Development*, 120(12), pp. 3621–3637.
- Feng, Q., Ma, Y., Mu, S., Wu, J., Chen, S., OuYang, L. and Lei, W. (2014) 'Specific reactions of different striatal neuron types in morphology induced by quinolinic acid in rats', *PLoS ONE*, 9(3). doi: 10.1371/journal.pone.0091512.
- Ferrante, R. J. (2009) 'Mouse models of Huntington's disease and methodological considerations for therapeutic trials.', *Biochimica et Biophysica Acta*, 1792(6), pp. 506–20. doi: 10.1016/j.bbadis.2009.04.001.
- Figueredo-Cardenas, G., Chen, Q. and Reiner, A. (1997) 'Age-dependent differences in survival of striatal somatostatin-NPY-NADPH-diaphorase-containing interneurons versus striatal projection neurons after intrastriatal injection of quinolinic acid in rats.', *Experimental Neurology*, 146(2), pp. 444–57. doi: 10.1006/exnr.1997.6549.
- Figueredo-Cardenas, G., Harris, C. L., Anderson, K. D. and Reiner, A. (1998) 'Relative resistance of striatal neurons containing calbindin or parvalbumin to quinolinic acid-mediated excitotoxicity compared to other striatal neuron types.', *Experimental Neurology*, 149(2), pp. 356–72. doi: 10.1006/exnr.1997.6724.
- Figueredo-Cardenas, G., Morello, M., Sancesario, G., Bernardi, G. and Reiner, a (1996) 'Colocalization of somatostatin, neuropeptide Y, neuronal nitric oxide synthase and NADPH-diaphorase in striatal interneurons in rats.', *Brain research*, 735(2), pp. 317–324. doi: 10.1016/0006-8993(96)00801-3.
- Fino, E. and Venance, L. (2011) 'Spike-timing dependent plasticity in striatal interneurons', *Neuropharmacology*. Elsevier Ltd, 60(5), pp. 780–788. doi: 10.1016/j.neuropharm.2011.01.023.
- Flames, N., Pla, R., Gelman, D. M., Rubenstein, J. L. R., Puellas, L. and Marín, O. (2007) 'Delineation of multiple subpallial progenitor domains by the combinatorial expression of transcriptional codes.', *Journal of Neuroscience*, 27(36), pp. 9682–9695. doi: 10.1523/JNEUROSCI.2750-07.2007.
- Flandin, P., Kimura, S. and Rubenstein, J. L. (2010) 'The progenitor zone of the ventral medial

- ganglionic eminence requires Nkx2-1 to generate most of the globus pallidus but few neocortical interneurons', *Journal of Neuroscience*, 30(8), pp. 2812–2823. doi: 10.1523/JNEUROSCI.4228-09.2010.
- Freeman, T. B., Cicchetti, F., Hauser, R. A., Deacon, T. W., Li, X. J., Hersch, S. M., Nauert, G. M., Sanberg, P. R., Kordower, J. H., Saporta, S. and Isacson, O. (2000) 'Transplanted fetal striatum in Huntington's disease: phenotypic development and lack of pathology.', *Proceedings of the National Academy of Sciences of the United States of America*, 97(25), pp. 13877–82. doi: 10.1073/pnas.97.25.13877.
- Fuccillo, M. V. (2016) 'Striatal circuits as a common node for autism pathophysiology', *Frontiers in Neuroscience*, 10(FEB). doi: 10.3389/fnins.2016.00027.
- Furuta, Y., Piston, D. W. and Hogan, B. L. (1997) 'Bone morphogenetic proteins (BMPs) as regulators of dorsal forebrain development.', *Development*, 124(11), pp. 2203–2212.
- Garriga-Canut, M., Agustín-Pavón, C., Herrmann, F., Sánchez, A. and Dierssen, M. (2012) 'Synthetic zinc finger repressors reduce mutant huntingtin expression in the brain of R6/2 mice', *Proceedings of the National Academy of Sciences of the United States of America*, 109(45). doi: 10.1073/pnas.1206506109/-/DCSupplemental.www.pnas.org/cgi/doi/10.1073/pnas.1206506109.
- Géral, C., Angelova, A. and Lesieur, S. (2013) 'From molecular to nanotechnology strategies for delivery of neurotrophins: Emphasis on brain-derived neurotrophic factor (BDNF)', *Pharmaceutics*, 5(1), pp. 127–167. doi: 10.3390/pharmaceutics5010127.
- Germain, N. D., Banda, E. C., Becker, S., Naegele, J. R. and Grabel, L. B. (2013) 'Derivation and isolation of NKX2.1-positive basal forebrain progenitors from human embryonic stem cells.', *Stem Cells and Development*, 22(10), pp. 1477–89. doi: 10.1089/scd.2012.0264.
- Ghiglieri, V., Bagnetta, V., Calabresi, P. and Picconi, B. (2012) 'Functional interactions within striatal microcircuit in animal models of Huntington's disease', *Neuroscience*. Elsevier Inc., 211, pp. 165–184. doi: 10.1016/j.neuroscience.2011.06.075.
- Giampà, C., DeMarch, Z., D'Angelo, V., Morello, M., Martorana, A., Sancesario, G., Bernardi, G. and Fusco, F. R. (2006) 'Striatal modulation of cAMP-response-element-binding protein (CREB) after excitotoxic lesions: Implications with neuronal vulnerability in Huntington's disease', *European Journal of Neuroscience*, 23(1), pp. 11–20. doi: 10.1111/j.1460-9568.2005.04545.x.
- Gittis, A. H., Hang, G. B., LaDow, E. S., Shoenfeld, L. R., Atallah, B. V., Finkbeiner, S. and Kreitzer, A. C. (2011) 'Rapid target-specific remodeling of fast-spiking inhibitory circuits after loss of dopamine', *Neuron*, 71(5), pp. 858–868. doi: 10.1016/j.neuron.2011.06.035.
- Gonzalez, V., Cif, L., Biolsi, B., Garcia-Ptacek, S., Seychelles, A., Sanrey, E., Descours, I., Coubes, C., de Moura, A. M., Corlobe, A., James, S., Roujeau, T. and Coubes, P. (2014) 'Deep brain stimulation for Huntington's disease: long-term results of a prospective open-label study.', *Journal of Neurosurgery*, 121(1), pp. 114–122. doi: 10.3171/2014.2.jns131722.
- Grasbon-Frodl, E. M., Nakao, N., Lindvall, O. and Brundin, P. (1996) 'Phenotypic development of the human embryonic striatal primordium: A study of cultured and grafted neurons from the lateral and medial ganglionic eminences', *Neuroscience*, 73(1), pp. 171–183.
- Grasbon-Frodl, E. M., Nakao, N., Lindvall, O. and Brundin, P. (1997) 'Developmental features of human striatal tissue transplanted in a rat model of Huntington's disease.', *Neurobiology of Disease*, 3(4), pp. 299–311. doi: 10.1006/nbdi.1996.0124.
- Graveland, G. A. and Difiglia, M. (1985) 'The frequency and distribution of medium-sized neurons with indented nuclei in the primate and rodent neostriatum', *Brain Research*, 327(1–2), pp. 307–311. doi: 10.1016/0006-8993(85)91524-0.



- Graybiel, A. M., Liu, F. C. and Dunnett, S. B. (1989) 'Intra-striatal grafts derived from fetal striatal primordia. I. Phenotypy and modular organization.', *Journal of Neuroscience*, 9(9), pp. 3250–3271.
- Grealish, S., Diguët, E., Kirkeby, A., Mattsson, B., Heuer, A., Bramouille, Y., Van Camp, N., Perrier, A. L., Hantraye, P., Björklund, A. and Parmar, M. (2014) 'Human ESC-derived dopamine neurons show similar preclinical efficacy and potency to fetal neurons when grafted in a rat model of Parkinson's disease', *Cell Stem Cell*, 15(5), pp. 653–665. doi: 10.1016/j.stem.2014.09.017.
- Guidetti, P., Bates, G. P., Graham, R. K., Hayden, M. R., Leavitt, B. R., MacDonald, M. E., Slow, E. J., Wheeler, V. C., Woodman, B. and Schwarcz, R. (2006) 'Elevated brain 3-hydroxykynurenine and quinolinate levels in Huntington disease mice', *Neurobiology of Disease*, 23(1), pp. 190–197. doi: 10.1016/j.nbd.2006.02.011.
- Guidetti, P., Luthi-Carter, R. E., Augood, S. J. and Schwarcz, R. (2004) 'Neostriatal and cortical quinolinate levels are increased in early grade Huntington's disease', *Neurobiology of Disease*, 17(3), pp. 455–461. doi: 10.1016/j.nbd.2004.07.006.
- Gulacsi, A. and Anderson, S. A. (2006) 'Shh maintains Nkx2.1 in the MGE by a Gli3-independent mechanism', *Cerebral Cortex*, 16(SUPPL. 1), pp. 89–95. doi: 10.1093/cercor/bhk018.
- Gunhaga, L., Marklund, M., Sjödal, M., Hsieh, J.-C., Jessell, T. M. and Edlund, T. (2003) 'Specification of dorsal telencephalic character by sequential Wnt and FGF signaling.', *Nature Neuroscience*, 6(7), pp. 701–707. doi: 10.1038/nn1068.
- Hagell, P., Schrag, A., Piccini, P., Jahanshahi, M., Brown, R., Rehncrona, S., Widner, H., Brundin, P., Rothwell, J. C., Odin, P., Wenning, G. K., Morrish, P., Gustavii, B., Björklund, A., Brooks, D. J., Marsden, C. D., Quinn, N. P. and Lindvall, O. (1999) 'Sequential bilateral transplantation in Parkinson's disease Effects of the second graft', *Clinical Neuroscience*, 122, pp. 1121–1132. doi: 10.1093/brain/122.6.1121.
- Hallett, P. J., Deleidi, M., Astradsson, A., Smith, G. A., Cooper, O., Osborn, T. M., Sundberg, M., Moore, M. A., Perez-Torres, E., Brownell, A. L., Schumacher, J. M., Spealman, R. D. and Isacson, O. (2015) 'Successful function of autologous iPSC-derived dopamine neurons following transplantation in a non-human primate model of Parkinson's disease', *Cell Stem Cell*. Elsevier Inc., 16(3), pp. 269–274. doi: 10.1016/j.stem.2015.01.018.
- Halliday, G., McRitchie, D., Macdonald, V., Double, K., Trent, R. and McCusker, E. (1998) 'Regional Specificity of Brain Atrophy in Huntington's Disease', *Experimental Neurology*, (154), pp. 663–672.
- Hansen, D. V, Lui, J. H., Flandin, P., Yoshikawa, K., Rubenstein, J. L., Alvarez-Buylla, A. and Kriegstein, A. R. (2013) 'Non-epithelial stem cells and cortical interneuron production in the human ganglionic eminences.', *Nature Neuroscience*, 16(11), pp. 1576–87. doi: 10.1038/nn.3541.
- Harper, S. Q., Staber, P. D., He, X., Eliason, S. L., Martins, I. H., Mao, Q., Yang, L., Kotin, R. M., Paulson, H. L. and Davidson, B. L. (2005) 'RNA interference improves motor and neuropathological abnormalities in a Huntington's disease mouse model.', *Proceedings of the National Academy of Sciences of the United States of America*, 102(16), pp. 5820–5. doi: 10.1073/pnas.0501507102.
- Hemmati-Brivanlou, A., Kelly, O. G. and Melton, D. A. (1994) 'Follistatin, an antagonist of activin, is expressed in the Spemann organizer and displays direct neuralizing activity.', *Cell*, 77(2), pp. 283–295. doi: 10.1016/0092-8674(94)90320-4.
- Heuer, A., Jönsson, M. E., Ulrich, P., Kirkeby, A. and Parmar, M. (2016) 'hESC-derived neural progenitors prevent xenograft rejection through neonatal desensitisation', *Experimental Neurology*, 282, pp. 78–85. doi: 10.1016/j.expneurol.2016.05.027.
- Hong, S., Hwang, D.-Y., Yoon, S., Isacson, O., Ramezani, A., Hawley, R. G. and Kim, K.-S. (2007)

'Functional analysis of various promoters in lentiviral vectors at different stages of in vitro differentiation of mouse embryonic stem cells.', *Molecular Therapy*, 15(9), pp. 1630–9. doi: 10.1038/sj.mt.6300251.

Hooi, H. K. and Hearn, M. T. W. (2005) 'A molecular recognition paradigm: Promiscuity associated with the ligand-receptor interactions of the activin members of the TGF- $\beta$  superfamily', *Journal of Molecular Recognition*, 18(5), pp. 385–403. doi: 10.1002/jmr.715.

Hooper, J. E. and Scott, M. P. (2005) 'Communicating with Hedgehogs.', *Nature Reviews Molecular Cell Biology*, 6(4), pp. 306–317. doi: 10.1038/nrm1622.

Hu, H., Gan, J. and Jonas, P. (2014) 'Fast-spiking, parvalbumin<sup>+</sup> GABAergic interneurons: from cellular design to microcircuit function.', *Science*, 345(6196), p. 1255263. doi: 10.1126/science.1255263.

Hu, J. S., Doan, L. T., Currle, D. S., Paff, M., Rheem, J. Y., Schreyer, R., Robert, B. and Monuki, E. S. (2008) 'Border formation in a BMP gradient reduced to single dissociated cells', *Proceedings of the National Academy of Sciences of the United States of America*, 105(9), pp. 3398–3403. doi: 10.1073/pnas.0709100105.

Huang, S.-M. a, Mishina, Y. M., Liu, S., Cheung, A., Stegmeier, F., Michaud, G. A., Charlat, O., Wiellette, E., Zhang, Y., Wiessner, S., Hild, M., Shi, X., Wilson, C. J., Mickanin, C., Myer, V., Fazal, A., Tomlinson, R., Serluca, F., Shao, W., Cheng, H., Shultz, M., Rau, C., Schirle, M., Schlegl, J., Ghidelli, S., Fawell, S., Lu, C., Curtis, D., Kirschner, M. W., Lengauer, C., Finan, P. M., Tallarico, J. A., Bouwmeester, T., Porter, J. a, Bauer, A. and Cong, F. (2009) 'Tankyrase inhibition stabilizes axin and antagonizes Wnt signalling', *Nature*, 461(7264), pp. 614–620. doi: 10.1038/nature08356.

Huelsken, J. and Behrens, J. (2002) 'The Wnt signalling pathway', *Journal of Cell Science*, 115(21), pp. 3977–3978. doi: 10.1242/jcs.00089.

Hughes, P. E., Alexi, T., Williams, C. E., Clark, R. G. and Gluckman, P. D. (1999) 'Administration of recombinant human activin-A has powerful neurotrophic effects on select striatal phenotypes in the quinolinic acid lesion model of Huntington's disease', *Neuroscience*, 92(1), pp. 197–209. doi: 10.1016/S0306-4522(98)00724-6.

Hynes, M., Stone, D. M., Dowd, M., Pitts-Meek, S., Goddard, A., Gurney, A. and Rosenthal, A. (1997) 'Control of cell pattern in the neural tube by the zinc finger transcription factor and oncogene Gli-1', *Neuron*, 19(1), pp. 15–26. doi: 10.1016/S0896-6273(00)80344-X.

Ivkovic, S. and Ehrlich, M. E. (1999) 'Expression of the striatal DARPP-32/ARPP-21 phenotype in GABAergic neurons requires neurotrophins in vivo and in vitro.', *Journal of Neuroscience*, 19(13), pp. 5409–5419.

Jaeger, I., Arber, C., Risner-Janiczek, J. R., Kuechler, J., Pritzsche, D., Chen, I.-C., Naveenan, T., Ungless, M. a. and Li, M. (2011) 'Temporally controlled modulation of FGF/ERK signaling directs midbrain dopaminergic neural progenitor fate in mouse and human pluripotent stem cells', *Development*, 138(20), pp. 4363–4374. doi: 10.1242/dev.066746.

Janowski, M., Jablonska, A., Kozłowska, H., Orukari, I., Bernard, S., Bulte, J. W. M., Lukomska, B. and Walczak, P. (2012) 'Neonatal desensitization does not universally prevent xenograft rejection.', *Nature Methods*, 9(9), p. 856–8; doi: 10.1038/nmeth.2146.

Jensen, J. B., Björklund, A. and Parmar, M. (2004) 'Striatal neuron differentiation from neurosphere-expanded progenitors depends on Gsh2 expression.', *Journal of Neuroscience*, 24(31), pp. 6958–6967. doi: 10.1523/JNEUROSCI.1331-04.2004.

Joannides, A. J., Webber, D. J., Raineteau, O., Kelly, C., Irvine, K.-A., Watts, C., Rosser, A. E., Kemp, P. J., Blakemore, W. F., Compston, A., Caldwell, M. A., Allen, N. D. and Chandran, S. (2007) 'Environmental

signals regulate lineage choice and temporal maturation of neural stem cells from human embryonic stem cells.', *Brain*, 130(Pt 5), pp. 1263–75. doi: 10.1093/brain/awm070.

Kallur, T., Darsalia, V., Lindvall, O. and Kokaia, Z. (2006) 'Human fetal cortical and striatal neural stem cells generate region-specific neurons in vitro and differentiate extensively to neurons after intrastriatal transplantation in neonatal rats', *Journal of Neuroscience Research*, 84(8), pp. 1630–1644. doi: 10.1002/jnr.21066.

Kanatani, S., Yozu, M., Tabata, H. and Nakajima, K. (2008) 'COUP-TFII is preferentially expressed in the caudal ganglionic eminence and is involved in the caudal migratory stream.', *Journal of Neuroscience*, 28(50), pp. 13582–13591. doi: 10.1523/JNEUROSCI.2132-08.2008.

Kawaguchi, Y. (1993) 'Physiological, morphological, and histochemical characterization of three classes of interneurons in rat neostriatum.', *Journal of Neuroscience*, 13(11), pp. 4908–4923. doi: 10.1016/S0921-8696(05)81133-8.

Kearns, N. A., Genga, R. M. J., Enuameh, M. S., Garber, M., Wolfe, S. A. and Maehr, R. (2014) 'Cas9 effector-mediated regulation of transcription and differentiation in human pluripotent stem cells.', *Development*, 141(1), pp. 219–23. doi: 10.1242/dev.103341.

Kelly, C. M., Precious, S. V., Scherf, C., Penketh, R., Amso, N. N., Battersby, A., Allen, N. D., Dunnett, S. B. and Rosser, A. E. (2009) 'Neonatal desensitization allows long-term survival of neural xenotransplants without immunosuppression.', *Nature Methods*, 6(4), pp. 271–273. doi: 10.1038/nmeth.1308.

Kendall, A. L., Rayment, F. D. and Torres, E. M. (1998) 'Functional integration of striatal allografts in a primate model of Huntington's disease', *Nature Medicine*, 4, pp. 727–729.

Kim, T.-G., Yao, R., Monnell, T., Cho, J.-H., Vasudevan, A., Koh, A., T., P. K., Moon, M., Datta, D., Bolshakov, V. Y., Kim, K.-S. and Chung, S. (2014) 'Efficient Specification of Interneurons from Human Pluripotent Stem Cells by Dorsoventral and Rostrocaudal Modulation', *Stem Cells*, pp. 1789–1804.

Kirkeby, A., Grealish, S., Wolf, D. A., Nelander, J., Wood, J., Lundblad, M., Lindvall, O. and Parmar, M. (2012) 'Generation of Regionally Specified Neural Progenitors and Functional Neurons from Human Embryonic Stem Cells under Defined Conditions', *Cell Reports*. The Authors, 1(6), pp. 703–714. doi: 10.1016/j.celrep.2012.04.009.

Kirwan, P., Turner-Bridger, B., Peter, M., Momoh, A., Arambepola, D., Robinson, H. P. C. and Livesey, F. J. (2015) 'Development and function of human cerebral cortex neural networks from pluripotent stem cells in vitro', *Development*, 142(18), pp. 3178–3187. doi: 10.1242/dev.123851.

Klein, A., Lane, E. L. and Dunnett, S. B. (2012) 'Brain repair in a unilateral rat model of Huntington's disease: new insights into impairments and restoration of forelimb movement patterns.', *Cell Transplantation*, 22, pp. 1735–1751. doi: 10.3727/096368912X657918.

Kopyov, O. V., Jacques, S., Lieberman, A., Duma, C. M. and Eagle, K. S. (1998) 'Safety of intrastriatal neurotransplantation for Huntington's disease patients.', *Experimental Neurology*, 149(1), pp. 97–108. doi: 10.1006/exnr.1997.6685.

Kordasiewicz, H. B., Stanek, L. M., Wancewicz, E. V., Mazur, C., McAlonis, M. M., Pytel, K. A., Artates, J. W., Weiss, A., Cheng, S. H., Shihabuddin, L. S., Hung, G., Bennett, C. F. and Cleveland, D. W. (2012) 'Sustained Therapeutic Reversal of Huntington's Disease by Transient Repression of Huntingtin Synthesis', *Neuron*, 74(6), pp. 1031–1044. doi: 10.1016/j.neuron.2012.05.009.

Kosinski, C. M., Cha, J. H., Young, A. B., Mangiarini, L., Bates, G., Schiefer, J. and Schwarz, M. (1999) 'Intranuclear inclusions in subtypes of striatal neurons in Huntington's disease transgenic mice.', *Neuroreport*, 10(18), pp. 3891–6. doi: 10.1097/00001756-199912160-00031.

- Kosinski, C. M., Cha, J. H., Young, A. B., Persichetti, F., MacDonald, M., Gusella, J. F., Penney, J. B. and Standaert, D. G. (1997) 'Huntingtin immunoreactivity in the rat neostriatum: differential accumulation in projection and interneurons.', *Experimental Neurology*, 144(2), pp. 239–47. doi: 10.1006/exnr.1997.6441.
- Kriks, S., Shim, J.-W., Piao, J., Ganat, Y. M., Wakeman, D. R., Xie, Z., Carrillo-Reid, L., Auyeung, G., Antonacci, C., Buch, A., Yang, L., Beal, M. F., Surmeier, D. J., Kordower, J. H., Tabar, V. and Studer, L. (2011) 'Dopamine neurons derived from human ES cells efficiently engraft in animal models of Parkinson's disease', *Nature*. Nature Publishing Group, 480(7378), pp. 547–551. doi: 10.1038/nature10648.
- Kuschel, S., Rütter, U. and Theil, T. (2003) 'A disrupted balance between BMP/Wnt and FGF signaling underlies the ventralization of the Gli3 mutant telencephalon', *Developmental Biology*, 260(2), pp. 484–495. doi: 10.1016/S0012-1606(03)00252-5.
- Lancaster, M., Renner, M., Martin, C., Wenzel, D., Bicknell, L., Hurles, M., Homfray, T., Penninger, J., Jackson, A. and Knoblich, J. (2013) 'Cerebral organoids model human brain development and microcephaly', *Nature*. Nature Publishing Group, 501, pp. 373–379. doi: 10.1002/mds.25740.
- Lee, J. K., Mathews, K., Schlaggar, B., Perlmutter, J., Paulsen, J. S., Epping, E., Burmeister, L. and Nopoulos, P. (2012) 'Measures of growth in children at risk for Huntington disease', *Neurology*, 79(7), pp. 668–674. doi: 10.1212/WNL.0b013e3182648b65.
- Lee, J., Platt, K. A., Censullo, P., Ruiz i Altaba, A. and Altaba, A. R. i (1997) 'Gli1 is a target of Sonic hedgehog that induces ventral neural tube development.', *Development*, 124(13), pp. 2537–2552.
- Lee, S. M., Tole, S., Grove, E. and McMahon, a P. (2000) 'A local Wnt-3a signal is required for development of the mammalian hippocampus.', *Development*, 127(3), pp. 457–467.
- Lelos, M. J., Robertson, V. H., Vinh, N.-N., Harrison, C., Eriksen, P., Torres, E. M., Clinch, S. P., Rosser, A. E. and Dunnett, S. B. (2015) 'Direct Comparison of Rat- and Human-Derived Ganglionic Eminence Tissue Grafts on Motor Function.', *Cell Transplantation*, 25(0), pp. 665–675. doi: 10.3727/096368915X690297.
- Li, X.-J., Zhang, X., Johnson, M. A., Wang, Z.-B., Lavaute, T. and Zhang, S.-C. (2009) 'Coordination of sonic hedgehog and Wnt signaling determines ventral and dorsal telencephalic neuron types from human embryonic stem cells.', *Development*, 136(23), pp. 4055–4063. doi: 10.1242/dev.036624.
- Liang, Z. Q., Wang, X. X., Wang, Y., Chuang, D. M., DiFiglia, M., Chase, T. N. and Qin, Z. H. (2005) 'Susceptibility of striatal neurons to excitotoxic injury correlates with basal levels of Bcl-2 and the induction of P53 and c-Myc immunoreactivity', *Neurobiology of Disease*, 20(2), pp. 562–573. doi: 10.1016/j.nbd.2005.04.011.
- Liu, Y., Weick, J. P., Liu, H., Krencik, R., Zhang, X., Ma, L., Zhou, G., Ayala, M. and Zhang, S.-C. (2013) 'Medial ganglionic eminence-like cells derived from human embryonic stem cells correct learning and memory deficits.', *Nature Biotechnology*. Nature Publishing Group, 31(5), pp. 440–7. doi: 10.1038/nbt.2565.
- Ludwig, T. E., Bergendahl, V., Levenstein, M. E., Yu, J. Y., Probasco, M. D. and Thomson, J. A. (2006) 'Feeder-independent culture of human embryonic stem cells', *Nature Methods*, 3(8), pp. 637–646. doi: 10.1038/nmeth902.
- Ma, L., Hu, B., Liu, Y., Vermilyea, S. C., Liu, H., Gao, L., Sun, Y., Zhang, X. and Zhang, S. C. (2012) 'Human embryonic stem cell-derived GABA neurons correct locomotion deficits in quinolinic acid-lesioned mice', *Cell Stem Cell*. Elsevier Inc., 10(4), pp. 455–464. doi: 10.1016/j.stem.2012.01.021.
- MacDonald, M. E., Ambrose, C. M., Duyao, M. P., Myers, R. H., Lin, C., Srinidhi, L., Barnes, G., Taylor,

- S. A., James, M., Groot, N., MacFarlane, H., Jenkins, B., Anderson, M. A., Wexler, N. S., Gusella, J. F., Bates, G. P., Baxendale, S., Hummerich, H., Kirby, S., North, M., Youngman, S., Mott, R., Zehetner, G., Sedlacek, Z., Poustka, A., Frischauf, A. M., Lehrach, H., Buckler, A. J., Church, D., Doucette-Stamm, L., O'Donovan, M. C., Riba-Ramirez, L., Shah, M., Stanton, V. P., Strobel, S. A., Draths, K. M., Wales, J. L., Dervan, P., Housman, D. E., Altherr, M., Shiang, R., Thompson, L., Fielder, T., Wasmuth, J. J., Tagle, D., Valdes, J., Elmer, L., Allard, M., Castilla, L., Swaroop, M., Blanchard, K., Collins, F. S., Snell, R., Holloway, T., Gillespie, K., Datson, N., Shaw, D. and Harper, P. S. (1993) 'A novel gene containing a trinucleotide repeat that is expanded and unstable on Huntington's disease chromosomes', *Cell*, 72(6), pp. 971–983. doi: 10.1016/0092-8674(93)90585-E.
- Maira, M., Long, J. E., Lee, A. Y., Rubenstein, J. L. R. and Stifani, S. (2010) 'Role for TGF- $\beta$  superfamily signaling in telencephalic GABAergic neuron development', *Journal of Neurodevelopmental Disorders*, 2(1), pp. 48–60. doi: 10.1007/s11689-009-9035-6.
- Marin, O., Anderson, S. A. and Rubenstein, J. L. (2000) 'Origin and molecular specification of striatal interneurons.', *Journal of Neuroscience*, 20(16), pp. 6063–6076. doi: 10934256.
- Marin, O., Yaron, A., Bagri, A., Tessier-Lavigne, M. and Rubenstein, J. L. R. (2001) 'Sorting of striatal and cortical interneurons regulated by Semaphorin-Neuropilin interactions', *Science*, 293(5531), pp. 872–875. doi: 10.1126/science.1061891.
- Maroof, A. M., Keros, S., Tyson, J. A., Ying, S.-W., Ganat, Y. M., Merkle, F. T., Liu, B., Goulburn, A., Stanley, E. G., Elefanty, A. G., Widmer, H. R., Eggan, K., Goldstein, P. A., Anderson, S. A. and Studer, L. (2013) 'Directed differentiation and functional maturation of cortical interneurons from human embryonic stem cells.', *Cell stem cell*. Elsevier Inc., 12(5), pp. 559–72. doi: 10.1016/j.stem.2013.04.008.
- Martín-Ibáñez, R., Crespo, E., Esgleas, M., Urban, N., Wang, B., Waclaw, R., Georgopoulos, K., Martínez, S., Campbell, K., Vicario-Abejón, C., Alberch, J., Chan, S., Kastner, P., Rubenstein, J. L. and Canals, J. M. (2012) 'Helios transcription factor expression depends on Gsx2 and Dlx1/2 function in developing striatal matrix neurons', *Stem Cells and Development*, 21(12), pp. 2239–2251. doi: 10.1089/scd.2011.0607.
- Massagué, J. (1998) 'TGF- $\beta$  signal transduction', *Annual Review of Biochemistry*, 67, pp. 753–91.
- Massouh, M., Wallman, M. J., Pourcher, E. and Parent, A. (2008) 'The fate of the large striatal interneurons expressing calretinin in Huntington's disease', *Neuroscience Research*, 62(4), pp. 216–224. doi: 10.1016/j.neures.2008.08.007.
- Mazzocchi-Jones, D., Döbrössy, M. and Dunnett, S. B. (2009) 'Embryonic striatal grafts restore bi-directional synaptic plasticity in a rodent model of Huntington's disease', *European Journal of Neuroscience*, 30(11), pp. 2134–2142. doi: 10.1111/j.1460-9568.2009.07006.x.
- Mazzocchi-Jones, D., Döbrössy, M. and Dunnett, S. B. (2011) 'Environmental enrichment facilitates long-term potentiation in embryonic striatal grafts.', *Neurorehabilitation and Neural Repair*, 25(6), pp. 548–557. doi: 10.1177/1545968311402090.
- McKinsey, G. L., Lindtner, S., Trzcinski, B., Visel, A., Pennacchio, L. A., Huylebroeck, D., Higashi, Y. and Rubenstein, J. L. R. (2013) 'Dlx1&2-dependent expression of Zfhx1b (Sip1, Zeb2) regulates the fate switch between cortical and striatal interneurons', *Neuron*. Elsevier Inc., 77(1), pp. 83–98. doi: 10.1016/j.neuron.2012.11.035.
- Monte, S. M. De, Vonsattel, J. and Richardson, E. P. (1988) 'Morphometric demonstration of atrophic changes in the cerebral cortex, white matter, and neostriatum in Huntington's disease', *Journal of Neuropathology and Experimental Neurology*, 47(5), pp. 516–525.

Moore, A. R., Zhou, W.-L., Jakovcevski, I., Zecevic, N. and Antic, S. D. (2011) 'Spontaneous electrical activity in the human fetal cortex in vitro.', *Journal of Neuroscience*, 31(7), pp. 2391–2398. doi: 10.1523/JNEUROSCI.3886-10.2011.

Nakao, N., Grasbon-Frodl, E. M., Widner, H. and Brundin, P. (1996) 'DARPP-32-rich zones in grafts of lateral ganglionic eminence govern the extent of functional recovery in skilled paw reaching in an animal model of Huntington's disease', *Neuroscience*, 74(4), pp. 959–970. doi: 10.1016/S0306-4522(96)00238-2.

Nambu, A., Tokuno, H. and Takada, M. (2002) 'Functional significance of the cortico-subthalamo-pallidal "hyperdirect" pathway', *Neuroscience Research*, 43(2), pp. 111–117. doi: 10.1016/S0168-0102(02)00027-5.

Nasir, J., Floresco, S. and O'Kusky, J. (1995) 'Targeted disruption of the Huntington's disease gene results in embryonic lethality and behavioral and morphological changes in heterozygotes', *Cell*, 81, pp. 811–823. doi: 10.1016/0092-8674(95)90542-1.

Nelson, A. B., Hammack, N., Yang, C. F., Shah, N. M., Seal, R. P. and Kreitzer, A. C. (2014) 'Striatal cholinergic interneurons drive GABA release from dopamine terminals', *Neuron*. Elsevier Inc., 82(1), pp. 63–70. doi: 10.1016/j.neuron.2014.01.023.

Nicholas, C. R., Chen, J., Tang, Y., Southwell, D. G., Chalmers, N., Vogt, D., Arnold, C. M., Chen, Y. J. J., Stanley, E. G., Elefanty, A. G., Sasai, Y., Alvarez-Buylla, A., Rubenstein, J. L. R. and Kriegstein, A. R. (2013) 'Functional maturation of hPSC-derived forebrain interneurons requires an extended timeline and mimics human neural development', *Cell Stem Cell*. Elsevier Inc., 12(5), pp. 573–586. doi: 10.1016/j.stem.2013.04.005.

Nicoleau, C., Varela, C., Bonnefond, C., Maury, Y., Bugi, A., Aubry, L., Viegas, P., Bourgois-Rocha, F., Peschanski, M. and Perrier, A. L. (2013) 'Embryonic stem cells neural differentiation qualifies the role of Wnt/ $\beta$ -Catenin signals in human telencephalic specification and regionalization', *Stem Cells*, 31(9), pp. 1763–1774. doi: 10.1002/stem.1462.

Nishino, H., Hida, H., Takei, N., Kumazaki, M., Nakajima, K. and Baba, H. (2000) 'Mesencephalic neural stem (progenitor) cells develop to dopaminergic neurons more strongly in dopamine-depleted striatum than in intact striatum.', *Experimental Neurology*, 164, pp. 209–214. doi: 10.1006/exnr.2000.7426.

Nóbrega-Pereira, S., Gelman, D., Bartolini, G., Pla, R., Pierani, A. and Marín, O. (2010) 'Origin and molecular specification of globus pallidus neurons.', *Journal of Neuroscience*, 30(8), pp. 2824–2834. doi: 10.1523/JNEUROSCI.4023-09.2010.

Nóbrega-Pereira, S., Kessar, N., Du, T., Kimura, S., Anderson, S. a. and Marín, O. (2008) 'Postmitotic Nkx2-1 Controls the Migration of Telencephalic Interneurons by Direct Repression of Guidance Receptors', *Neuron*, 59(5), pp. 733–745. doi: 10.1016/j.neuron.2008.07.024.

Nopoulos, P. C., Aylward, E. H., Ross, C. A., Mills, J. A., Langbehn, D. R., Johnson, H. J., Magnotta, V. A., Pierson, R. K., Beglinger, L. J., Nance, M. A., Barker, R. A. and Paulsen, J. S. (2011) 'Smaller intracranial volume in prodromal Huntington's disease: evidence for abnormal neurodevelopment', *Brain*, 134, pp. 137–142. doi: 10.1093/brain/awq280.

Onorati, M., Castiglioni, V., Biasci, D., Cesana, E., Menon, R., Vuono, R., Talpo, F., Goya, R. L., Lyons, P. A., Bulfamante, G. P., Muzio, L., Martino, G., Toselli, M., Farina, C., Barker, R. A., Biella, G. and Cattaneo, E. (2014) 'Molecular and functional definition of the developing human striatum', *Nature Neuroscience*. Nature Publishing Group, 17(12), pp. 1804–1815. doi: 10.1038/nn.3860.

Palfi, S., Condé, F., Riche, D., Brouillet, E., Dautry, C., Mittoux, V., Chibois, A., Peschanski, M. and

- Hantraye, P. (1998) 'Fetal striatal allografts reverse cognitive deficits in a primate model of Huntington disease.', *Nature Medicine*, 4(8), pp. 963–966. doi: 10.1038/nm0898-963.
- Di Pardo, A., Amico, E., Favellato, M., Castrataro, R., Fucile, S., Squitieri, F. and Maglione, V. (2014) 'FTY720 (fingolimod) is a neuroprotective and disease-modifying agent in cellular and mouse models of huntington disease', *Human Molecular Genetics*, 23(9), pp. 2251–2265. doi: 10.1093/hmg/ddt615.
- Pauly, M.-C., Döbrössy, M. D., Nikkhah, G., Winkler, C. and Piroth, T. (2013) 'Organization of the human fetal subpallium.', *Frontiers in Neuroanatomy*, 7(January), p. 54. doi: 10.3389/fnana.2013.00054.
- Penrod, R. D., Kourrich, S., Kearney, E., Thomas, M. J. and Lanier, L. M. (2011) 'An embryonic culture system for the investigation of striatal medium spiny neuron dendritic spine development and plasticity', *Journal of Neuroscience Methods*. Elsevier B.V., 200(1), pp. 1–13. doi: 10.1016/j.jneumeth.2011.05.029.
- Perea, G., Navarrete, M. and Araque, A. (2009) 'Tripartite synapses: astrocytes process and control synaptic information', *Trends in Neurosciences*, 32(8), pp. 421–431. doi: 10.1016/j.tins.2009.05.001.
- Perrier, A. L., Tabar, V., Barberi, T., Rubio, M. E., Bruses, J., Topf, N., Harrison, N. L. and Studer, L. (2004) 'Derivation of midbrain dopamine neurons from human embryonic stem cells.', *Proceedings of the National Academy of Sciences of the United States of America*, 101(34), pp. 12543–12548. doi: 10.1073/pnas.0404700101.
- Peschanski, M., Cesaro, P. and Hantraye, P. (1995) 'Rationale for intrastriatal grafting of striatal neuroblasts in patients with Huntington's disease', *Neuroscience*, 68(2), pp. 273–285. doi: 10.1016/0306-4522(95)00162-C.
- Piek, E., Heldin, C. H. and Ten Dijke, P. (1999) 'Specificity, diversity, and regulation in TGF-beta superfamily signaling.', *FASEB*, 13(15), pp. 2105–2124.
- Pilz, G.-A., Shitamukai, A., Reillo, I., Pacary, E., Schwausch, J., Stahl, R., Ninkovic, J., Snippert, H. J., Clevers, H., Godinho, L., Guillemot, F., Borrell, V., Matsuzaki, F. and Götz, M. (2013) 'Amplification of progenitors in the mammalian telencephalon includes a new radial glial cell type.', *Nature Communications*, 4, p. 2125. doi: 10.1038/ncomms3125.
- Plotkin, J. L., Wu, N., Chesselet, M. F. and Levine, M. S. (2005) 'Functional and molecular development of striatal fast-spiking GABAergic interneurons and their cortical inputs', *European Journal of Neuroscience*, 22(5), pp. 1097–1108. doi: 10.1111/j.1460-9568.2005.04303.x.
- Pundt, L., Kondoh, T., Conrad, J. and Low, W. (1996) 'Transplantation of human fetal striatum into a rodent model Huntington's disease ameliorates locomotor deficits', *Neuroscience Research*, 24, pp. 415–420.
- Rallu, M., Machold, R., Gaiano, N., Corbin, J. G., McMahon, A. P. and Fishell, G. (2002) 'Dorsoventral patterning is established in the telencephalon of mutants lacking both Gli3 and Hedgehog signaling.', *Development*, 129(21), pp. 4963–4974.
- Reddington, A. E., Rosser, A. E. and Dunnett, S. B. (2014) 'Differentiation of pluripotent stem cells into striatal projection neurons: a pure MSN fate may not be sufficient', *Frontiers in Cellular Neuroscience*, 8, pp. 1–15. doi: 10.3389/fncel.2014.00398.
- Reiner, A., Shelby, E., Wang, H., Demarch, Z., Deng, Y., Guley, N. H., Hogg, V., Roxburgh, R., Tippett, L. J., Waldvogel, H. J. and Faull, R. L. M. (2013) 'Striatal parvalbuminergic neurons are lost in Huntington's disease: Implications for dystonia', *Movement Disorders*, 28(12), pp. 1691–1699. doi: 10.1002/mds.25624.
- Robertson, V. H., Evans, A. E., Harrison, D. J., Precious, S. V., Dunnett, S. B., Kelly, C. M. and Rosser, A. E.

- (2013) 'Is the adult mouse striatum a hostile host for neural transplant survival?', *Neuroreport*, 24(18), pp. 1010–5. doi: 10.1097/WNR.0000000000000066.
- Roberts, R., Ahn, A., Swartz, K., Beal, M. and Difiglia, M. (1993) 'Intrastriatal injections of quinolinic acid or kainic acid: Differential patterns of cell survival and the effects of data analysis on outcome', *Experimental Neurology*, 124, pp. 274–282.
- Rohr, K. B., Barth, K. A., Varga, Z. M. and Wilson, S. W. (2001) 'The Nodal pathway acts upstream of Hedgehog signaling to specify ventral telencephalic identity', *Neuron*, 29(2), pp. 341–351. doi: 10.1016/S0896-6273(01)00210-0.
- Ross, C. A. and Tabrizi, S. J. (2011) 'Huntington's disease: From molecular pathogenesis to clinical treatment', *Lancet Neurology*. Elsevier Ltd, 10(1), pp. 83–98. doi: 10.1016/S1474-4422(10)70245-3.
- Rosser, A. E., Barker, R. A., Harrower, T., Watts, C., Farrington, M., Ho, a K., Burnstein, R. M., Menon, D. K., Gillard, J. H., Pickard, J. and Dunnett, S. B. (2002) 'Unilateral transplantation of human primary fetal tissue in four patients with Huntington's disease: NEST-UK safety report ISRCTN no 36485475.', *Journal of Neurology, Neurosurgery and Psychiatry*, 73(6), pp. 678–685. doi: 10.1136/jnnp.73.6.678.
- Rosser, A. E., Tyers, P. and Dunnett, S. B. (2000) 'The morphological development of neurons derived from EGF- and FGF-2-driven human CNS precursors depends on their site of integration in the neonatal rat brain', *European Journal of Neuroscience*, 12(7), pp. 2405–2413. doi: 10.1046/j.1460-9568.2000.00135.x.
- Rubenstein, J. L. R., Shimamura, K., Martinez, S. and Puelles, L. (1998) 'Regionalization of the prosencephalic neural plate', *Annual Review of Neuroscience*, 21, pp. 445–477.
- Ruiz I Altaba, A. (1998) 'Combinatorial Gli gene function in floor plate and neuronal inductions by Sonic hedgehog.', *Development*, 125, pp. 2203–2212.
- Rushton, D. J., Mattis, V. B., Svendsen, C. N., Allen, N. D. and Kemp, P. J. (2013) 'Stimulation of GABA-induced Ca<sup>2+</sup> influx enhances maturation of human induced pluripotent stem cell-derived neurons', *PLoS ONE*, 8(11), pp. 1–16. doi: 10.1371/journal.pone.0081031.
- Samata, B., Kikuchi, T., Miyawaki, Y., Morizane, A., Mashimo, T., Nakagawa, M., Okita, K. and Takahashi, J. (2015) 'X-linked severe combined immunodeficiency (X-SCID) rats for xenotransplantation and behavioral evaluation', *Journal of Neuroscience Methods*, 243, pp. 68–77. doi: 10.1016/j.jneumeth.2015.01.027.
- Sanberg, P. R., Borlongan, C. V., Koutouzis, T. K., Norgren, R. B., Cahill, D. W. and Freeman, T. B. (1997) 'Human fetal striatal transplantation in an excitotoxic lesioned model of Huntington's disease.', *Annals of the New York Academy of Sciences*, 831, pp. 452–460.
- Sasai, Y., Lu, B., Steinbeisser, H., Geissert, D., Gont, L. K. and Robertis, E. M. De (1994) 'Xenopus chordin: A novel dorsalizing factor activated by organizer-specific homeobox genes', *Cell*, 79, pp. 779–790.
- Sato, T., Vries, R. G., Snippert, H. J., van de Wetering, M., Barker, N., Stange, D. E., van Es, J. H., Abo, A., Kujala, P., Peters, P. J. and Clevers, H. (2009) 'Single Lgr5 stem cells build crypt-villus structures in vitro without a mesenchymal niche.', *Nature*. Nature Publishing Group, 459(7244), pp. 262–5. doi: 10.1038/nature07935.
- Schwarcz, R., Guidetti, P., K., S. and Muchowski, P. J. (2011) 'Of Mice, Rats and Men: Revisiting the quinolinic acid hypothesis of Huntington's disease', *Progress in Neurobiology*, 90(2), pp. 230–245. doi: 10.1016/j.pneurobio.2009.04.005.OF.
- Schwartz, S. D., Hubschman, J., Heilwell, G., Franco-Cardenas, V., Pan, C. K., Ostrick, R. M., Mickunas,



- E., Gay, R., Klimanskaya, I. and Lanza, R. (2012) 'Embryonic stem cell trials for macular degeneration: a preliminary report', *Lancet*. Elsevier Ltd, 379(9817), pp. 713–720. doi: 10.1016/s0140-6736(12)60028-2.
- Semenov, M. V., Tamai, K., Brott, B. K., Kühl, M., Sokol, S. and He, X. (2001) 'Head inducer dickkopf-1 is a ligand for Wnt coreceptor LRP6', *Current Biology*, 11(12), pp. 951–961. doi: 10.1016/S0960-9822(01)00290-1.
- Shi, Y. and Massagué, J. (2003) 'Mechanisms of TGF- $\beta$  signaling from cell membrane to the nucleus', *Cell*, 113(Figure 2), pp. 685–700. doi: 10.1016/S0092-8674(03)00432-X.
- Simpson, E. H., Kellendonk, C. and Kandel, E. (2010) 'A possible role for the striatum in the pathogenesis of the cognitive symptoms of schizophrenia', *Neuron*. Elsevier Inc., 65(5), pp. 585–596. doi: 10.1016/j.neuron.2010.02.014.
- Sinha, S. and Chen, J. K. (2006) 'Purmorphamine activates the Hedgehog pathway by targeting Smoothened.', *Nature Chemical Biology*, 2(1), pp. 29–30. doi: 10.1038/nchembio753.
- Smith, W. C. and Harland, R. M. (1992) 'Expression cloning of noggin, a new dorsalizing factor localized to the Spemann organizer in *Xenopus* embryos.', *Cell*, 70(5), pp. 829–40. doi: 10.1016/0092-8674(92)90316-5.
- Song, M., Mohamad, O., Chen, D. and Yu, S. P. (2013) 'Coordinated development of voltage-gated Na<sup>+</sup> and K<sup>+</sup> currents regulates functional maturation of forebrain neurons derived from human induced pluripotent stem cells.', *Stem cells and development*, 22(10), pp. 1551–63. doi: 10.1089/scd.2012.0556.
- Spemann, H. and Mangold, H. (1924) 'Induction of embryonic primordia by implantation of organizers from a different species', *Development Genes and Evolution*, 100, pp. 599–638. doi: 10.1007/BF02108133.
- Starr, P. A., Kang, G. A., Heath, S., Shimamoto, S. and Turner, R. S. (2008) 'Pallidal neuronal discharge in Huntington's disease: Support for selective loss of striatal cells originating the indirect pathway', *Experimental Neurology*, 211(1), pp. 227–233. doi: 10.1016/j.expneurol.2008.01.023.
- Süssmuth, S. D., Haider, S., Landwehrmeyer, G. B., Farmer, R., Frost, C., Tripepi, G., Andersen, C. A., Di Bacco, M., Lamanna, C., Diodato, E., Massai, L., Diamanti, D., Mori, E., Magnoni, L., Dreyhaupt, J., Schiefele, K., Craufurd, D., Saft, C., Rudzinska, M., Ryglewicz, D., Orth, M., Brzozy, S., Baran, A., Pollio, G., Andre, R., Tabrizi, S. J., Darpo, B. and Westerberg, G. (2015) 'An exploratory double-blind, randomized clinical trial with selisistat, a SirT1 inhibitor, in patients with Huntington's disease', *British Journal of Clinical Pharmacology*, 79(3), pp. 465–476. doi: 10.1111/bcp.12512.
- Swijnenburg, R. J., Schrepfer, S., Govaert, J. A., Cao, F., Ransohoff, K., Sheikh, A. Y., Haddad, M., Connolly, A. J., Davis, M. M., Robbins, R. C. and Wu, J. C. (2008) 'Immunosuppressive therapy mitigates immunological rejection of human embryonic stem cell xenografts', *Proceedings of the National Academy of Sciences of the United States of America*, 105(35), pp. 12991–12996. doi: 10.1073/pnas.0805802105.
- Szucsik, J. C., Witte, D. P., Li, H., Pixley, S. K., Small, K. M. and Potter, S. S. (1997) 'Altered forebrain and hindbrain development in mice mutant for the Gsh-2 homeobox gene.', *Developmental Biology*, 191(2), pp. 230–42. doi: 10.1006/dbio.1997.8733.
- Takahashi, K., Tanabe, K., Ohnuki, M., Narita, M., Ichisaka, T., Tomoda, K. and Yamanaka, S. (2007) 'Induction of pluripotent stem cells from adult human fibroblasts by defined factors', *Cell*, 131(5), pp. 861–872. doi: 10.1016/j.cell.2007.11.019.
- Tam, P. P. and Steiner, K. A. (1999) 'Anterior patterning by synergistic activity of the early gastrula

organizer and the anterior germ layer tissues of the mouse embryo.', *Development*, 126(22), pp. 5171–5179.

Tang, B., Di Lena, P., Schaffer, L., Head, S. R., Baldi, P. and Thomas, E. A. (2011) 'Genome-wide identification of Bcl11b gene targets reveals role in brain-derived neurotrophic factor signaling', *PLoS ONE*, 6(9). doi: 10.1371/journal.pone.0023691.

Telezhkin, V., Schnell, C., Yarova, P. L., Yung, S., Sanders, P., Cope, E., Hughes, A., Thompson, B. A., Geater, C., Hancock, J. M., Joy, S., Badder, L., Connor-Robson, N., Comella, A., Straccia, M., Bombau, G., Brown, J. T., Canals, J. M., Randall, A. D., Allen, N. D. and Kemp, P. J. (2015) 'Forced cell-cycle exit and modulation of GABAA, CREB and GSK3 $\beta$  signaling promote functional maturation of induced pluripotent stem cell-derived neurons', *American Journal of Physiology*, p. ajpcell.00166.2015. doi: 10.1152/ajpcell.00166.2015.

Telias, M., Segal, M. and Ben-Yosef, D. (2014) 'Electrical maturation of neurons derived from human embryonic stem cells', *F1000Research*, 196, pp. 1–12. doi: 10.12688/f1000research.4943.1.

The HD iPSC Consortium (2012) 'Induced pluripotent stem cells from patients with huntington's disease show cag-repeat-expansion-associated phenotypes', *Cell Stem Cell*, 11(2), pp. 264–278. doi: 10.1016/j.stem.2012.04.027.

Thomson, J. A., Itskovitz-Eldor, J., Shapiro, S. S., Waknitz, M. A., Swiergiel, J. J., Marshall, V. S. and Jones, J. M. (1998) 'Embryonic stem cell lines derived from human blastocysts.', *Science*, 282(5391), pp. 1145–1147. doi: 10.1126/science.282.5391.1145.

Threlfell, S., Lalic, T., Platt, N. J., Jennings, K. A., Deisseroth, K. and Cragg, S. J. (2012) 'Striatal dopamine release is triggered by synchronized activity in cholinergic interneurons', *Neuron*, 75(1), pp. 58–64. doi: 10.1016/j.neuron.2012.04.038.

Toresson, H., Mata de Urquiza, A., Fagerström, C., Perlmann, T. and Campbell, K. (1999) 'Retinoids are produced by glia in the lateral ganglionic eminence and regulate striatal neuron differentiation.', *Development*, 126(6), pp. 1317–1326.

Toresson, H., Potter, S. S. and Campbell, K. (2000) 'Genetic control of dorsal-ventral identity in the telencephalon: opposing roles for Pax6 and Gsh2.', *Development*, 127(20), pp. 4361–4371.

Tozzi, A., de Iure, A., Bagetta, V., Tantucci, M., Durante, V., Quiroga-Varela, A., Costa, C., Di Filippo, M., Ghiglieri, V., Latagliata, E. C., Wegrzynowicz, M., Decressac, M., Giampà, C., Dalley, J. W., Xia, J., Gardoni, F., Mellone, M., El-Agnaf, O. M., Ardah, M. T., Puglisi-Allegra, S., Björklund, A., Spillantini, M. G., Picconi, B. and Calabresi, P. (2015) 'Alpha-Synuclein produces early behavioral alterations via striatal cholinergic synaptic dysfunction by interacting with GluN2D N-Methyl-D-Aspartate receptor subunit', *Biological Psychiatry*. Elsevier, 79(5), pp. 402–414. doi: 10.1016/j.biopsych.2015.08.013.

Traiffort, E., Angot, E. and Ruat, M. (2010) 'Sonic Hedgehog signaling in the mammalian brain', *Journal of Neurochemistry*, 113(3), pp. 576–590. doi: 10.1111/j.1471-4159.2010.06642.x.

Tyson, J. A., Goldberg, E. M., Maroof, a. M., Xu, Q., Petros, T. J. and Anderson, S. A. (2015) 'Duration of culture and sonic hedgehog signaling differentially specify PV versus SST cortical interneuron fates from embryonic stem cells', *Development*, 142(7), pp. 1267–1278. doi: 10.1242/dev.111526.

Urbán, N., Martín-Ibáñez, R., Herranz, C., Esgleas, M., Crespo, E., Pardo, M., Crespo-Enríquez, I., Méndez-Gómez, H. R., Waclaw, R., Chatzi, C., Alvarez, S., Alvarez, R., Duester, G., Campbell, K., de Lera, A. R., Vicario-Abejón, C., Martinez, S., Alberch, J. and Canals, J. M. (2010) 'Nol3 promotes striatal neurogenesis through the regulation of retinoic acid signaling.', *Neural Development*, 5, p. 21. doi: 10.1186/1749-8104-5-21.

Victor, M. B., Richner, M., Hermansteyne, T. O., Ransdell, J. L., Sobieski, C., Deng, P.-Y., Klyachko, V. A.,

- Nerbonne, J. M. and Yoo, A. S. (2014) 'Generation of Human Striatal Neurons by MicroRNA-Dependent Direct Conversion of Fibroblasts', *Neuron*. Elsevier Inc., 84(2), pp. 311–323. doi: 10.1016/j.neuron.2014.10.016.
- Vierbuchen, T., Ostermeier, A., Pang, Z., Kokubu, Y., Suedhof, T. and Wernig, M. (2010) 'Direct conversion of fibroblasts to functional neurons', *Nature*, 463, pp. 1035–1041. doi: 10.1016/j.wneu.2011.11.002.
- Villar-Cerviño, V., Kappeler, C., Nóbrega-Pereira, S., Henkemeyer, M., Rago, L., Nieto, M. A. and Marín, O. (2015) 'Molecular mechanisms controlling the migration of striatal interneurons.', *Journal of Neuroscience*, 35(23), pp. 8718–29. doi: 10.1523/JNEUROSCI.4317-14.2015.
- Vonsattel, J.-P., Myers, R. H., Stevens, T. J., Ferrante, R. J., Bird, E. D. and Richardson, E. P. (1985) 'Neuropathological classification of Huntington's disease', *Journal of Neuropathology and Experimental Neurology*, 44(6), pp. 559–577. doi: 10.1097/00005072-198511000-00003.
- Vonsattel, J. and Difiglia, M. (1998) 'Huntington Disease', *Journal of Neuropathology and Experimental Neurology*, 57(5), pp. 369–384. doi: 10.1017/CBO9781107415324.004.
- Walker, F. O. (2007) 'Huntington's disease', *Lancet*, 369(9557), pp. 218–228. doi: 10.1016/S0140-6736(07)60111-1.
- Wang, B., Fallon, J. F. and Beachy, P. A. (2000) 'Hedgehog-regulated processing of Gli3 produces an anterior/posterior repressor gradient in the developing vertebrate limb', *Cell*, 100(4), pp. 423–434. doi: 10.1016/S0092-8674(00)80678-9.
- Wang, C., You, Y., Qi, D., Zhou, X., Wang, L., Wei, S., Zhang, Z., Huang, W., Liu, Z., Liu, F., Ma, L. and Yang, Z. (2014) 'Human and monkey striatal interneurons are derived from the medial ganglionic eminence but not from the adult subventricular zone', *Journal of Neuroscience*, 34(33), pp. 10906–10923. doi: 10.1523/JNEUROSCI.1758-14.2014.
- Wang, Q., Hong, P., Gao, H., Chen, Y., Yang, Q., Jiang, M. and Li, H. (2016) 'An interneuron progenitor maintains neurogenic potential in vivo and differentiates into GABAergic interneurons after transplantation in the postnatal rat brain', *Scientific Reports*. Nature Publishing Group, 6(November 2015), p. 19003. doi: 10.1038/srep19003.
- Watts, C., Brasted, P. J. and Dunnett, S. B. (2000) 'Embryonic donor age and dissection influences striatal graft development and functional integration in a rodent model of Huntington's disease.', *Experimental Neurology*, 163(1), pp. 85–97. doi: 10.1006/exnr.1999.7341.
- Wenning, G. K., Odin, P., Morrish, P., Rehncrona, S., Widner, H., Brundin, P., Rothwell, J. C., Brown, R., Gustavii, B., Hagell, P., Jahanshahi, M., Sawle, G., Björklund, A., Brooks, D. J., Marsden, C. D., Quinn, N. P. and Lindvall, O. (1997) 'Short- and long-term survival and function of unilateral intrastriatal dopaminergic grafts in Parkinson's disease', *Annals of Neurology*, 42(1), pp. 95–107. doi: 10.1002/ana.410420115.
- Wichterle, H., Garcia-Verdugo, J. M., Herrera, D. G. and Alvarez-Buylla, A. (1999) 'Young neurons from medial ganglionic eminence disperse in adult and embryonic brain.', *Nature Neuroscience*, 2(5), pp. 461–466. doi: 10.1038/8131.
- Victorin, K. and Björklund, A. (1989) 'Connectivity of striatal grafts implanted into the ibotenic acid-lesioned striatum-II. Cortical afferents', *Neuroscience*, 30(2), pp. 297–311. doi: 10.1016/0306-4522(89)90255-8.
- Victorin, K., Isacson, O., Fischer, W., Nothias, F., Peschanski, M. and Björklund, A. (1988) 'Connectivity of striatal grafts implanted into the ibotenic acid-lesioned striatum-I. Subcortical afferents', *Neuroscience*, 27(2), pp. 547–562. doi: 10.1016/0306-4522(89)90255-8.

- Victorin, K., Simerly, R. B., Isacson, O., Swanson, L. W. and Björklund, A. (1989) 'Connectivity of striatal grafts implanted into the ibotenic acid-lesioned striatum-III. Efferent projecting graft neurons and their relation to host afferents within the grafts', *Neuroscience*, 30(2), pp. 313–330. doi: 10.1016/0306-4522(89)90256-X.
- Williams, H. J., Norton, N., Dwyer, S., Moskvina, V., Nikolov, I., Carroll, L., Georgieva, L., Williams, N. M., Morris, D. W., Quinn, E. M., Giegling, I., Ikeda, M., Wood, J., Lencz, T., Hultman, C., Lichtenstein, P., Thiselton, D., Maher, B. S., Malhotra, A. K., Riley, B., Kendler, K. S., Gill, M., Sullivan, P., Sklar, P., Purcell, S., Nimgaonkar, V. L., Kirov, G., Holmans, P., Corvin, A., Rujescu, D., Craddock, N., Owen, M. J. and O'Donovan, M. C. (2011) 'Fine mapping of ZNF804A and genome-wide significant evidence for its involvement in schizophrenia and bipolar disorder.', *Molecular Psychiatry*, 16(4), pp. 429–441. doi: 10.1038/mp.2010.36.
- Wu, Y. and Parent, A. (2000) 'Striatal interneurons expressing calretinin, parvalbumin or NADPH-diaphorase: A comparative study in the rat, monkey and human', *Brain Research*, 863(1–2), pp. 182–191. doi: 10.1016/S0006-8993(00)02135-1.
- Xu, Q., Guo, L., Moore, H., Waclaw, R. R., Campbell, K. and Anderson, S. A. (2010) 'Sonic Hedgehog signaling confers ventral telencephalic progenitors with distinct cortical interneuron fates', *Neuron*, 65(3), pp. 328–340. doi: 10.1016/j.neuron.2010.01.004.
- Yamaguchi, T. P. (2001) 'Heads or tails : Wnts and anterior – posterior patterning', *Current Biology*, pp. 713–724.
- Zhang, N., An, M. C., Montoro, D. and Ellerby, L. M. (2010) 'Characterization of human Huntington's disease cell model from induced pluripotent stem cells', *PLoS Currents*, (2), pp. 1–11. doi: 10.1371/currents.RRN1193.
- Zhang, S. C., Wernig, M., Duncan, I. D., Brüstle, O. and Thomson, J. a (2001) 'In vitro differentiation of transplantable neural precursors from human embryonic stem cells.', *Nature Biotechnology*, 19(12), pp. 1129–1133. doi: 10.1038/nbt1201-1129.
- Zhao, C., Eisinger, B. and Gammie, S. C. (2013) 'Characterization of GABAergic neurons in the mouse lateral septum: A double fluorescence in situ hybridization and immunohistochemical study using tyramide signal amplification', *PLoS ONE*, 8(8). doi: 10.1371/journal.pone.0073750.
- Zietlow, R., Precious, S. V., Kelly, C. M., Dunnett, S. B. and Rosser, A. E. (2012) 'Long-term expansion of human foetal neural progenitors leads to reduced graft viability in the neonatal rat brain', *Experimental Neurology*. Elsevier Inc., 235(2), pp. 563–573. doi: 10.1016/j.expneurol.2012.03.010.
- Zimmerman, L. B., De Jesús-Escobar, J. M. and Harland, R. M. (1996) 'The Spemann organizer signal noggin binds and inactivates bone morphogenetic protein 4', *Cell*, 86(4), pp. 599–606. doi: 10.1016/S0092-8674(00)80133-6.